PROPOSED DESIGN OF AN OPTIMAL CONTROLLER TO MAXIMISE THE EFFICIENCY OF FLAT PLATE SOLAR COLLECTOR

by

Abubakar Sani Muhammad

Submitted to the Institute of Graduate Studies in Science and Engineering

in partial fulfillment of the requirements for the degree of

Master of Science

in

Electrical-Electronic Engineering

Mevlana (Rumi) University

2014

PROPOSED DESIGN OF AN OPTIMAL CONTROLLER TO MAXIMISE THE EFFICIENCY OF FLAT PLATE SOLAR COLLECTOR

Submitted by **Abubakar Sani Muhammad** in partial fulfillment of the requirements for the degree of Master of Science in Electrical and Electronic Engineering Department, Mevlana (Rumi) University

APPROVED BY:

Examining Committee Members:

Assoc. Prof. Dr. Hossein Valizadeh . . . . . .

(Thesis Supervisor)

Assoc. Prof. Dr. Essam Aboserie . . . . . .

Assoc. Prof. Dr. Musa Aydin . . . . . .

Assist. Prof. Dr. Alaa Elyan . . . . . .

Head of Department, Electrical-Electronic Engineering (Acting)

Assoc. Prof. Dr. Ali Sebetci . . . . . .

Director, Institute of Graduate Studies in Science and Engineering

DATE OF APPROVAL (/ / 2014)

I hereby declare that all information in this document has been obtained and presented in accordance with academic rules and ethical conduct. I also declare that, as required by these rules and conduct, I have fully cited and referenced all material and results that are not original to this work.

Abubakar Sani Muhammad

Signature:

ABSTRACT

PROPOSED DESIGN OF AN OPTIMAL CONTROLLER TO MAXIMISE THE EFFICIENCY OF FLAT PLATE SOLAR COLLECTOR

Abubakar Sani Muhammad

M.Sc. Thesis/2014

Thesis Supervisor: Assoc. Prof. Dr. Hossein Valizadeh

Keywords: Solar Collector, Controller, Solar Water Heating, Extremum Seeking Controller.

In a solar water heating system, a closed loop control system plays a vital role in maximizing the efficiency of the solar collector. In this thesis, this type of controller is considered. Water is pumped through the collector by means of a motor pump, and the quantity of water to be pumped at a certain moment will be decided when the net power which is the thermal power less the parasitic pumping power is fed through a logic decision unit called an extremum seeking controller which provides an output signal that either increases or decreases average power that drives the pump and as such the quantity of water fed into the solar collector is dependent on the intensity of the solar radiation striking the collector`s absorber, the flow rate converted to equivalent frequency and the pumping power. The complete system that manipulates these variables and gives the desired output response is referred to as an optimal control system.

DEDICATION

To My Parents

ACKNOWLEDGEMENTS

I am wholeheartedly thankful to my supervisor, Assoc. Prof. Dr. Hossein Valizadeh for giving me an opportunity to work under his supervision. This work would not have been successful without his patience, guidance, advice and encouragement. I indeed never forget your generosity sir!

I am also grateful to the management of Mevlana University Konya, Turkey, members of Engineering Faculty, and Electrical and Electronics Engineering Department for giving me this opportunity to undergo a master degree in this great university.

I would like to personally express my deep gratitude to the government of Kano State under the leadership of His Excellency, Engr. Dr. Rabiu Musa Kwankwaso for sponsoring my study.

TABLE OF CONTENTS

LIST OF TABLES

LIST OF FIGURES

LIST OF SYMBOLS/ABBREVIATIONS

Symbol	Explanation
α	Absorption rate of the absorber/ Resistance temperature
δ	Plate thickness
$\Delta\bar{x}$	Average thickness of insulating material
ε	Emittance of the absorber surface
ε_g	Emission of glass tube
ε_p	Emission of the absorber plate
η_c	Global collector efficiency
η_o	Optimal efficiency
η_t	Thermal efficiency
σ	The Stefan-Boltzmann constant
τ	Rate of transmission of the cover
$\tau\alpha$	Multiplying factor
A	Collector surface area
A_c	Collector area
A_g	Area of the glass tube
A_p	Area of the absorber plate
A_r	Surface area of receiver or absorber
c	Specific heat capacity of fluid
cp	Specific heat capacity of the fluid
c_b	Bond conductance between the conduit and absorber plate
CL.	Clocking
D	Outside diameter
D_i	Inside diameter
F	Frequency
F	Fin efficiency
F'	Collector efficiency
F_R	Heat removal factor

$\bar{h}_c$	Average overall convective transfer coefficient
$h_{f,i}$	Heat transfer coefficient between the fluid and the tube wall
h_g	Convection heat transfer coefficient from glass tube to ambient air
I	Intensity of solar radiation
k	Thermal conductivity of the absorber plate
$\bar{k}$	Equivalent average conductance
$\dot{m}$	Mass flow rate through the fluid conduit
P_p	Pump power
P_{TH}	Thermal power
Q_i	Collector heat input
$\dot{Q}_{loss\ convection}$	Convection loss
$\dot{Q}_{loss\ conduction}$	Conduction loss
$Q_{loss\ radiation}$	Radiation loss
Q_o	Heat loss
S	Solar radiation on the absorber plate
T_a	Ambient air temperature
T_c	Collector temperature
T_g	Temperature of glass tube
T_i	Fluid inlet temperature
T_r	Average temperature of receiver
T_{sky}	Equivalent black body temperature of the sky
U_L	Overall heat transfer coefficient
V_{pv}	Pump voltage
w	Width of the absorber plate
D.D	Darlington driver
L.E.D	Light emitting diode
MONO	Monostable
PIC	Programmable interface controller

PLC	Programmable logic controller
TRIG	Trigger

CHAPTER ONE

INTRODUCTION

1.1. General

Generation of large percentage of electricity in many countries of the world is allocated for heating water in some places such as family houses, industries and hospitals. In many developing countries, there is great challenge of power insufficiency and there is great inconsistency between demand and supply of electricity. To reduce this insufficiency, the best alternative is to employ solar hot water system so that huge amount of electricity can be saved for other purposes and hence the gap between supply and demand can be cut down substantially.

To achieve this desired objective, the solar hot water system has to be developed with an automatic control system to optimize the system performance there by maximizing efficiency. The system mainly constitute of the storage tank, solar collector, the pipe line connection and the controller [1].

The automatic solar hot water system has a lot of advantages among which the ones outlined below:

- The system utilizes solar energy that is obtained freely and is always renewable source because it is directly conveyed from sun to earth through radiation and cannot be exhausted unlike the case of fossil fuel provided the sun is existing and shining.
- The system employs solar energy which results in reducing reliance on fossil fuels, thereby providing enough energy security and exploring the alternative sources of energy and hence this can reduce dependence on foreign fuel import which is expensive compared to this source of energy.
- under sunny and warm condition, there is cost effectiveness with solar water heating system that has sufficient insolation.
- There are some incentive in many countries when solar water heating systems are installed.
- There is low maintenance cost and the payback period is around 5-10 years which is an imperessive period.
- The automatic solar water heating system can be easily built and the chart on how to construct them can be found.

Apart from abundant opportunities available there are also some disadvantages such as the ones below.

- There is upfront cost which must be accounted for initially and this is the main disadvantage.
- Electrical, gas or other fuel backup are required for continous operation during the winter period.
- There is need for and efficient protection against freeze and overheating.
- There is great variation in payback period based on regional sun (when there is high insolation, there will be shorter payback period) [2].

1.2. Controllers

In many process control generally there are three basic type of controllers employed, bang-on-bang-off (on-off), proportional and optimal (PID). Either of these controllers can be used to control a process depending on the type of system under consideration.

1.2.1. Bang-on-bang-off

The control regarded as simplest temperature controller, where the output only existing in two states on or off, and has no intermediate state. With a set point, the output will only be switched on when the temperature is above that set point. For example, in a heating control the output is off when the temperature is above the set point and on when it is below the set point.

Cycling in the process temperature will be continuous with the temperature crossing and changing the output state. In the heating system where damages to some components such as valves and contactors are to be prevented, hysteresis or on-off differential in the controller operation should be added. Based on the temperature differential operation, set point should be exceeded by a certain amount before the output becomes on or off again. Where precise control should not be used necessarily, on-off control can be used directly. When the frequent on and off in a system cannot be handled and the system mass is so great, an extremely slow change in temperatures can be experienced.

A limit controller is a special type of on-off control that can be used for alarm. A latching relay is used by the controller which should be reset manually and the used for shutting down a process the temperature a certain value.

1.2.2. Proportional

On-off control cycling can be eliminated by proportional controls which are usually designed for this purpose. This type of controller can increase the average power supplied to a pumping machine in a solar collector or decrease it for a heater when the set point of the temperature is approached. The heater with this effect slows down or the pumping machine speed increases and hence the set point will not be overshooted but will be approached gradually and a stable temperature will be maintained. The controller can accomplish the proportioning action when the on and off turning of the output is within some short intervals. Close to the set point temperature, the proportioning action can be implemented around a "proportional band". The controller functions as on and off outside the band, where the output is either below the band (fully on for the heater and fully off for the pumping machine) or above the band (fully off for the heater and fully on for the pumping machine).

However, from the set point, the measurement difference ratio will determine where the output will be turned on and off. When the proportional band midpoint (set point) is reached, the on: off ratio of the output will be 1:1, which implies that both on and of time will be equal. As the temperature is away from the set point, there would be variation in the on-and-time proportional to the difference in temperature. But if the temperature goes below the set point, the on-time of the output is much longer (longer off time for the pumping machine); and if the temperature goes above, the off-time is much longer (longer on time for the pumping machine).

A percentage of full scale or degrees can be used for expressing the proportional band. In other words, this is the gain which is also the reciprocal of the band. At the startup or when there is significant change in the process condition, a small adjustment by an operator may be needed for bringing the temperature to the set point.

For systems that have wide cycling of temperature, a proportional controller is needed. The control can either be a simple proportional or PID based, by considering the precision needed or the process. A wide proportional band is used where the process has large maximum rates of rise and longtime lags in order to eliminate oscillation. A large offset is encountered as the

load changes with the wide band. These offsets can be eliminated with automatic reset (integral). For the long time delays in a process, derivative (rate) action is used after disturbance of a process to speed up recovery.

1.2.3. Proportional Integral and Derivative

This is the last type of controller with Proportional Integral and Derivative (PID) control. Two additional adjustments are involved in this type of controller, which are integral and derivative controls in time-based unit's expression with their reciprocals represented respectively as RESET and RATE.

The three terms proportional, integral and derivative controls can be adjusted individually using trial and error by tuning to a particular system. Among all the three types of controllers PID gives a control with highest stability and accuracy, and operate satisfactorily in relatively systems that have small mass with quick reaction to the energy changes on the process.

In order to select a controller, certain features are mostly considered like self-or auto-tuning, in which the proportional band, rate and reset values are automatically calculated by the instrument for precise control which include serial communications with the unit talking to a host computer for data tuning, analysis and storage. In addition, timers marking beginning/end of an event or time elapsed etc.[3]

1.3. Control Strategy in Solar Collector

In any solar heat collector, the principle of operation is to expose the absorber plate of the collector to solar radiation. The absorber is a conductive plate (metal coated by a thin film of dark material). Upon the impingement of the radiation on the absorber the energy of the incoming radiation is converted to heat in the absorber. This is then transferred away from the collector by any suitable heat transfer means, usually a set of metal pipes (carrying air or water) welded to the back of the absorber or heat pipe.

The efficiency of the system depends on the ability of the coated film on the absorber plate to convert maximum amount of the incoming energy to heat and also depends on how fast the collected heat is transferred from the collector to the storage tank. This project is concerned with the latter [4].

The collector itself is attached to a water-pump. The water-pump is however, controlled by a very simple controller, which switches the pump on when substantial solar energy is available, and off when it is not. It decides to build a more complex controller which would maximize the efficiency of the solar collector system.

Basically all the three types of controllers are employed; the first is Bang-on-bang-off controller. This controller switches the pump on to some fixed speed when the temperature of the fluid at the collector outlet T_o exceeds the temperature of the fluid in the storage tank T_s by a fixed value $\Delta T_{on}{}^{o}c$. The pump is then switched off when T_o - T_s falls to a value $\Delta T_{off}{}^{o}c$. Where $\Delta T_{off}{}^{o}c$ is less than $\Delta T_{on}{}^{o}c$. The second controller type is the proportional controller. In this case, the mass flow rate $\dot{m}$ is zero for T_o - T_s less than some value $\Delta T_{off}{}^{o}c$. For T_o - T_s greater than some value $\Delta T_{on}{}^{o}c$, $\dot{m}$ is fixed at $\dot{m}_{max}$. Finally for T_o - T_s between $\Delta T_{off}{}^{o}c$ and $\Delta T_{on}{}^{o}c$, $\dot{m}$ varies linearly between zero and $\dot{m}_{max}$. The third controller is the optimal controller. This is a controller which by some means always drives the pump at that speed which yields a maximum net power output from the solar energy system, net power being the thermal power collected less the associated parasitic pumping power. The objective of this thesis is to design optimal controller and to investigate compatibility with a solar energy system [5].

CHAPTER TWO

EFFICIENCY OF SOLAR WATER HEATERS

2.1. Types Of Flat Plate Panels and Description Of Efficiency

Flat-plate collector is one of the major types of collectors available used for either space or water heating and sometimes in applications with temperature less than 100. It constitutes of three main parts: insulated metal box with glazing, absorber plates and heating pipes. The absorber plate mostly with a selective coating designed to have low emissivity and high absorptivity for better efficiency receives the energy in the solar radiation and and then transfers it to the fluid flowing in the pipes attached to the absorber plates. Mostly the absorbers for this type of collector are manufactured from aluminum or copper sheets because of their good heat conductivity especially copper which is less vulnerable to corrosion. There are basically two types of a collector based on application, the liquid and air collectors.

2.1.1. Liquid Collector

In this type, solar energy is absorbed by the liquid flowing through tubes attached to the absorber plates, and the flow tubes are arranged in parallel with inlet and outlet headers or in a serpentine form for uniformity of flow and elimination of possible header leakage. For systems where the tubes must completely drain for freeze protection, serpentine arrangement has to be avoided. Liquid collector can either be direct (open-loop) where the liquid mostly water passes directly through the collector while being heated and then flows out directly to storage tank where it will be used for laundry, bathing etc. or indirect (closed-loop) where a heat-transfer fluid flows through the collector while absorbing heat and then moves through a heat exchanger until it reaches the water in the storage tank where the heat will be extracted and the whole process is then repeated. Liquid collectors can be glazed or unglazed. The glazed one is used for household water heating while the other is used for warming swimming pool. A typical liquid collector is shown in Figure 2.1.

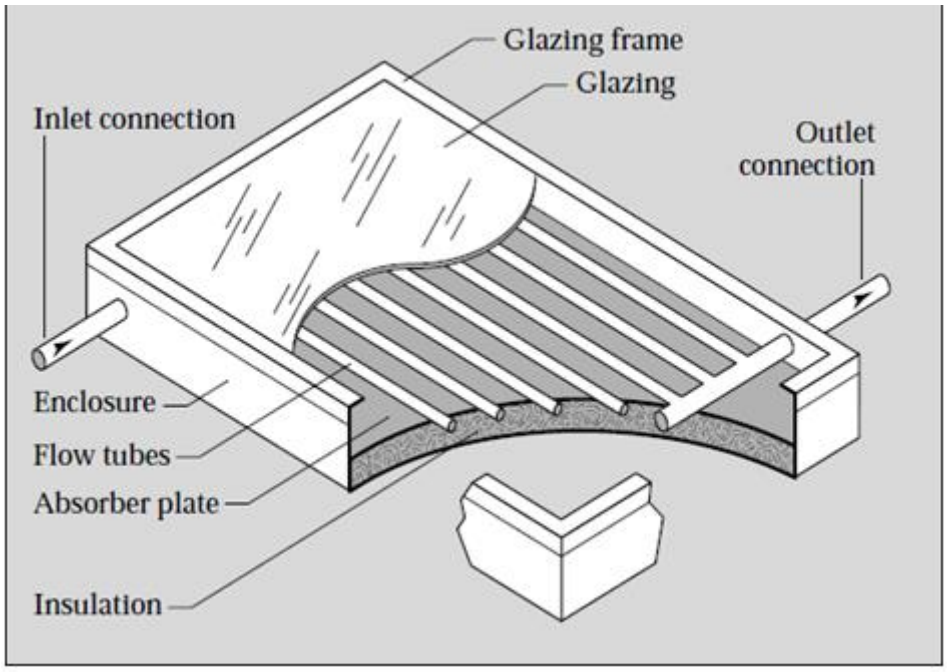

Figure 2.1: Water type Flat-Plate Collector [6].

2.1.2. Air Collector

In air Flat-plate collector, the air flows either by using a fan or by natural convection, through an inlet and passes the absorber through an outlet. The air conducts less; only small percentage of the heat will be transferred between the absorber and the air. Sometimes, the absorber is made with corrugation in order to create more turbulence for improving transfer of heat between the absorber and the air; even though more power will be needed to move fan for more air and thus the operating cost of the system will increase. Cheap materials such as plastic glazing can be used by air collector due to their low operating temperatures compared with liquid collectors. The air collector is shown in the Figure 2.2 [6].

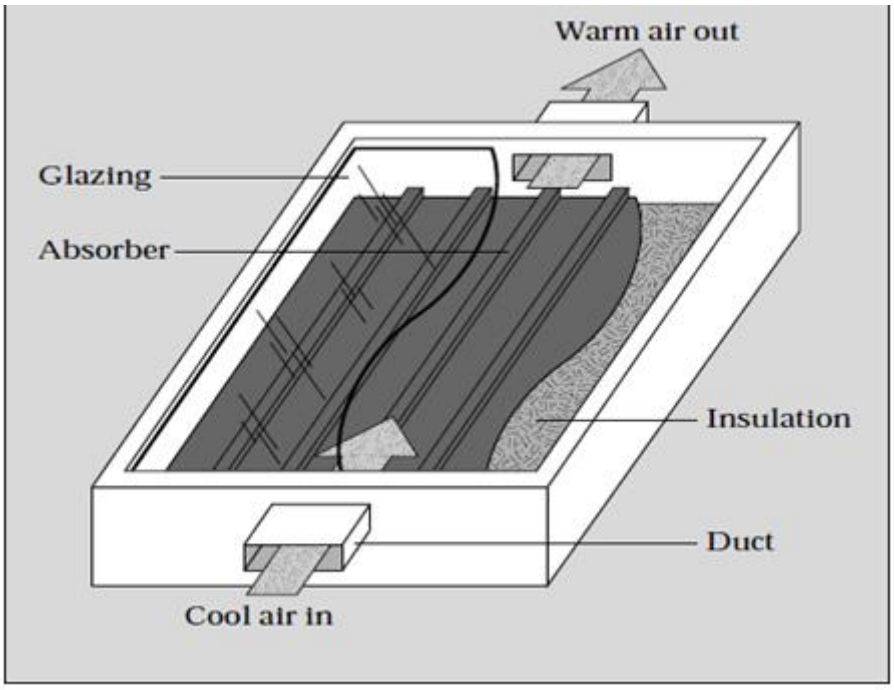

Figure 2.2: Air type Flat-plate Collector [6].

2.1.3. Description of Efficiency

Generally the efficiency of a solar collectors is dependent on certain factors, such as the design parameters, intensity of light , climatic condition, minimum temperature of demand, extraction rate of heat, fluctuation in the environmental temperature (with highest efficiency around the afternoon by overcoming the thermal inertia)

Under thermal operating condition, for any solar thermal collector, the global efficiency is given as:

$$\eta_c = \eta_o \times \eta \tag{2.1}$$

Where

$\eta_c =$ Global collector efficiency of the solar collector

$\eta_o =$ Optical efficiency (dependent on the angle of incidence of light)

$\eta_t =$ Thermal efficiency (dependent on the light intensity and system temperature)

Nowadays, many flat-plate collectors have an optical efficiency within a range of 75% to 80% when a transmission efficiency of 85% for ordinary glass at a perpendicular light incidence and an absorber with 5% to 10% reflectance are considered

The average temperature obtained between the inlet and outlet of the collector determines its thermal efficiency which increases with a decrease in average temperature. The amount of extracted heat and the efficiency would be zero as a result of heat flow stoppage, when there is equilibrium between radiation coming in on the one hand and the convective, radiative and conductive losses on other hand. The thermal efficiency can attain a value closer to 100% when there is very high heat extraction with the inlet temperature approaching ambient temperature making all the parasitic losses negligible. As just a compromise between a zero efficiency at high temperature and high efficiency at low temperature, an intermediate operating point is selected with a temperature below 100^{o}c and moderate efficiency.

Due to variation in solar intensity as a result of absorptions in atmosphere either in the evening or in the morning, average performance of the system cannot reach the maximum value or hence maximum efficiency cannot be attained. Depending on the site of the solar collector , the average efficiency is mostly below expectation due to effect of haze, clouds and other kinds of losses caused by some absorptions in atmosphere on the solar intensity, but it is much higher where sunny climate is abundantly available [7].

In the case of Flat-plate collectors, the conductivity of air is less compared with that of a liquid, the amount of heat transferred in the liquid collector is higher than that of the air collector, but in some systems turbulence in corrugations made on the absorber can be used to improve efficiency of the air collector. Therefore the air type is less efficient than the liquid collectors [6].

2.2. Factors Affecting Efficiency

The loss mechanisms that occurred in form of heat as a result of temperature difference between the absorber and the surroundings, when the solar energy with short wavelength radiations striking the absorber surface of the solar collector (thereby raising the temperature above the ambient temperature) are conduction, convection and radiation losses. There

should be a balance maintained between the heat removed from the collector and the heat losses by the three loss mechanisms which defines the collector's temperature operating point. This implies that the temperature of the absorber would be low if much heat is removed by the fluid and high if less heat is removed (which mostly happens due to interruption of the heat transfer fluid flow). The three loss mechanisms that affect the thermal efficiency are described below:

Convection loss: This type of loss is dependent on certain parameters which include the temperature difference between the surface of the absorber, air surrounding the environment and the absorber's surface area.

$$\dot{Q}_{loss\ convection} = \bar{h}_c A_r (T_r - T_a) \quad (W) \tag{2.2}$$

Where:

$\bar{h}_c$ – average overal convective heat transfer coefficient $(W / m^2 K)$
A_r – surface area of receiver or absorber(m^2)
T_r – average temperature of receiver (K)
T_a – ambient air temperature (K)

Convection loss takes place in two stages, one between the coversheet and the absorber and the other between the outside air and the cover sheet. For thorough analysis of heat loss due to convection, wind (which causes variation in heat transfer coefficient) must be included. However absorber's temperature is a variable quantity because the temperature around the heat transfer fluid outlet will be higher than that near the outlet , and both will be lower than that of the intermediate surface that does not have contact with fluid flowing through the absorber. Due to the surface phenomenon of convection, the temperature may not necessarily be that of the metal below the black paint or coating on the surface.

As with the other heat loss equations below, this is a simplified, instructive model. Usually there are a number of convective processes that cause an absorber or receiver to loose heat to the surroundings. For example, a flat-plate collector often has a glass cover sheet between the absorber plate and outside ambient air. There is one convection process between the hot absorber and the cover sheet, and a second between the cover sheet and outside air. Also, wind increases the heat transfer coefficient on the cover sheet and must be included in any serious analysis of convective heat loss. Regardless of these imperfections, the heat loss due

to convection is considered to be proportional to difference between the ambient and some average temperature and the surface area of the absorber.

Radiation loss: losses due to radiation are mostly noticed when the collector's temperature is slightly greater than ambient and becomes more effective when the temperature is very high. The rate of heat loss due to radiation is directly proportional to the surface emittance of the absorber and temperature difference to the fourth power as shown in Equation (2.3).

$$\dot{Q}_{loss\ radiation} = \varepsilon \sigma A_r (T^4 - T_{sky}^4) \quad (W) \tag{2.3}$$

ε – emittance of the absorber surface
σ – the stefan-Boltzmann constant ($5.670 \times 10^{-8} W/m^2K^2$)
T_{sky} – the equivalent black body temperature of the sky (K)

The figure below gives a graphical comparison between heat loss due to convection and radiation, where the convection loss becomes very high at high temperature compared with the radiation loss which is linear.

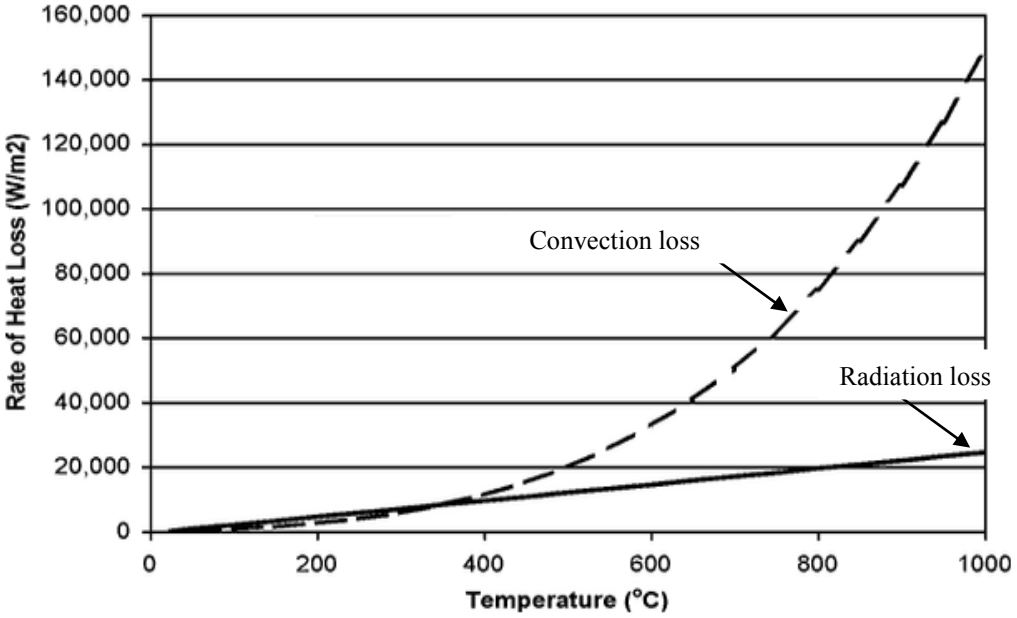

Figure 2.3: Comparison of Radiation and Convection Heat Loss for a Black, Vertical Surface in Free Air at 25°C [8].

The two parameters of this equation that can be controlled are the receiver's surface area and the emittance. By concentrating the solar energy on the receiver and reducing its surface area, the radiation losses can be minimized. While for the emittance, surfaces with low emittance can as well have low absorptance implying that the only small amount of the solar energy would be absorbed. But with a special type of surface coating known as selective coating, which at a low temperature has low emittance value and high absorptance.

Due to the operation of the solar collector in open space, there would be radiation exchange with the sky. The equivalent temperature of the radiation for the sky is dependent on the sky moisture content and air density. At sea level and a relatively high humidity, the sky temperature and the ambient air temperature are assumed to be equal. However, the temperature become 6^0C to 8^0C less than ambient air temperature at high altitude.

Conduction loss: Heat loss due to conduction is the last mechanism to be considered in designing a collector and is characterized by some parameters including cross-section area, the material constant and the thickness of the material.

$$\dot{Q}_{loss\ conduction} = \bar{k}\,\Delta\bar{x}A_r(T_r - T_a) \tag{2.4}$$

Where

$\bar{k}$ – equivalent average conductance (W/mK)
$\Delta\bar{x}$ – the average thickness of insulating material

When compared with other forms of losses, conduction has the least and is mostly combined with loss due to convection. In order to make the heat loss less significant, for example in a flat-plate collector, good and thick insulation (with low k) is made at both the back and sides surface of the absorber plate. This loss can further be reduced when a low conductance material (mostly made from stainless steel) for the frame and support structure attached to the absorber is used [8].

2.3. Role of Selective Coating

The flat plate collector can also be classified base on the selective property of the absorber plate by considering the type of the selective coating applied on the surface. The selectivity

implies that the absorber has high absorptance of the incoming radiation and low emittance of thermal radiation within the temperature range in which the surface radiates energy. A flat-black paint can absorb major percentage of the solar energy striking its surface and as well much of this energy is radiated in large quantity that depends on the absorber plate temperature and the glazing [6].

The fully efficient surface is a selective one in which all the solar wavelengths are absorbed and none of them are emitted there by causing more heat flowing in the working fluid. This can only exist when the absorptance is one and the emittance is zero. Many absorbers available commercially are designed to approach this ideal value. Many thin black metallic oxides placed on a bright metal surface constitutes a good selective absorber, among which the best one can have up to 0.95 absorptivity and transparent to longer wavelength thermal radiation , neither emitting nor absorbing 3 to 30 micro radiation.

The efficiency of the selective surface is determined by its absorptivity (which is supposed to be high at low wavelength) and its emissivity (supposed to be low at high wavelength). From the table below the surface formed from a black chrome coating on a substrate has an absorptance almost equal to 0.93 implying that about 93% of the incomings solar energy is absorbed, emittance of 0.10 which is 10% of the absorbed energy is emitted as radiation and a good resistance to humidity so far is the most efficient surface. The absorber made with this has the highest efficiency but is the most expensive type. Other types of surfaces with various efficiencies based on their absorptivity and emissivity and hierarchy of preference are shown in the Table 2.1[9].

Table 2. 1: Selective Surface Coatings and their Properties [9].

Selective Coatings	**Absorptance**	**Emittance**	**Absorptance/emittance**
Black chrome	0.93	0.10	9.3
Black Nickel on Polished Nickel	0.92	0.11	8.4
Black Nickel on galvanized Iron	0.89	0.12	7.4
CuO on nickel	0.81	0.17	4.7
Co_3O_4 on silver	0.90	0.27	3.3
CuO on Aluminum	0.93	0.11	8.5
CuO on anodized Aluminum	0.85	0.11	7.7
Sol chrome	0.96	0.12	8.0
Black paint	0.96	0.88	1.09

2.4. Factors Leading to Development of Evacuated Solar Collectors

Under warm and sunny climatic conditions, a flat-plate solar collector is found to be very efficient in absorbing the solar energy and transforming it to heat. During windy, cold and cloudy days, the efficiency becomes greatly affected. Low performance and system failure due to internal material deterioration could also happen as result meteorological influence such as moisture and condensation. In flat-plate collector, the angle of incidence also affects the performance of the flat panel. These are some of the inconveniences lead to development of an evacuated tube solar collector.

The evacuated tube collector is made up of a black copper heat pipe placed in a vacuum-sealed tube. At the top of each glass tube is a metal tip protruding and is attached to the pipe sealed inside the tube. This is called a condenser. A small quantity of fluid such as methanol is placed inside the pipe and when exposed to solar radiation, the fluid changes to vapor and

moves to the heat sink location around the condenser, releasing its latent heat , transforming back to liquid and the whole process keeps on repeating. Glycol or water flowing through the heat exchanger extracts heat from the collector's tube through the condensers and then circulates through another manifold (heat exchanger) and releases the heat to either a process or to water stored in a collector's storage tank. The schematic diagram of the evacuated heat collector is shown in the Figure 2.4.

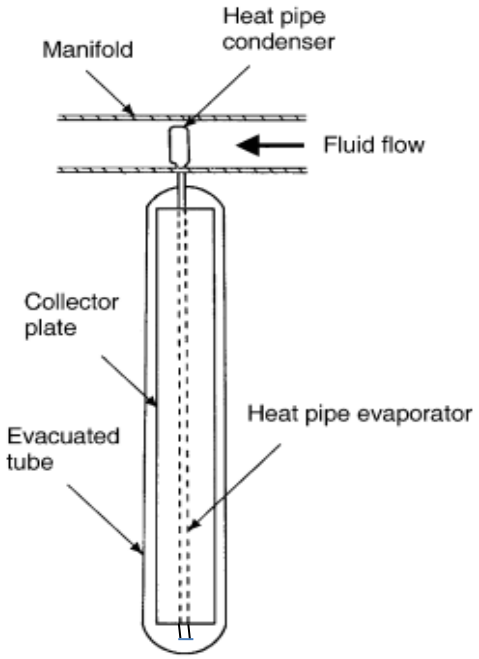

Figure 2.4: Schematic Diagram of Evacuated Tube Collector [10].

One unique feature of the evaporated tube collector is its ability to limit its temperature automatically, because no condensation or evaporation is possible above the phase-change temperature, thus the heat pipe gives inherent protection against freezing and overheating. It is also observed that an evacuated tube collector with a good convective suppressor and a selective surface performs effectively. The conduction and convection losses are also reduced by the vacuum envelope. At low incidence angle, the efficiency is very high [10].

.

CHAPTER THREE

DESCRIPTION OF A COMPLETE SOLAR WATER HEATING SYSTEM

3.1. Systems Using Flat Plate Collector

Solar water heating system (using flat plate collector as the absorber plate) is a system in which heat coming from the sun is captured and then transferred to a liquid placed in a storage tank. Trapping the solar thermal heat is achieved by means of a "greenhouse effect" in which both short wave radiations are transmitted and long wave radiation are reflected by an absorber's surface [11]

The solar water heating systems are classified based on the following characteristics:

- **Direct or Open Loop:** The water is directly heated while flowing through the absorber and then moves back to storage tank.
- **Indirect or Closed Loop:** The heat is transferred through a heat exchanger(with a heat carrying fluid inside such as water or glycol) from the collecor's absorber to the water in the storage tank without mixing with the heat exchange fluid.
- **Passive:** The heat is transferred by natural convection from collector to the water without influence of any external force.
- **Active:** The heat exchange fluid is forced to circulate in the system by using a pump [12].

3.1.1. Direct Pumped System

There are two types of the direct pumped system as outlined below:

3.1.1.1. Differential controller operated system

In a direct pumped system, water is circulated using a pump from a storage tank through a collector and back to the tank again. There is no heat exchanger involved where the heat is directly transferred to the water flowing through the collector and then flows back to the tank for usage.

The differential controller of the system is attached to two sensors for measuring temperature difference, one at the collector's outlet while the other at the position of the coldest water

stored in the tank. The pump is switched on when the temperature of the water in the collector $15^0F - 20^0F$ above the temperature in the storage tank. The pump is switched off when the temperature is below $3^0F - 5^0F$.

In order to provide protection against freezing, a freeze protection valve (flush - type) located close to the collector is let opened for the warm water to circulate through the collector when the temperature is very low and almost approaching freezing point. Freeze protection can also be achieved by automatically recirculating the warm water in the storage tank when the collector's temperature is approaching a freezing point.

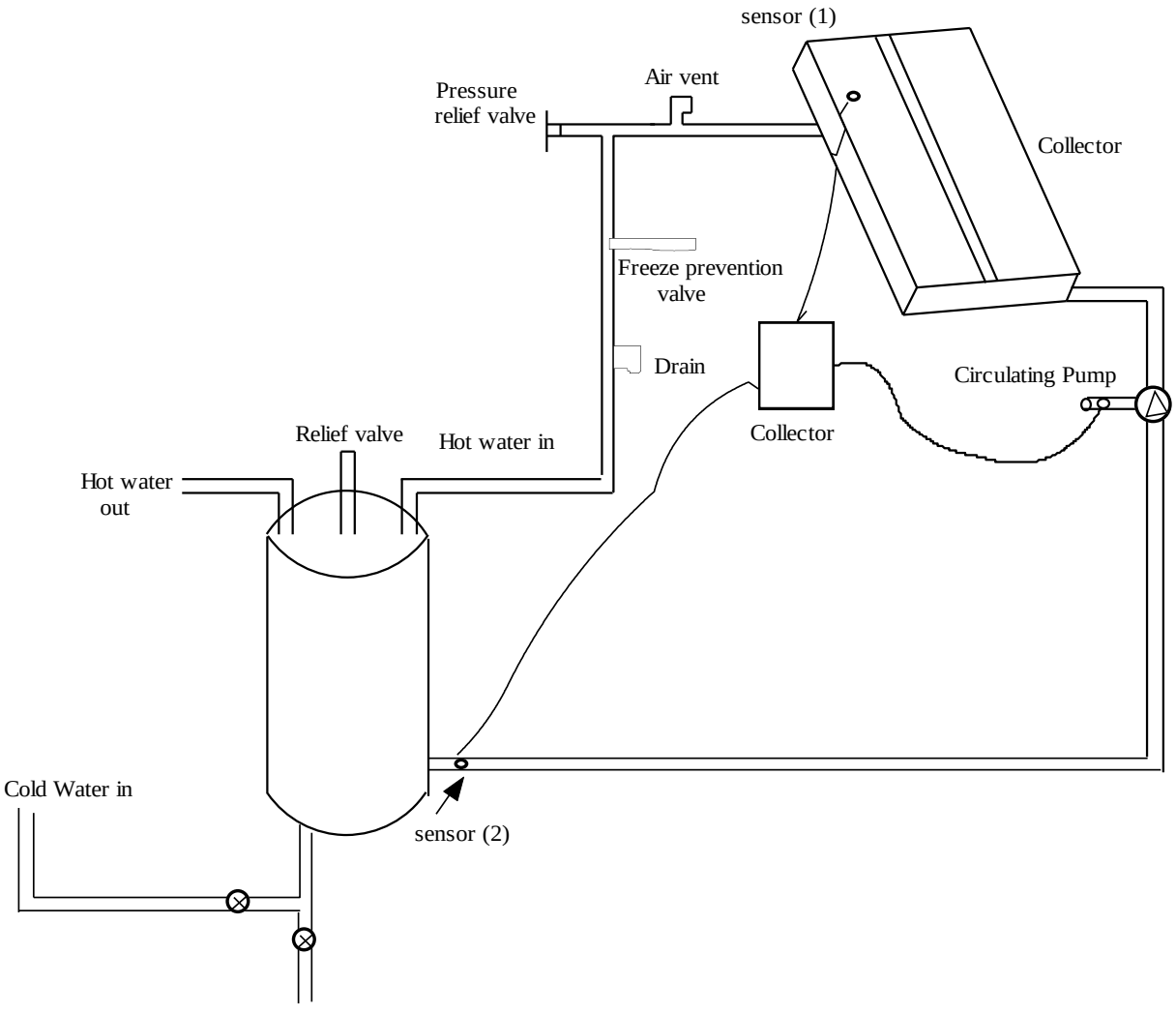

Figure 3.1: Typical Direct Pump System (with differential controller operation)

3.1.1.2. Photovoltaic Operated System

In this system photovoltaic panel is used to convert solar energy into electricity which supplies power to the dc pump and hence water is circulated through the collector and back to storage tank. This implies that water circulation through the collector is possible only during a shining day.

Efficient performance can be achieved only when there is matching between the dc pump and PV panel. The pump operation is dependent upon the available solar energy. It operates only when there is enough solar radiation for heating the collector and turns off when the solar energy is insufficient. Freeze protection is also provided by a thermally operated valve as in the case of differential controller operated system.

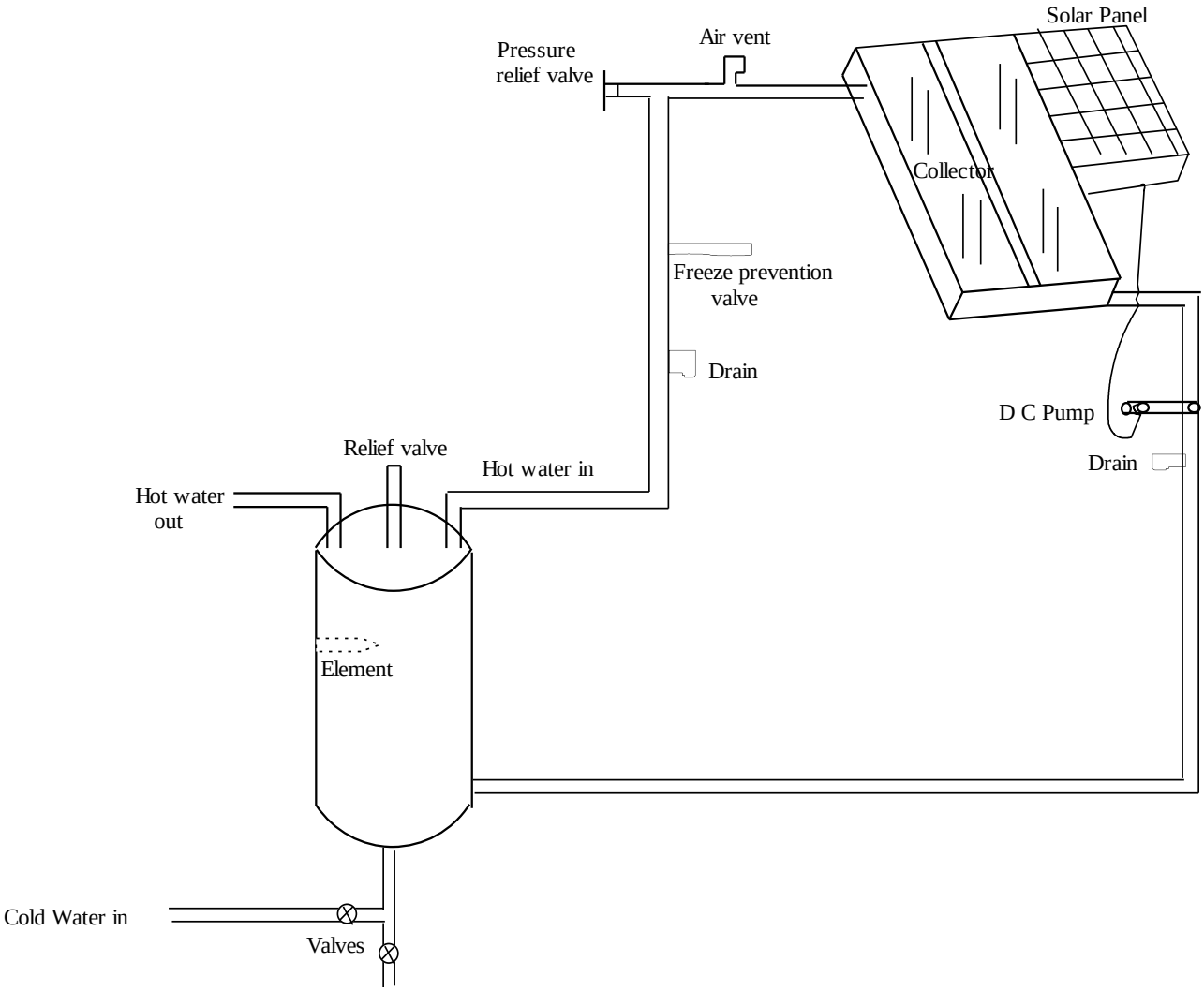

Figure 3.2: Direct System with Photovoltaic Powered – pump

3.1.2. Indirect Pumped System

In climates where freezing weather is frequent, an indirect pumped system is used. The water in the tank is not heated directly but an antifreeze solution (mostly a mixture of antifreeze and distilled water) circulating through the collector is used to transfer the heat to the water in the storage tank through a heat exchanger. If the exchange fluid is toxic, a double-walled exchange should be employed to prevent leakage and the exchanger is mostly located in the storage tank around the lower half.

A closed loop used to pump the heat exchange fluid through the collector consists of a tank, heat exchanger, the pump, collector and connecting piping. The heat exchanger can be placed either in the lower half of the storage tank in form of coil or wrapped around the tank. A controller attached to collector and the coldest part of the tank is used to determine appropriate amount of fluid flowing at a given time an when the circulation should be stopped [13].

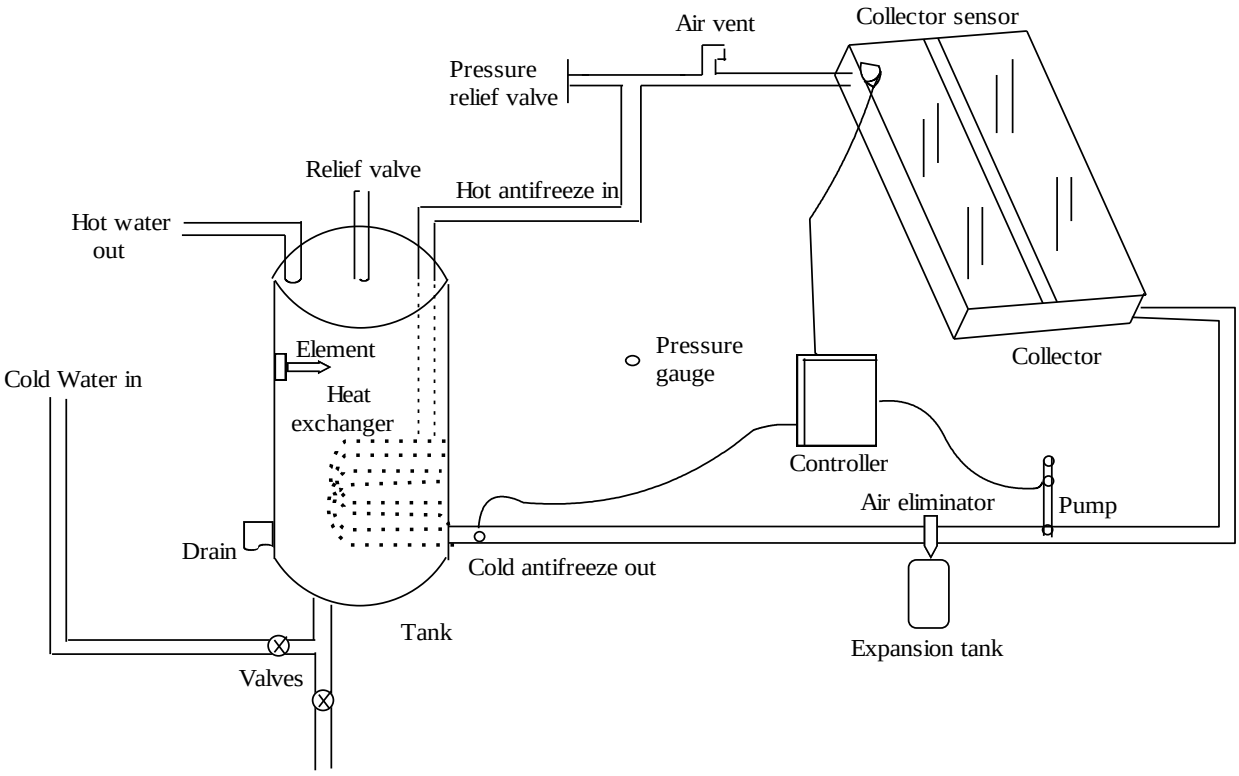

Figure 3.3: Indirect Pumped System using Antifreeze Solution

For a thirty gallon storage tank, about 7mm of a heat exchange coil of 20mm internal diameter of a standard copper pipe is needed in order heat the water using the solar heating system.

When a wrap-around heat exchanger is used, the major advantage is that there is no contamination of the domestic potable hot water by the antifreeze solution. However the system has several disadvantages such as the ones outlined below:

- All other components will be disabled if one component fails and there would be less design flexibility.
- Wrapping around the outside is mechanically not an easy task.
- The thermal contact between the heat exchanger pipe and the body of the tank is always poor.
- It needs good thermal insulation
- All the above make the system very labour intensive and hence too expensive [13].

3.1.3. Thermosiphon systems

In a thermo siphon system, the storage tank is installed at a position above the collector. When the water inside the flow-tubes of the solar collector is heated, it expands and becomes less heavy than the water in the storage tank. This will cause the water in the storage tank to flow and push the expanded water to move into the tank and thus heats the water inside the storage tank. As can be seen from the setup, neither a controller nor a pump is needed, because water is supplied directly from city water line and the heat transfer is by thermo siphoning [14].

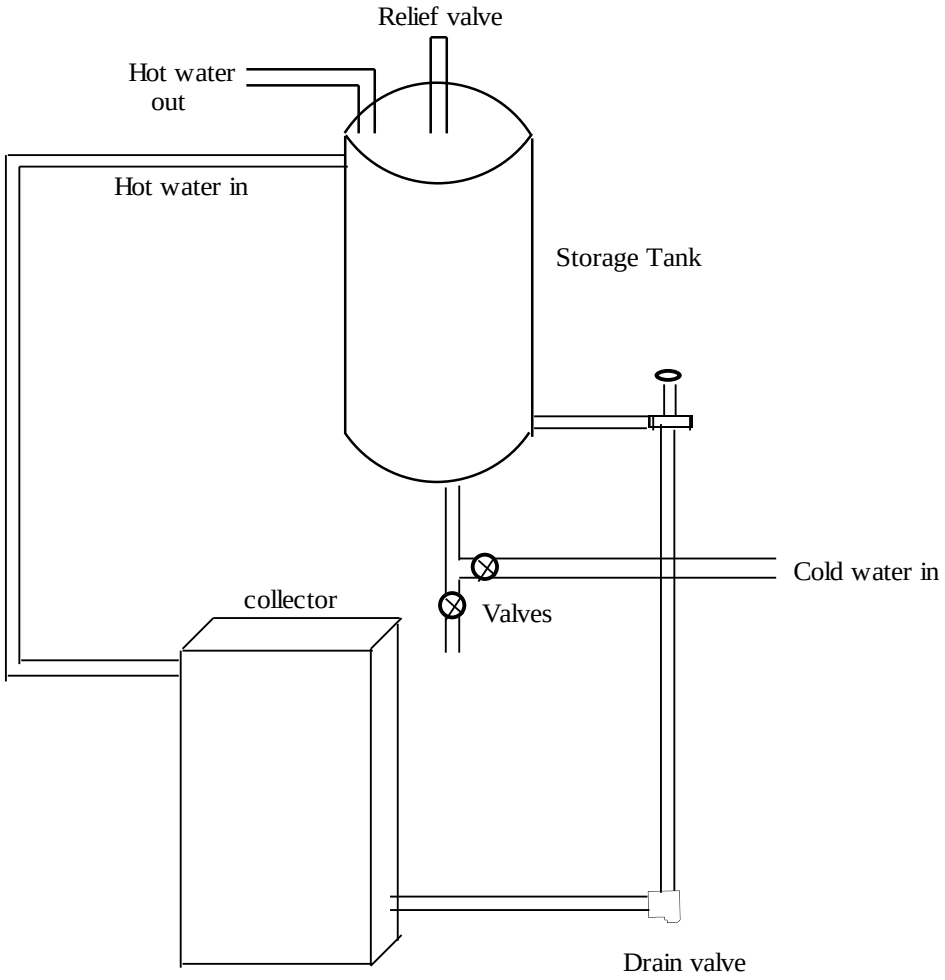

Figure 3.4: Thermo siphon System

3.1.2. Thermal Analysis Using Flat plate Collector

The efficiency of a solar collector i.e. the thermal performance or useful energy gain can be examined by making the following analysis. The allocation of the incoming solar thermal

energy on different parts of the collector panel is shown in Figure 3.5.

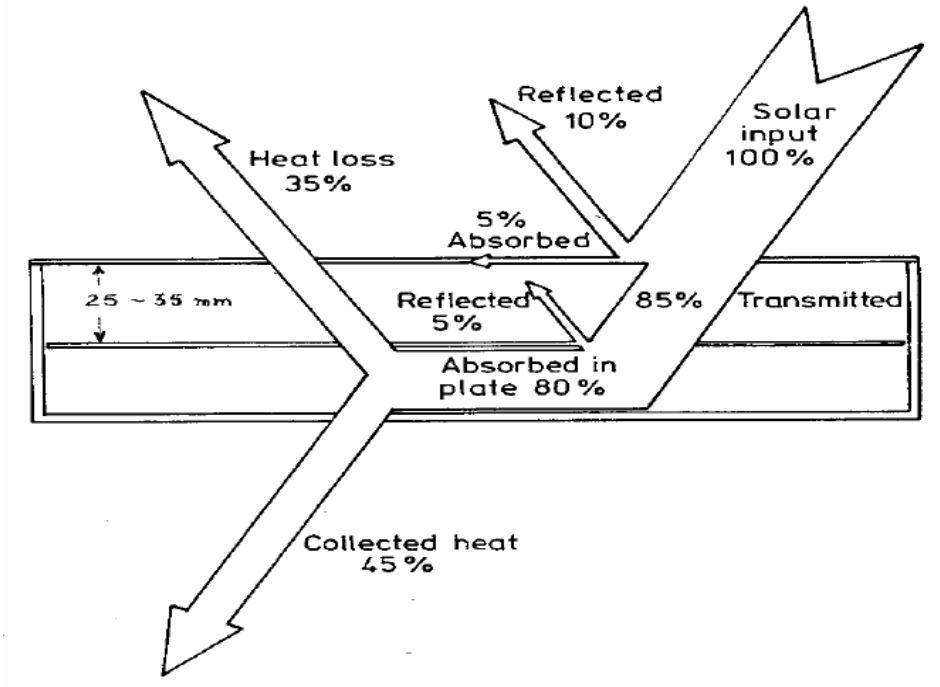

Figure 3.5: Energy Distribution on the Flat-Plate Collector Component

This analysis is carried out by considering the schematic of the collector system shown in Figure 3.5.

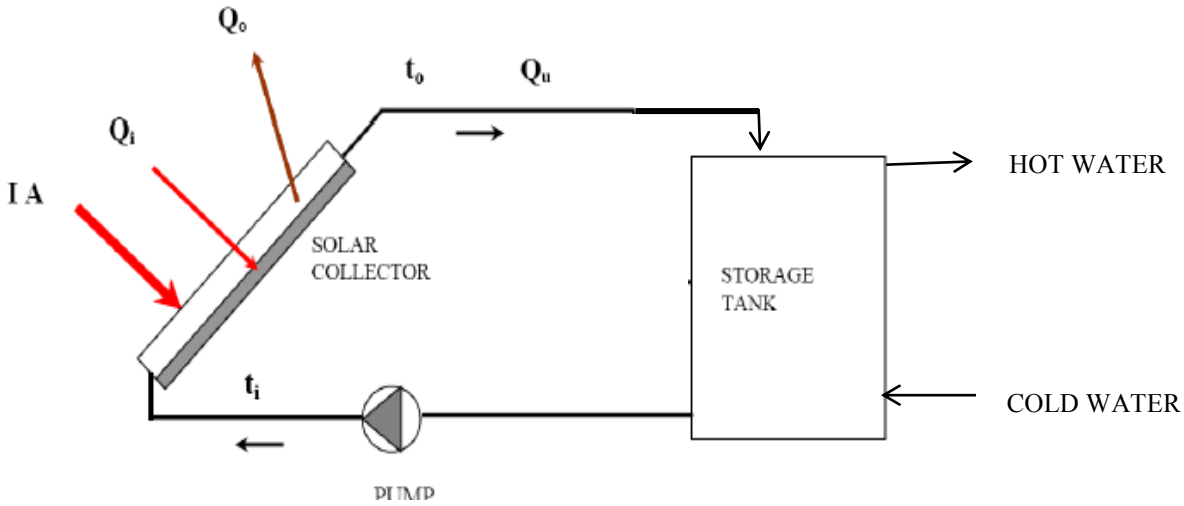

Figure 3.6: Schematic Diagram of the Collector System.

From the above figure, the amount of solar radiation which the collector receives is given as

$$Q_i = I.A \tag{3.1}$$

Where

$Q_i =$ Collector heat input

$I =$ Intensity of solar radiation

$A =$ Collector surface area

As seen from figure 2.3 some portion of the solar radiation is lost either as reflection back to sky or absorption by the glazing while the rest transmitted in form of short waves reaching the absorber plate. To know the exact quantity of the solar radiation being absorbed, then a new equation is obtained as follows by multiplying with a factor.

$$Q_i = I(\tau\alpha).A \tag{3.2}$$

$\tau\alpha =$ Multiplying factor

$\tau =$ Rate of transmission of the cover

$\alpha =$ Absorption rate of the absorber

The heat lost (Q_O) due to convection and radiation from the absorber as a result of rise in temperature is given as

$$Q_O = U_L A(T_c - T_a) \tag{3.3}$$

$U_L =$ Overall heat transfer coefficient

$T_c =$ Collector temperature

$T_a =$ Ambient temperature

The useful energy extracted by the collector can be expressed as

$$Q_u = Q_i - Q_o = I\tau\alpha.A - U_L A(T_c - T_a) \tag{3.4}$$

The amount of heat passed through the fluid can also be used to measure the rate of heat extraction from the collector.

$$Q_u = mcp(T_o - T_i) \tag{3.5}$$

$cp =$ Specific heat capacity of the fluid

There is need to define the relationship between actual energy gain and useful energy gain of the collector called "the collector heat removal factor (F_R)" when the whole surface were at the fluid inlet temperature.

$$F_R = \frac{mcp(T_o - T_i)}{A[I\tau\alpha - U_L(T_i - T_a)]} \tag{3.6}$$

The actual useful energy gain used in measurement of collector energy gain is called " Hottel whillier – Bliss equation "

$$Q_u = F_R A[I\tau\alpha - U_L(T_i - T_a)] \tag{3.7}$$

With regard to previous analysis of the heat flow the collector thermal efficiency over a particular period of time:

$$\eta = \frac{\int Q_u dt}{A\int Idt} \tag{3.8}$$

The collector thermal efficiency at any instant is:

$$\eta = \frac{Q_u}{AI} \tag{3.9}$$

This can further be expressed as

$$\eta = \frac{F_R A[I\tau\alpha - U_L(T_i - T_a)]}{AI} \tag{3.10}$$

$$\eta = F_R\tau\alpha - F_R U_L\left(\frac{T_i - T_a}{I}\right)$$

(3.11)

The efficiency is a linear function of three parameters which are ambient air temperature (T_a), solar irradiance (I) and fluid inlet temperature (T_i) if F_R, τ, α,u_L are assumed to be constant.

When the collector efficiency is plotted against $(T_i - T_a)/I$, a straight line with negative slope ($-F_R$, u_L) representing the rate of heat loss is obtained as shown in the Figure 3.9 below:

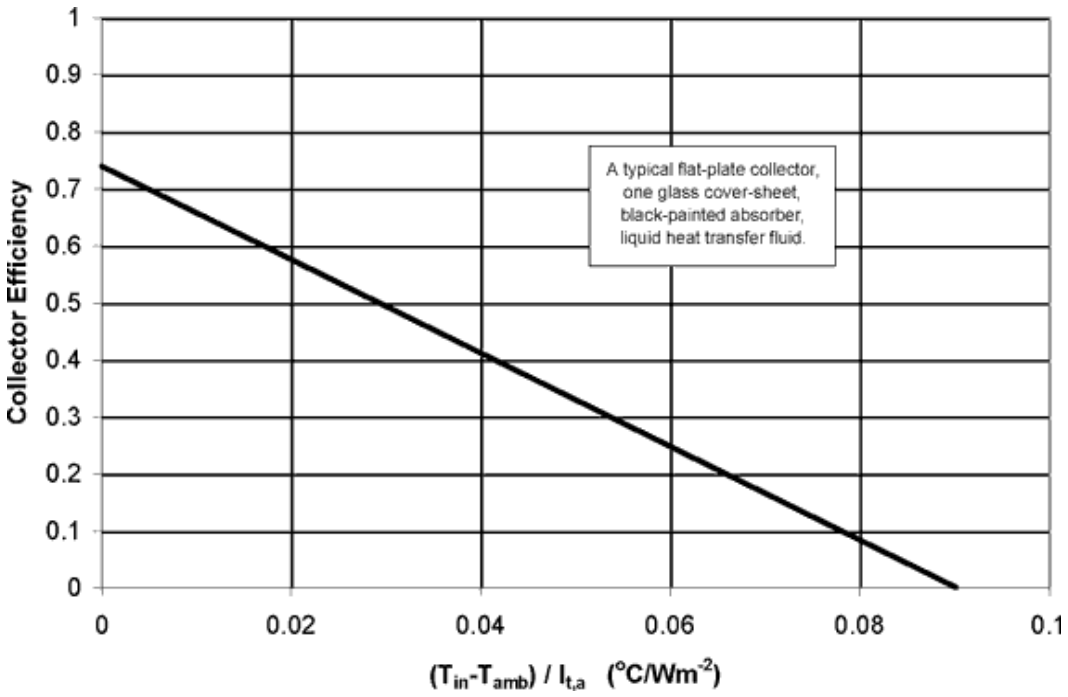

Figure 3.7: A Graph of Collector Efficiency against $(T_i - T_a)/I$.

From the figure above, the maximum efficiency occurs where the ambient temperature is equal to the fluid temperature and intercept is zero. The other point of interest is the intercept at the x – axis when the efficiency is zero. Under this condition there is no heat removal from the collector and the temperature of the absorber rises until it is equal to the heat loss. The temperature can further rise causing the fluid boiling or in some absorbers, the plate will be melting [15].

3.2. System using Evacuated Tube Collectors

All the systems that were described using flat plate collectors are the same for the evacuated tube collector systems except that the absorber plate is made up of the evacuated tube. The thermal analysis of the collector is carried out below:

3.2.1. Thermal Analysis of Evacuated Tube Collector

The analysis is carried out by considering the figure 3.10 below which shows a cross - section of a single evacuated with the fluid conduit and the absorber.

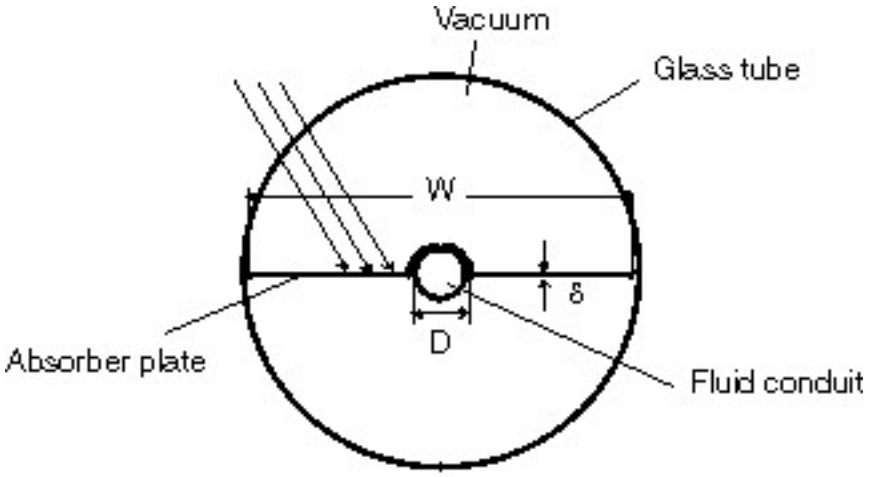

Figure 3.10: A cross-section of Evacuated Tube Collector

For the figure 3.10, to be modeled, some simple assumptions are made below:

1. The situation must be steady state.
2. The temperature of the absorber plate along the radial direction is much higher than in the axial direction, the sheet of the absorber plate should be of very conduction and the thickness should be small.
3. The properties should not be dependent on temperature.
4. The absorber plate shading should be negligible.
5. Dirt and dust are negligible on the glass tube.

The useful energy is expressed as

$$Q_u = A_c F_R [S - U_L (T_i - T_a)] \tag{3.12}$$

Where

A_c = collector area
F_R = collector heat removal
S = solar radiation on the absorber plate
T_i = inlet temperature
T_a = ambient temperature

F_R = collector heat removal factor

F_R is given as follows :

$$F_R = \frac{\dot{m}c_p}{A_c U_L}[1 - e^{-(\frac{A_c U_L F'}{\dot{m}c_p})}] \tag{3.13}$$

Where

$\dot{m}$ = mass flow rate through the fluid conduit
c_p = specific heat capacity of the fluid
F' = collector efficiency given by the following equation

$$F' = \frac{\frac{1}{U_L}}{w[\frac{1}{U_L[D + (w - D)F]} + \frac{1}{c_b} + \frac{1}{\pi D_i h_{f,i}}]} \tag{3.14}$$

Where

D = outside diameter
D_i = inside diameter
w = is the width of the absorber plate
c_b = bond conductance between the conduit and absorber plate
$h_{f,i}$ = heat transfer coefficient between the fluid and the tube wall
F = Fin efficiency

$$F = \frac{[\tanh m(W - D)/2]}{m(W - D)/2} \tag{3.15}$$

Where m is given as

$$m = \sqrt{U_L / k\delta} \tag{3.16}$$

where

k = thermal conductivity of the absorber plate

δ = plate thickness

The overall heat coefficient of the evacuated tube collector is developed as follows based on the fact that the conduction and convection heat transfer from the absorber plate to the glass tube is ignored. At certain location on the plate where the temperature is T_p, the absorbed solar energy S is distributed as the useful energy gain and thermal losses through the glass tube. The loss due to radiation from the both sides of the absorber plates to the glass tube is given as:[7]

$$Q_{loss} = \frac{2\sigma(T_p^4 - T_g^4)}{\frac{1-\varepsilon_p}{\varepsilon_p A_c} + \frac{1}{A_p} + \frac{1-\varepsilon_g}{\varepsilon_g A_g}} = h_g(T_g - T_a) + \varepsilon_g \sigma(T_g^4 - T_s^4) \tag{3.17}$$

Where

ε_p = emissivity of the absorber plate

ε_g = emissivity of glass tube

h_g = convection heat transfer coefficient from the glass tube to ambient air

A_p = area of the absorber plate

A_g = area of the glass tube

σ = stefan-boltzman constant

T_g = temeperature of the glass tube

3.3. Comparison of Flat Plate and Evacuated Systems with Regard to Efficiency

The efficiency of the two collectors is compared in the following Table 3.1 [18]

Table 3. 1 : Comparison of Flat Plate and Evacuated Systems With Regard To Efficiency [18]

Evacuated Tube Collectors	Flat-plate solar panels
Due to the sealing of the solar collector inside a glass tube which is evacuated, heat losses due to conduction and convection are eliminated and the performance does not change throughout the lifespan of the collector.	There are heat losses occurring between the cover pane and the absorber of the collector , especially during windy and cold days. The performance is affected by corrosion due to condensation.
There is no water entering into the collector as heat-pipe with extremely efficient heat conduction is used.	The water is circulated inside an insulated area which may encounter some flow restriction as a result of air lock and is vulnerable to corrosion and leakage.
The thermal flow is unidirectional as in the operation principle of thermal diode from collector to water and never flows in reverse direction.	When the collector is colder than the temperature of the water, the absorbed heat can be robbed by the Flat-plate collector.
They can be easily maintained and installed as individually sealed collector tubes are integrated into the system during installation.	Installation and maintenance are not easily carried out, because the entire panels are installed collectively by hoisting them onto the roof, and when leakage is found, the whole collector should be shut down and then removed for maintenance.
There is freedom in aesthetic and architectural setup due to insensitivity of the collector to placement angle.	The collector has to be accurately elevated and exposed to south for maximum energy collection.

CHAPTER FOUR

PROBLEM WITH OPERATION OF BANG ON BANG OFF CONTROL SYSTEM WITH REGARD TO EFFICIENCY

As already stated before, this type of controller has only two stable states, either fully on or fully off and the major problem with the operation of the controller is its oscillatory nature and this makes it unsuitable for applications where accurate temperature control is needed, because it can over shoot either below or above the set point, and thus the maximum efficiency of the system cannot be derived. For this reason a more temperature sensitive control is needed to take care of the imperfections encountered in bang on bang off controller [19] [20].

The other problem is its constant pumping speed. So the removal of the collected heat is not as efficient as it should be. For example, when the incoming radiation of the sun's energy is low, then the pumping speed does not need to be high. A slower speed will be more appropriate.

On the other hand, when the intensity of the incoming solar rays is high, then the collected heat must be removed as fast as possible. Hence a faster pumping will be most appropriate. As a result a Bang on Bang off system cannot be as efficient as it should be [21].

CHAPTER FIVE

PROPOSED DESİGN FOR THE NEW TEMPERATURE SENSİTİVE CONTROL SYSTEM

5.1. Thermal Power Transducer

The design was based on the hardware requirements for the optimal controller as shown in Fig. 5.1. Four main elements were required as shown in Figure 5.1.

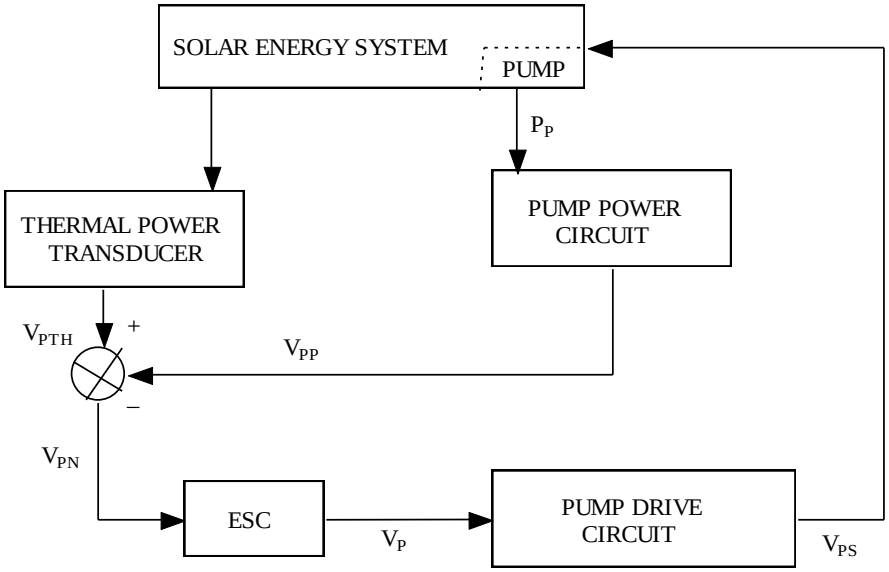

Figure 5.1: Thermal Power Transducer.

This is required to provide a D.C voltage, V_{pth}, proportional to thermal power, P_{TH}. The thermal power being transferred to fluid (water) travelling at mass flow rate, $\dot{m}$ in kg/s is given in Equation (5.1).

$$P_{TH} = \dot{m}c(\Delta T) \tag{5.1}$$

Where,

c = Specific heat capacity of the fluid J/kg.k

$\Delta T = T_o - T_s$ = temperature differential across collector ($^o c$)

Thus in order to obtain V_{pth}, we require;

- Temperature Transducers: Providing a voltage $V_{\Delta T}$, proportional to pump power.
- Flow Transducer: Providing a voltage , proportional to $V_{\dot{m}}$

- An Analog Multiolier: To multiply $V_{\dot{m}}$ and $V_{\Delta T}$, giving a voltage

$$V_{pth} = K_1 V_{\dot{m}} V_{\Delta T} \tag{5.2}$$

Where K_1 can be adjusted as required.

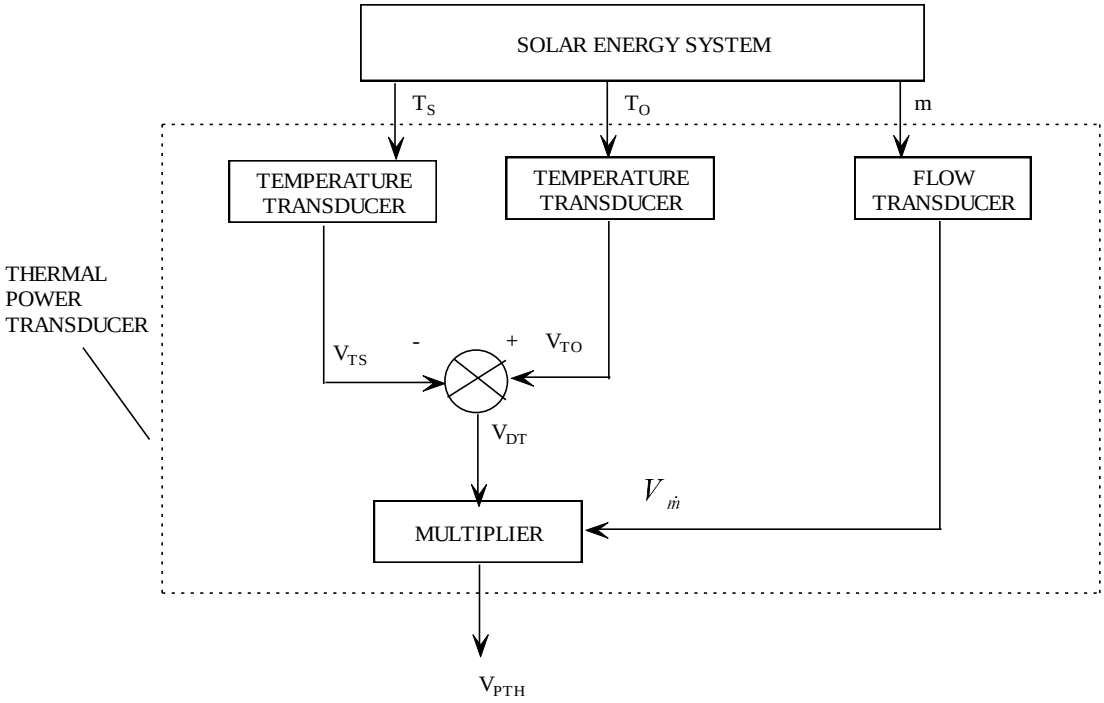

Figure 5.2: A detail of thermal power transducer

5.2. Pump Power Circuit

This is required to provide a D.C voltage, V_{pp} , proportional to pump power, P_p .

P_p = (voltage across pump) $\times$ (current to pump)

The design requirement is therefore, as shown in Fig 5.3

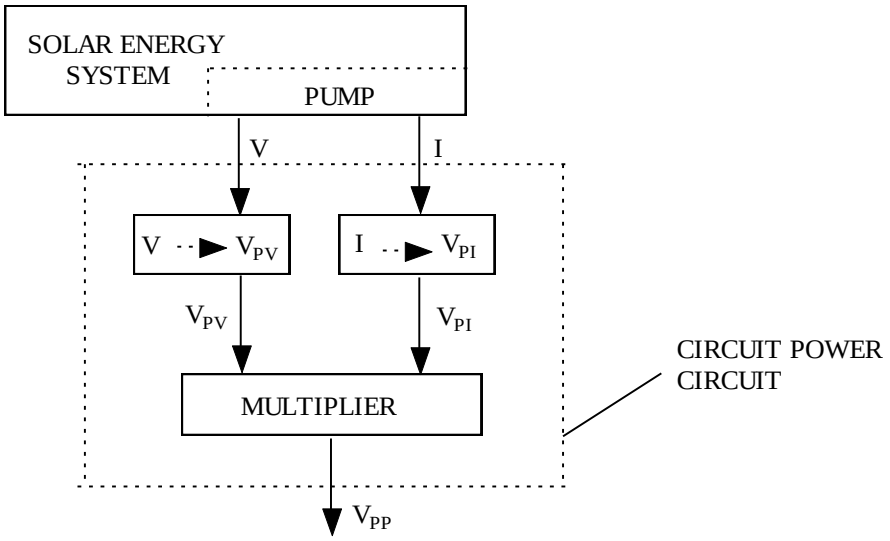

Figure 5.3: A detail of pump power transducer

- A small D.C voltage, V_{pv}, proportional to the large mains – derived D.C pump voltage, V
- A small D.C voltage, V_{PI}, proportional to the pump current, I.
- A Multiplier to give

$$V_{pp} = K_2 V_{PV} V_{PI} \tag{5.3}$$

Where K_2 is a constant to be selected.

5.3. The ESC

This is the intelligence of the control system.

5.4. The Pump Drive Circuit

In this circuit, the output of the ESC (a small voltage V_F, typically 2 volts) is used to control the mains – derived D.C voltage across the motor of the pump.

A phase – controlled rectification circuit was envisaged, at this stage, to supply the pump with an average D.C voltage, V_{PS}, proportional to V_F.

5.5. Development

The solar energy system in rich view, for which it is anticipated the optimal controller will eventually be used, could not be used in the laboratory development of the aforesaid controller. Thus a simulation of the system can be constructed in the laboratory. This is shown in a photograph in the schematic diagram of Fig. 5.4.

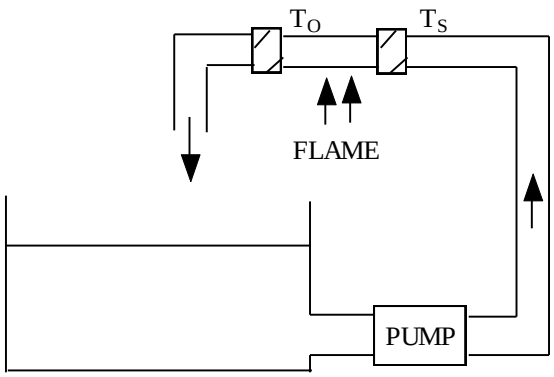

Figure 5.4: Simulation of the Solar Collector System.

In the simulation, the solar panel is represented by a copper tube (insulated at both ends), which is heated directly using a gas flame. This simulates the photo thermal process in a real collector. A centrifugal pump was used, driven by a universal motor supplied with rectified mains voltage. The motor is to be rated 100 watts.

5.5.1. Thermal Power Transducers

5.5.1.1. Temperature Transducers

Platinum resistances, R_1 and R_2 , attached to pipe fittings were used to detect the temperatures T_S and T_o.

For R_1

$$R_1 = K_1[1+T_S\alpha] \tag{5.4}$$

Where

K_1 = some constant for R_1

α = the resistance temperature coefficient for platinum

Similarly

$$R_2 = K_2[1 + T_o\alpha] \tag{5.5}$$

Thus

$$T_o - T_S = K_A'[R_2 - K_B'R_1] \tag{5.6}$$

Where

K_A', K_B' are constants.

If a constant current source passes a current, I_c through both R_1 and R_2, then the resistances are proportional to the voltages across them.

Thus

$$\Delta T = T_o - T_S = K_A[V_2 - K_B V_1] \tag{5.7}$$

Where

K_A and K_B are constants.

And hence,

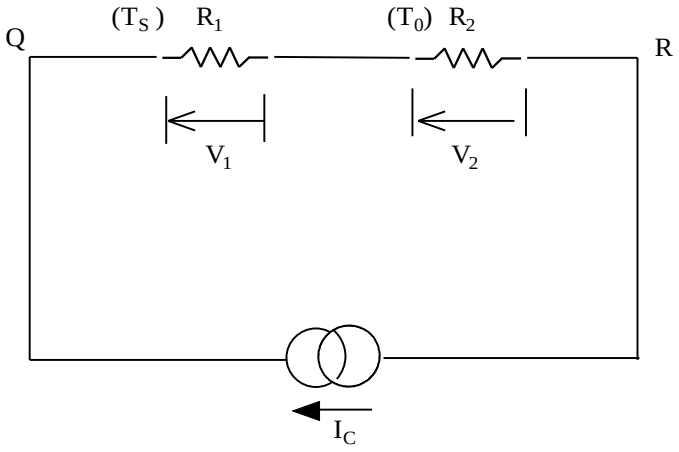

Figure 5.5: A Schematic diagram of the Temperature Transducers

$$V_{\Delta T} = K_{\Delta T}[V_2 - K_B V_1] \tag{5.8}$$

The circuit required to implement this equation is shown in block form in Fig. 5.6. The differential amplifier, gain and subtraction are easily implemented using simple operational amplifier configurations.

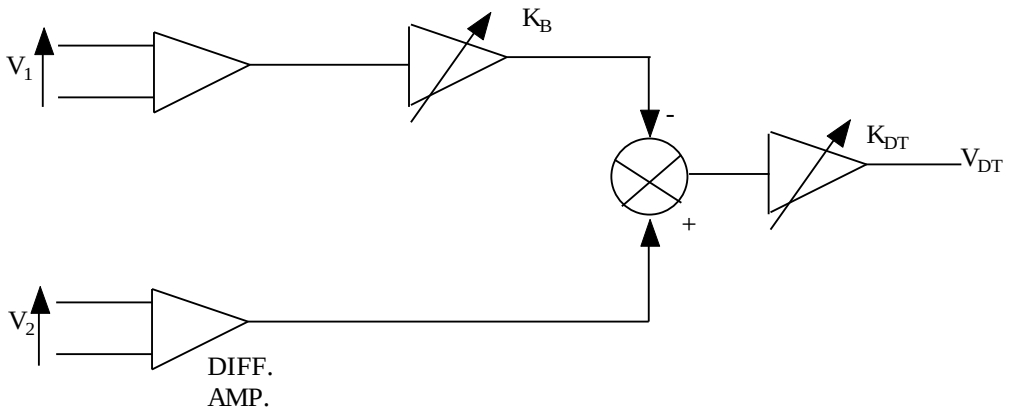

Figure 5.6: A Circuit for determining $V_{\Delta T}$.

The resistor in the gain element K_B can be adjusted while both platinum resistances are at the same temperature so as to give a zero output, $V_{\Delta T}$. K_B Should then be left fixed. $K_{\Delta T}$ may then be adjusted to give some suitable volt/K for the output, typically 0.5volt/K. 0.3 Ω/K is expected to the increase in temperature.

The value of R_1 and R_2 is approximately 100Ω. It is necessary, therefore that:

1. Differential amplifier inputs are taken at the resistances themselves and not at , for example, points Q and R above, as lead resistances is significant.
2. The input resistance of the differential amplifier is given by :

$$\frac{R_{IN}\Omega}{100\Omega} >> \frac{100\Omega}{0.3\Omega} \qquad (5.9)$$

R_{IN} of $1M\Omega$ was chosen for the differential operational amplifiers.

In this way an accurate measurement of V_1 and V_2 and hence $V_{\Delta T}$ is possible.

5.5.1.2. Flow Transducer

The flow transducer used was one which gave a square wave output (between 12 volts supply rail and ground) whose frequency was proportional to the flow.

The basic principle of operation was as follows:

A metallic fin, set revolving by the flow of water, is shaped so that light from a fixed light emitting diode is reflected onto fixed photodiode for some fraction of one fin revolution.

Thus each time the fin passed the L.E.D, a square pulse was detected by the photodiode. The faster the fin revolved, the more pulses detected per second.

A frequency to voltage converter converted the square wave into the required D.C voltage, .

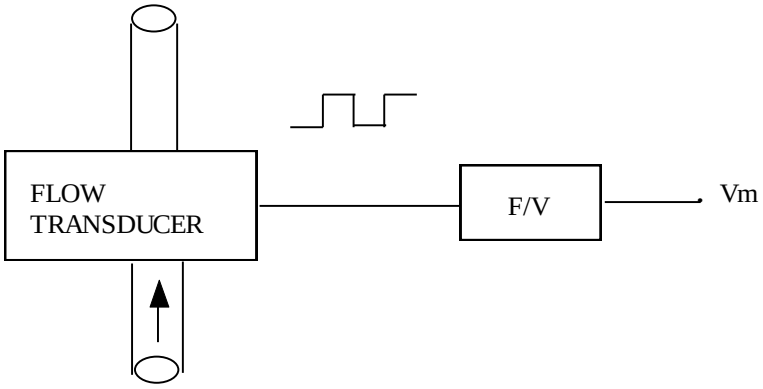

Figure 5.7: A Schematic diagram of Flow Transducer

The fully detailed circuit is shown in Figure 5.8

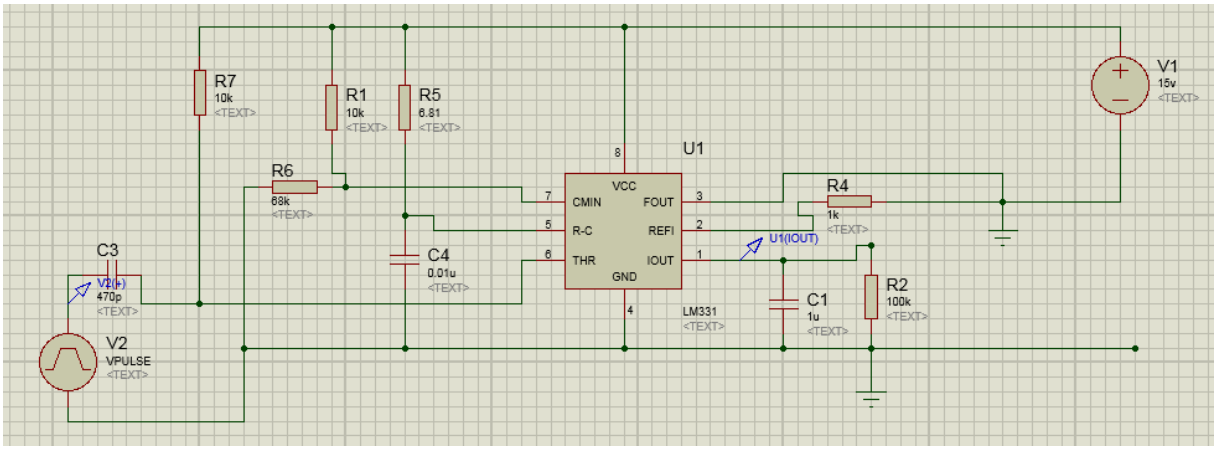

Figure 5.8: A Circuit diagram of Flow Transducer [22]

When the frequency is set at 1 kHz, the output of the frequency to voltage converter is about 11.5v at the set values of the circuit components, as shown in the figure 5.9.

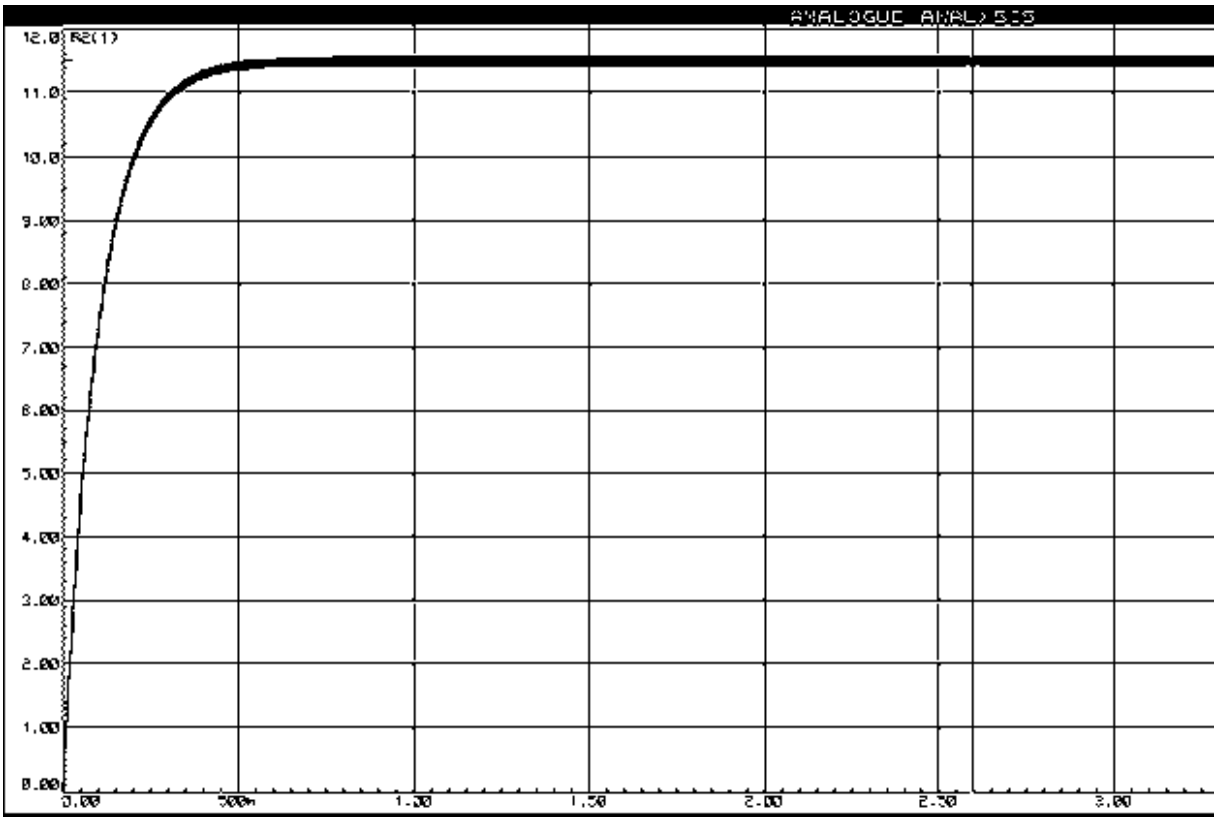

Figure 5.9: Output of the Flow Transducer Circuit at a f = 1KHz.

When f = 15Hz, the average output is 400mV.

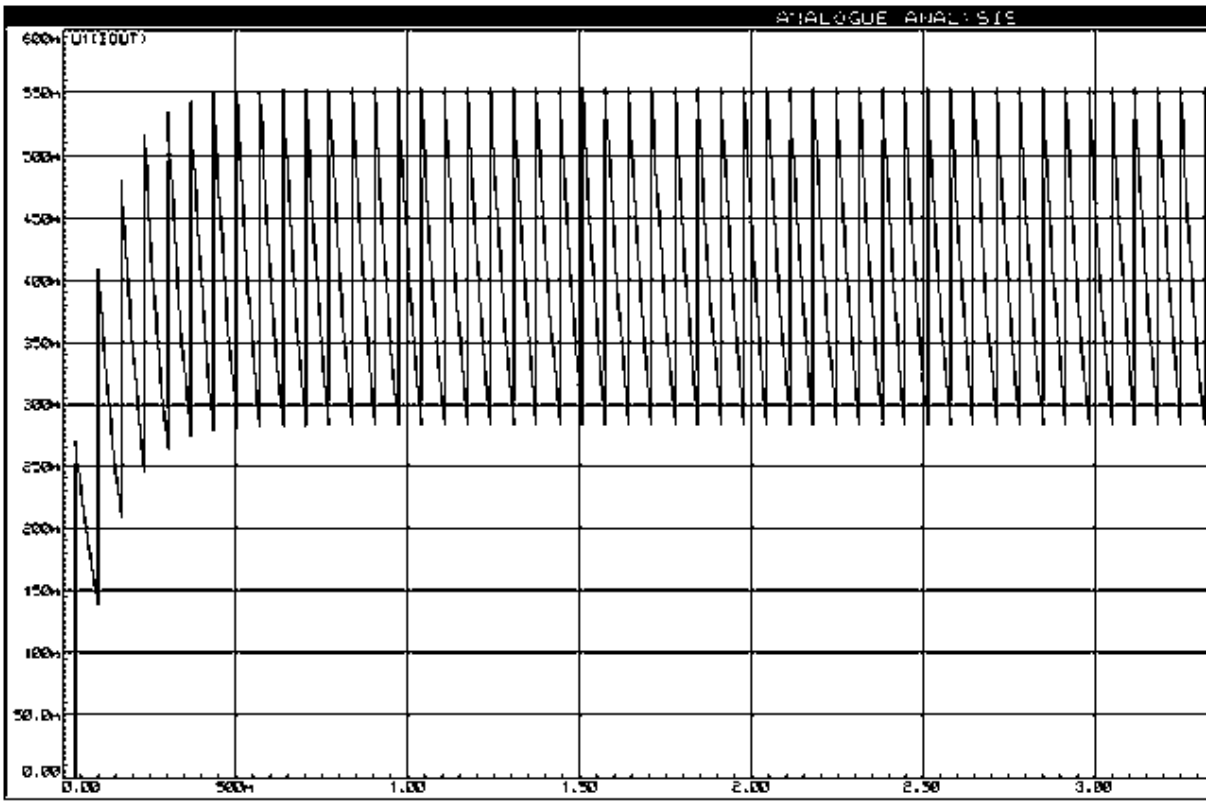

Figure 5.10: Output of the Flow Transducer circuit at a f = 15Hz.

5.5.1.3. Analog Multiplier

As no commercial analogue multiplier was available, it was necessary to design one. The basic circuit used is illustrated in Fig. 5.11.

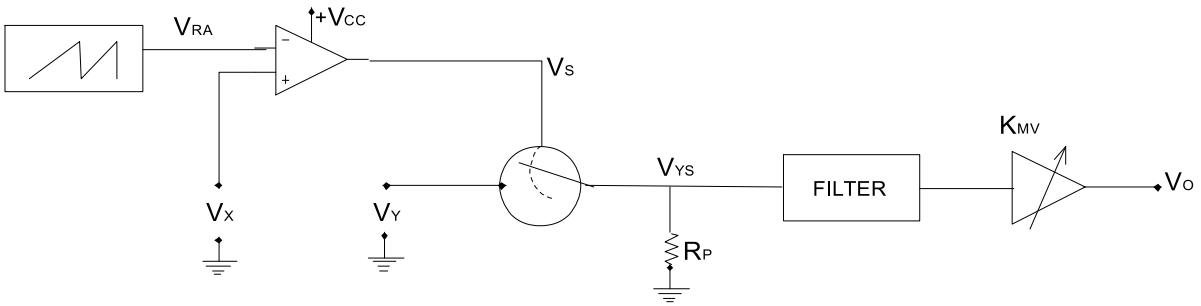

Figure 5.11: Schematic of the Analog Multiplier Circuit

The principle employed is that a square wave, V_{YS} be derived from V_X and V_Y , the two voltages to be multiplied, so that the amplitude of the square wave is equal V_Y to and its width proportional to V_X .

Both a ramp voltage and V_X are fed into a comparator. The output V_S is a square wave whose width is proportional to the ramp voltage, V_{RA} . This fraction is in turn proportional to V_X itself. This is clear from fig 5.12.

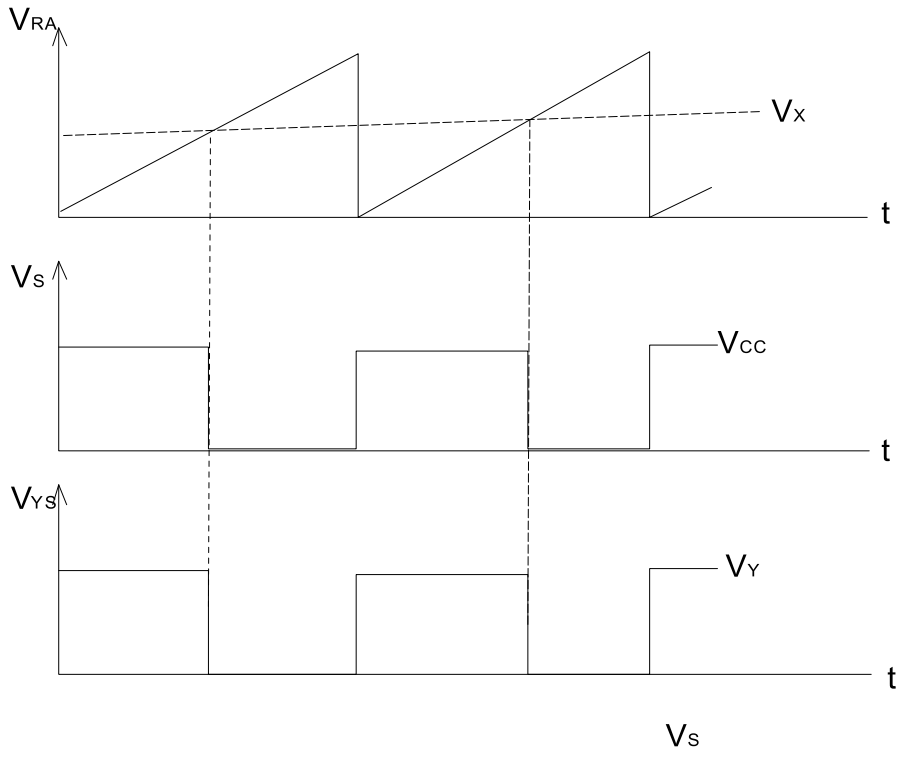

Figure 5.12: A Sample of Analog Multiplier Circuit Output

V_S is applied to a voltage controlled solid state switch which switches V_Y through to V_{YS} when V_S is high is high. When V_S is low, the switch is open and V_{YS} is pulled down by R_P to ground. Hence the waves form of V_{YS} in Fig. 5.12.

Now, the width of the square wave pulse of V_{YS} is proportional to V_X and the amplitude of V_{YS} is proportional to V_Y .

Thus the area V_{YS} under is proportional to V_X , V_Y . Hence by filtering V_{YS} , the output V_o is given by:

$$V_o = K_{MU} K V_X V_Y \tag{5.10}$$

K_{MU} Can be adjusted and K is a fixed constant.

5.5.1.4. Ramp Generator

The ramp voltage is generated using the circuit in Fig. 5.13.

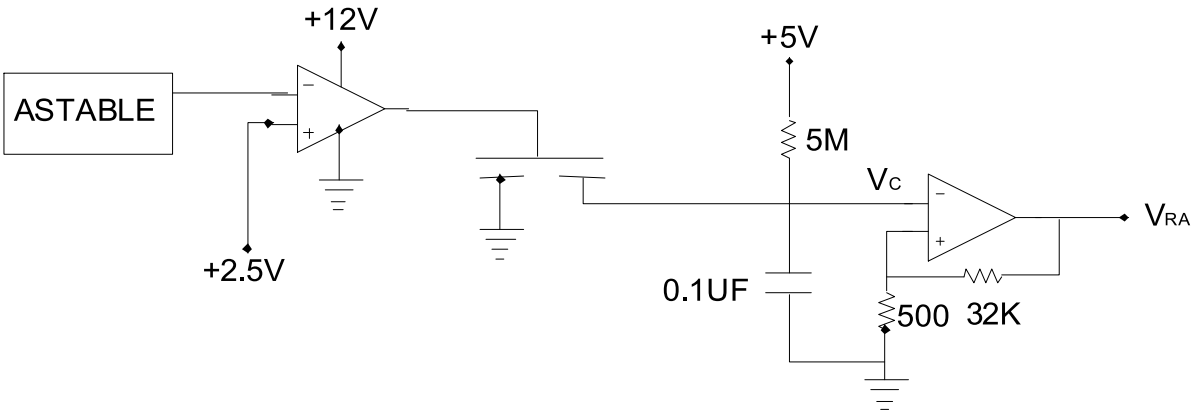

Figure 5.13: Ramp Generator Circuit.

The output of the astable is for 12ms and zero for 0.8ms of every period of 12.8ms. the switch is closed for 0.8ms of every period. The 0.1uF capacitor will, therefore, charge up for 12ms and discharge fully in 0.8ms of every period. Thus, provided the capacitor charges linearly with time, will be a ramp voltage, 12.8ms. With $R = 5M\Omega$, $RC >> 12.8ms$ and thus linear charging is assured. Since in 12.8ms, the capacitor will have charged to only 118mv, a gain element is required to ensure the peak of the ramp is equal to the maximum value that will take (7.5 volts approximately).

5.5.1.5. Filter

A simple RC filter is used with $RC = 0.82$ seconds. This ensures that $RC >> 12.8ms$ and hence the multiplier output is a D.C voltage.

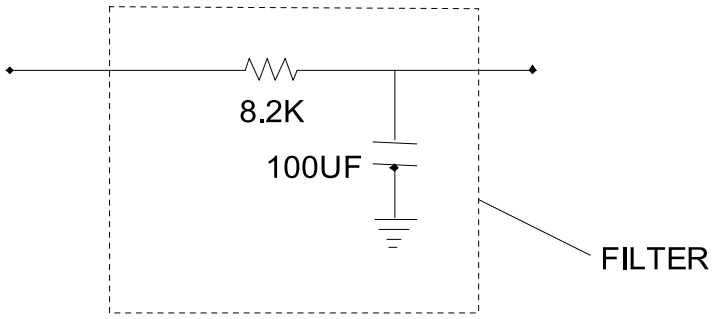

Figure 5.14: A Filter Circuit

The output ripple is 0.2%.

A full circuit of the multiplier is shown in figure 5.15All elements required to obtain have now been completed.

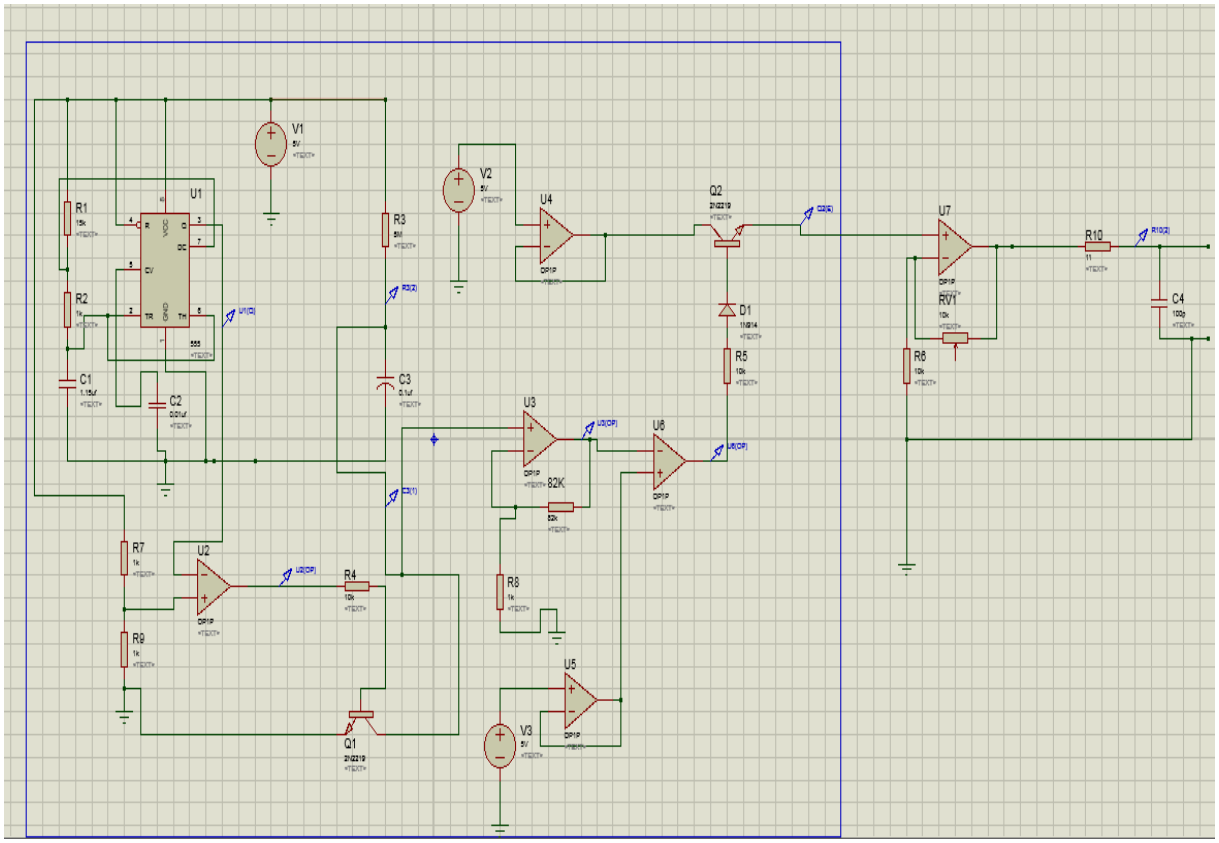

Figure 5.15: Analog Multiplier Circuit [23][24]

The output of the ramp generator is as shown with voltage of approximately 140mv

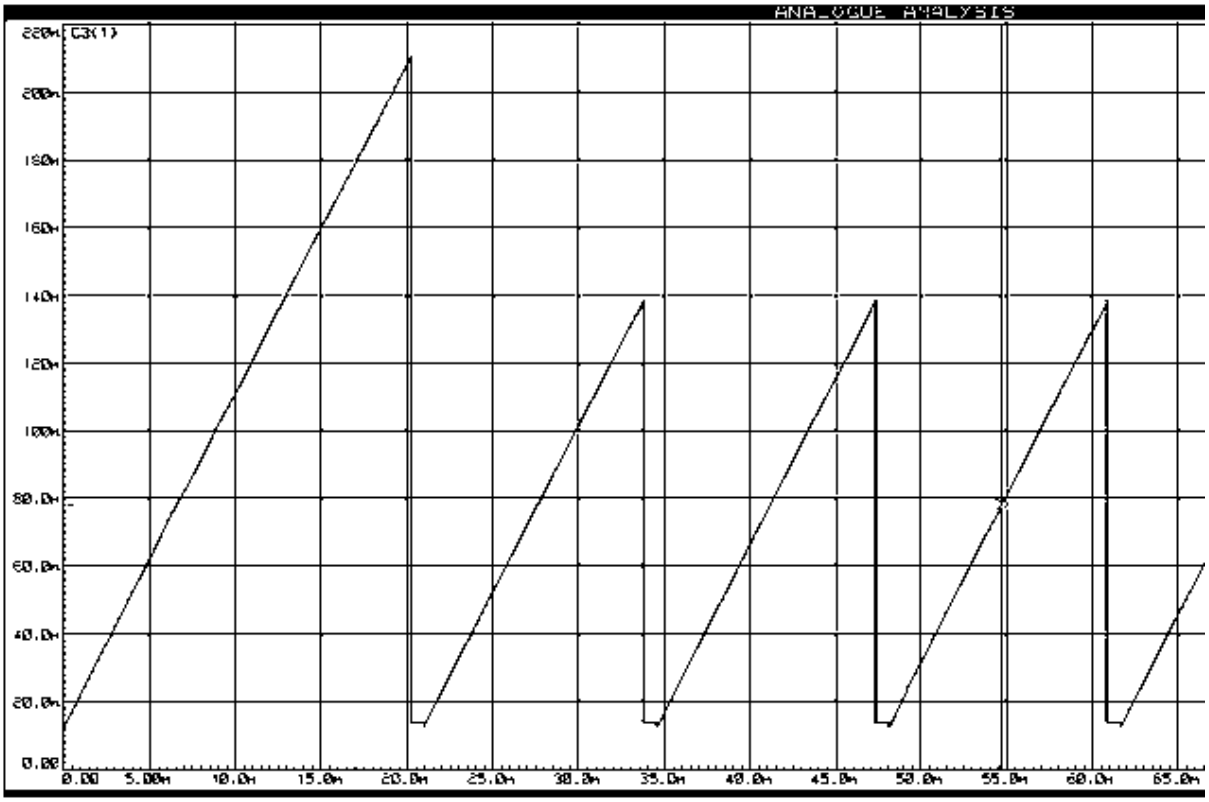

Figure 5.16: Ramp Generator Output before Amplification

After amplification the output is about 10v as shown below:

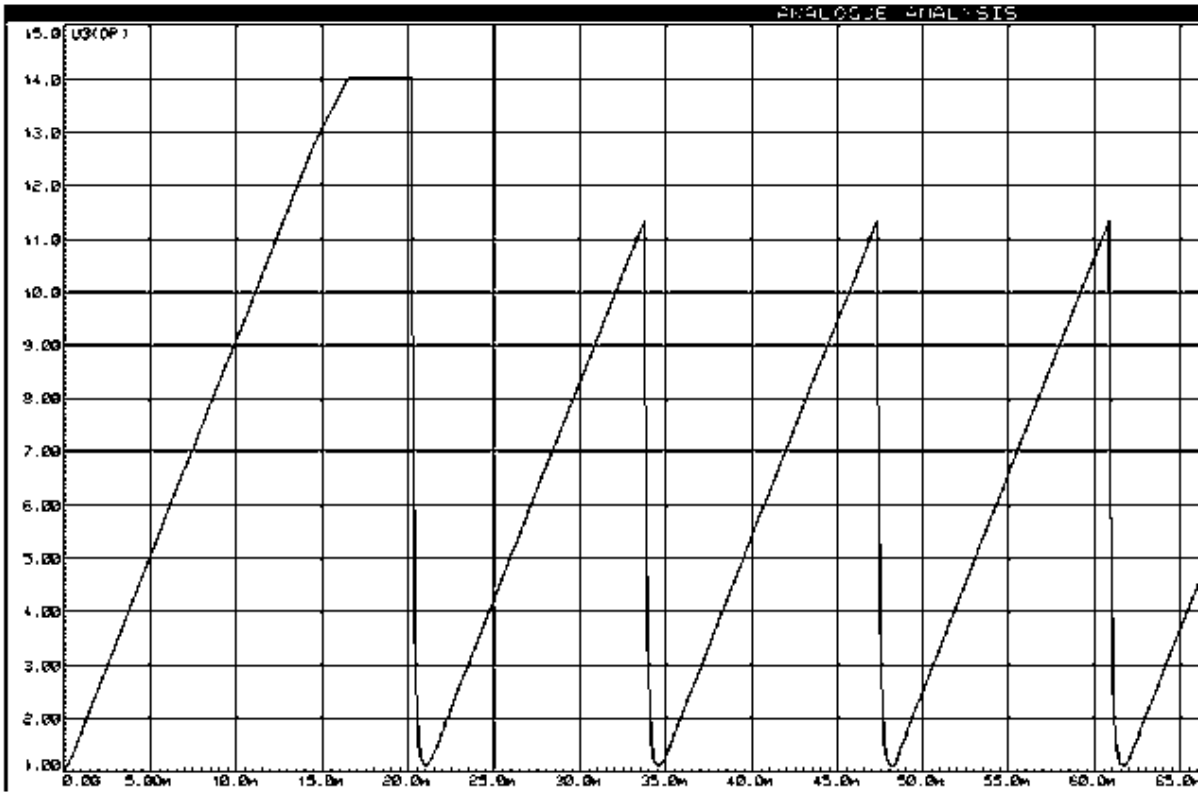

Figure 5.17: Ramp Generator Output after Amplification

The combined voltage each 5v for the two inputs is shown below

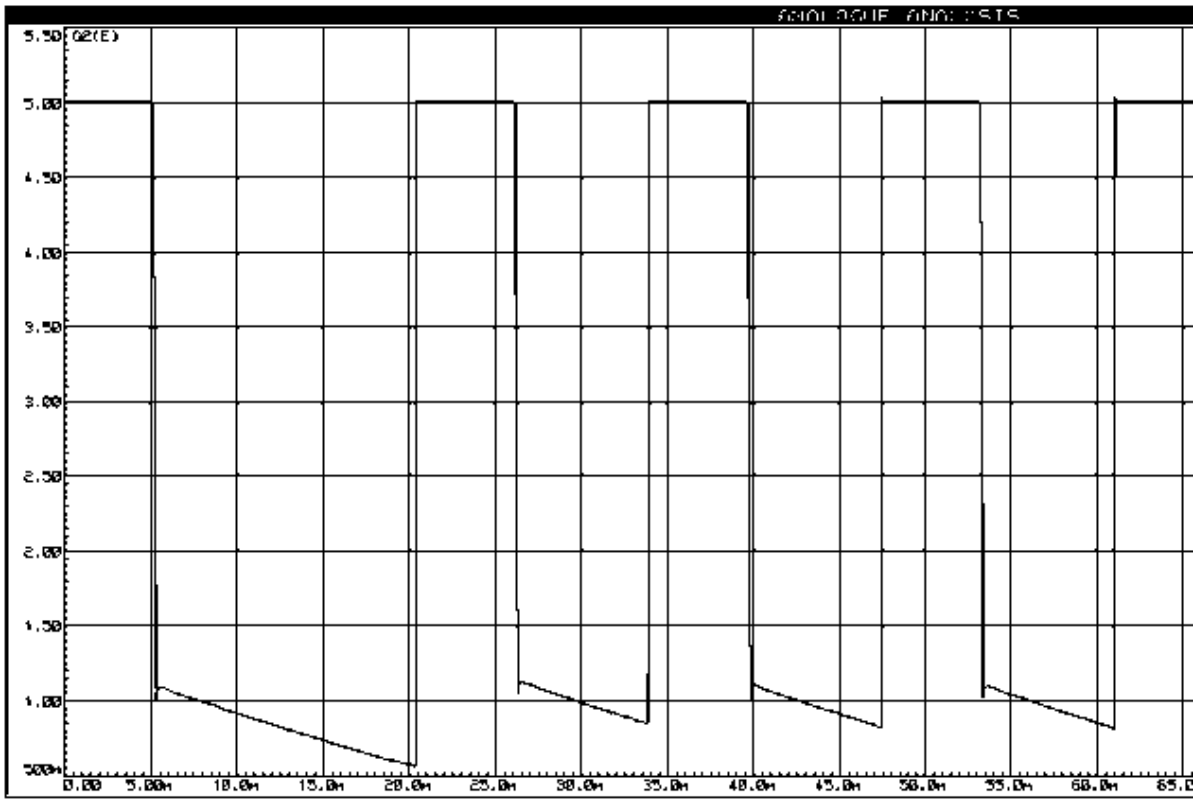

Figure 5.18: The Multiplied Output Voltage before amplification

After the amplifier with an output of 5.5v.

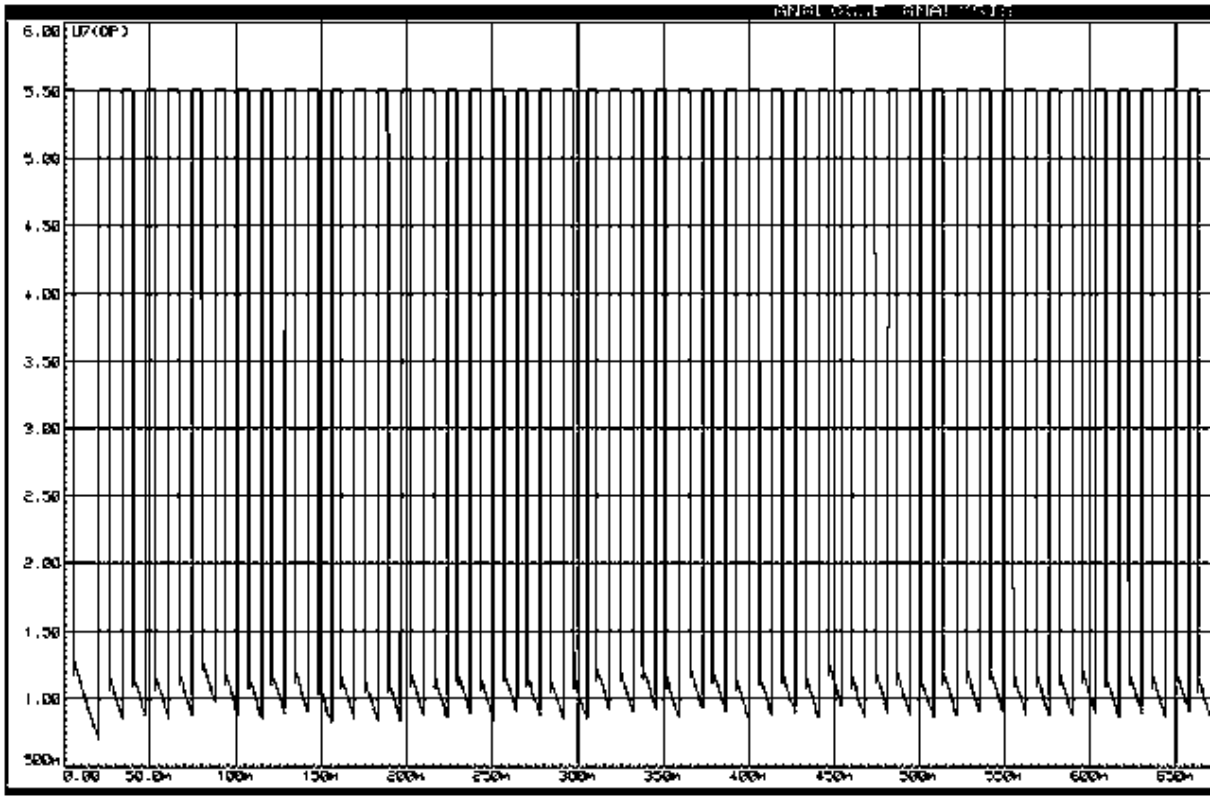

Figure 5.19: The multiplied Output Voltage after amplification

After the filter

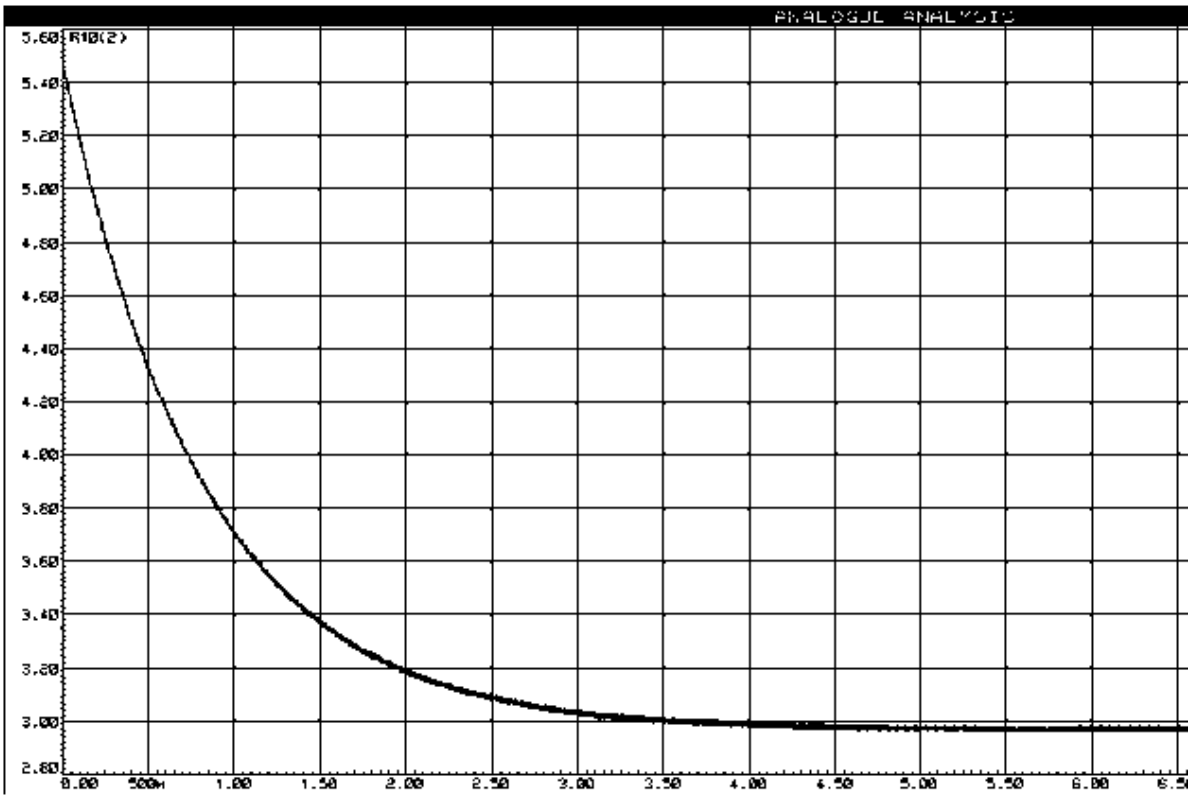

Figure 5.20: The Multplied Output Voltage after the filter

5.5.2. Pump Power Circuit

(a) Pump Voltage, (b) Current Signals

The low level voltages, V_{PV} and V_{PI} , proportional to the actual pump voltage and current respectively are obtained using the circuit illustrated in Fig. 5.21.

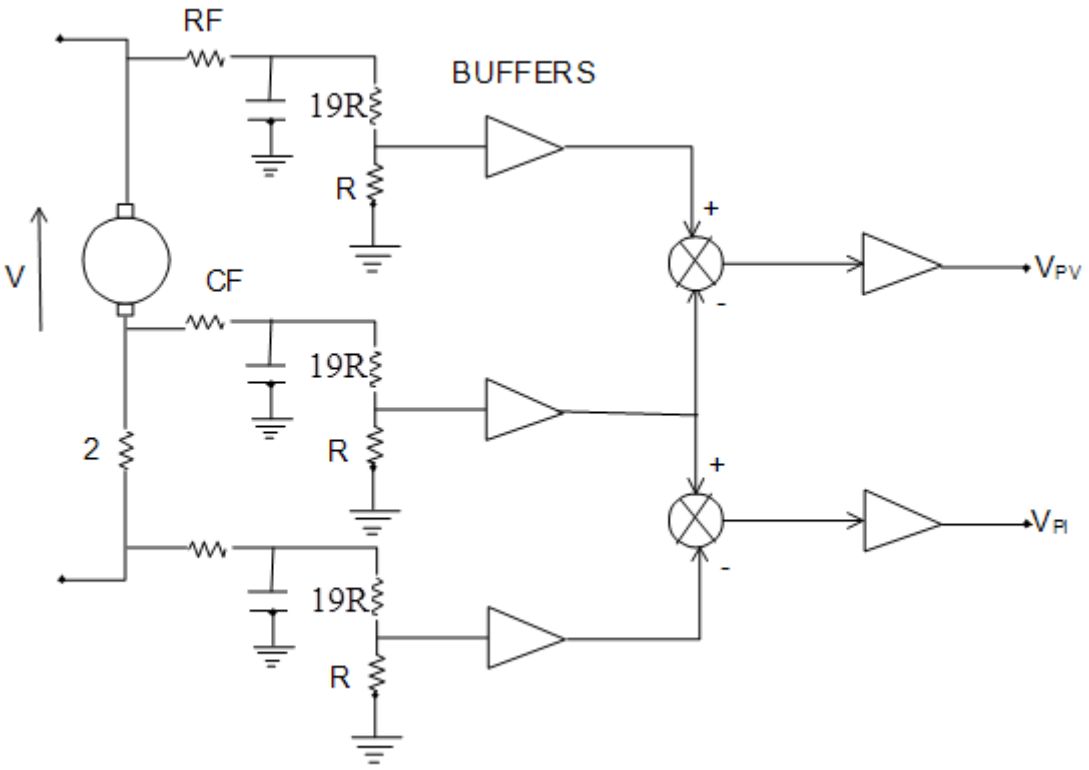

Figure 5.21: A Schematic of Pump Power Circuit

The voltage across the pump motor is mains-derived and thus neither end of the motor is at ground potential.

The detection of motor current is equivalent to the detection of the voltage across the resistor which was used. Three voltages are smoothed using simple filters and 20:1 potentiometer (19R and R) attenuate these voltages which may be as high as 240 volts (approx.). The attenuated voltages can be subtracted as shown, using operational amplifier circuits, to give the required V_{PV} and V_{PI}.

The following points show how component values were selected:

1. R_F had to be sufficiently large such that the power dissipated in it would be less than 0.5 watts. For $R_F = 100K\Omega$, the maximum power dissipated wuould satisfy this requirement.
2. C_F was required to satisfy

   $R_F C_F >> 0.02uF$

   Where the period of the 50Hz mains voltages is 0.02 seconds.

   C_F = 2.2uF was selected

   C_F was required to take voltages of up to 200V (approx.).

Thus a 250V capacitor was selected.

3. R was chosen to ensure

   $20R >> R_F$

   R was chosen as $0.5M\Omega$.

4. Finally, because R was required to be so large, a buffer was necessary to ensure the scaling factor R:20R was not disturbed by an input resistance to the subtractor of the order R. The buffer had an input resistance of $10^{12}\Omega$.

   Where

   $10^{12}\Omega >> 5 * 10^{6}$

A full circuit of the feedback is shown in Fig. With all the other resistors equal to 100K except for that of the divider (9.5M and 0.5M ohms), voltage gain (30K and 10K ohms) and current gain (20K and 300K).

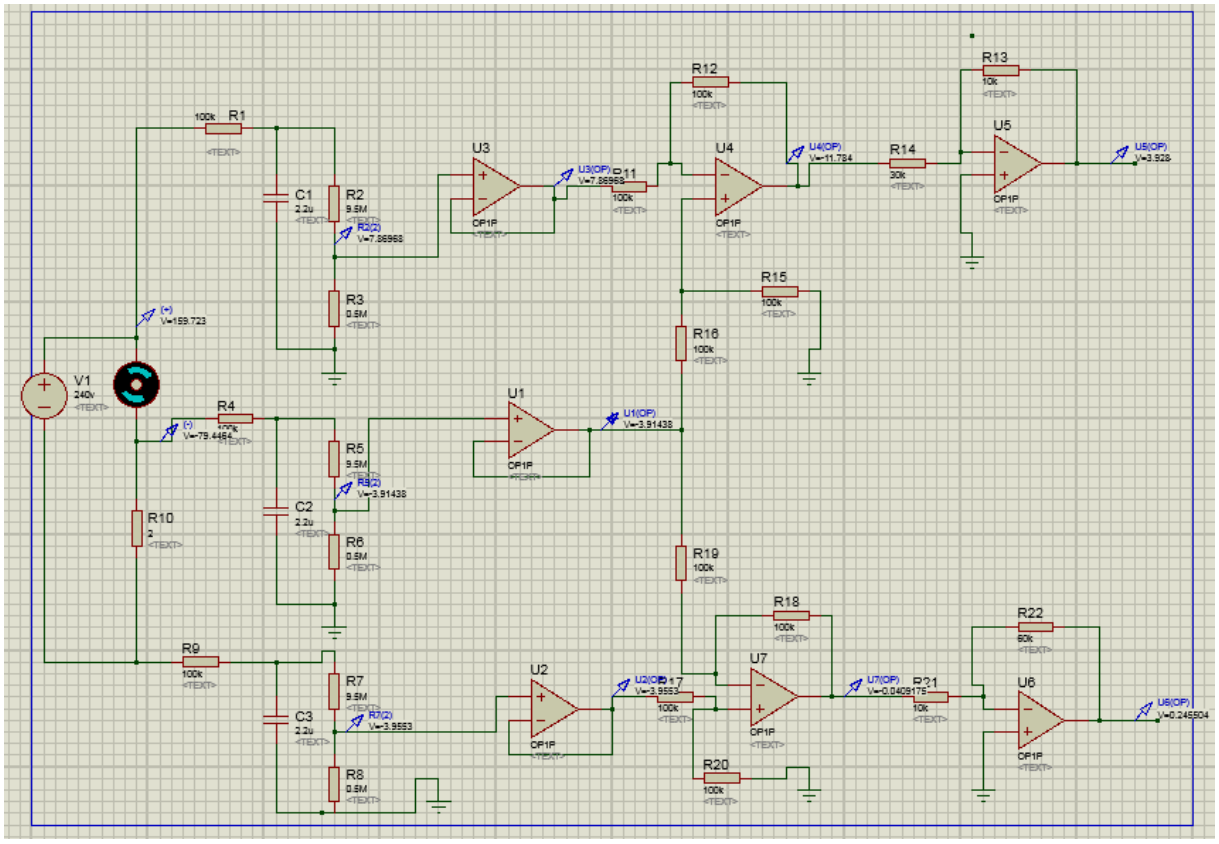

Figure 5.22: Pump Power Circuit [24]

The proportional pump voltage, Vpv with a gain, k of 1/3 gives an output of approximately 3.93volts as shown in the Fig. 5.23.

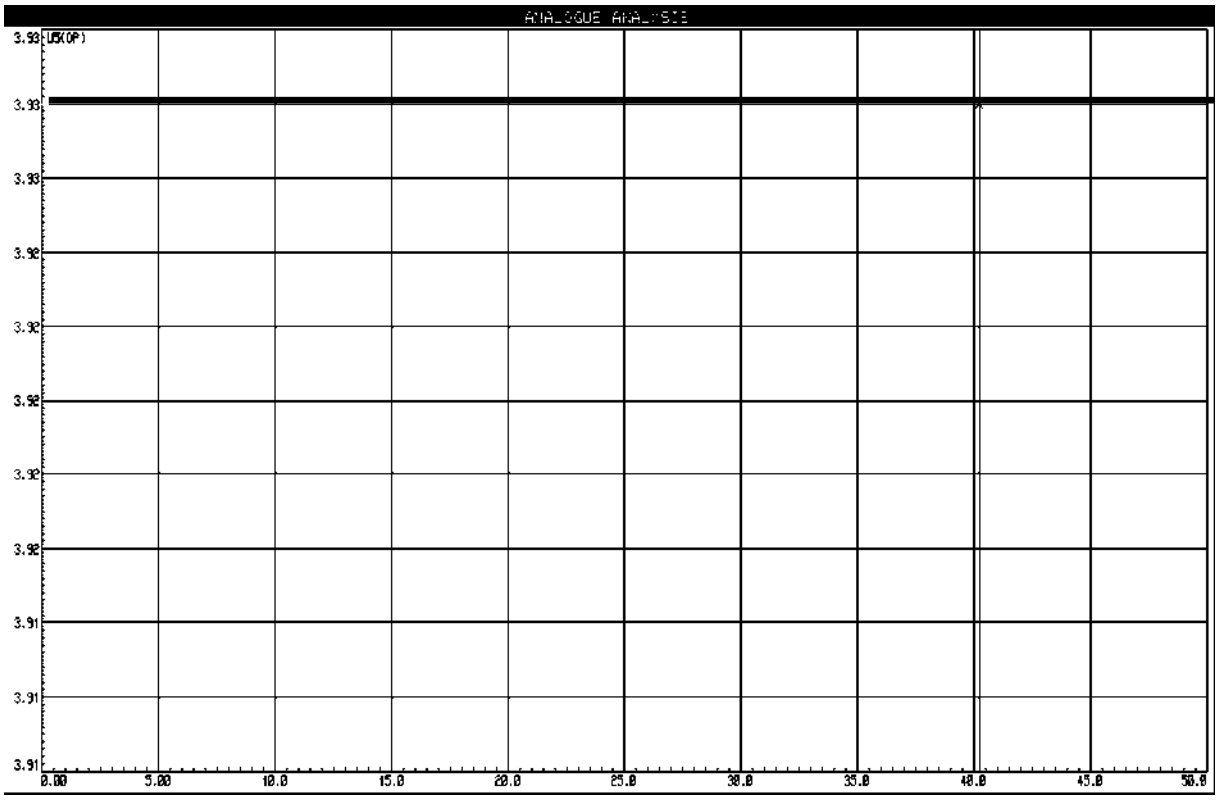

Figure 5.23: D.C Voltage Output Proportional to Pump Voltage

The V_{PI} with a gain, k of 10 gives an output of approximately 2.45volts as shown in the figure. 5.24.

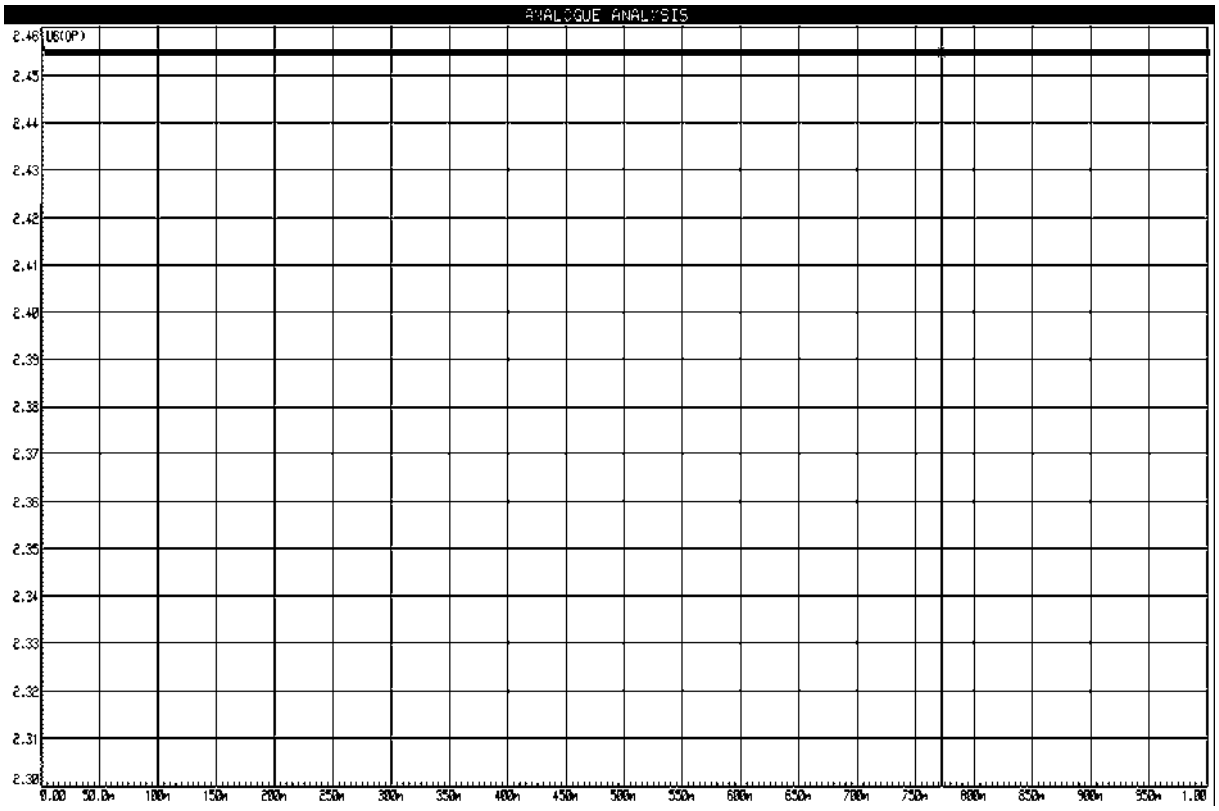

Figure 5.24: D.C Voltage Output Proportional to Pump Current

(c) Analog Multiplier

This element, required to multiply V_{PV} and V_{PI} to give the pump power voltage, V_{PP}, has already been discussed.

Elements were built and connected as required by the design diagram of Fig. Thus giving the voltage V_{PP}, proportional to pump power. A simple operational amplifier sub tractor was now used to subtract V_{PP} from V_{PTH} giving the net power, V_{PN}, proportional to net power.

5.5.3. The Extremum Seeking Controller

This is a single input, single output element. Its input is V_{PN}, the quantity to be maximized. Its output is V_F, a voltage which through the pump drive circuit, will control the pump speed. Both pump speed and flow will vary monotonically with V_F .

Every T seconds the ESC will either increase or decrease V_F by a fixed amount. Each such increase/decrease is a “decision” of the ESC. If the ESC´s nth decision (nT seconds after it is

switched on) is to increase V_F , we will say that ΔF^n is positive and assign the binary bit,1, to ΔF^n .

If the ESC's nth decision is to decrease V_F , we will say that ΔF^n is negative and assign the binary bit, 0, to ΔF^n .

Also, if V_{PN} at nT seconds is greater than at (n-1) * T seconds, we will say that ΔP^n is positive and assign the binary bit, 1, to ΔP^n . If V_{PN} at nT seconds is less than V_{PN} at (n-1) * T seconds, we will say that ΔP^n is negative and assign the binary bit, 0, to ΔP^n .

At any time nT, the ESC must have available to it the signs of ΔF^{n-1} and ΔP^n to decide what should be the sign of ΔF^n . There are four possibilities as shown in the truth table.

Table 5. 1: Truth Table for the ESC

ΔF^{n-1}	ΔP^n	ΔF^n
0	0	1
0	1	0
1	0	0
1	1	1

The truth value of ΔF^n is a consequence of the ESC logic, a summary of which follows:

If $\Delta F^n = \Delta P^n$ (truth values), then $\Delta F^n = 1$

Otherwise

$\Delta F^n = 0$

5.5.3.1. Implementing ESC Logic

İs best implemented in practice as shown in Fig. 5.25.

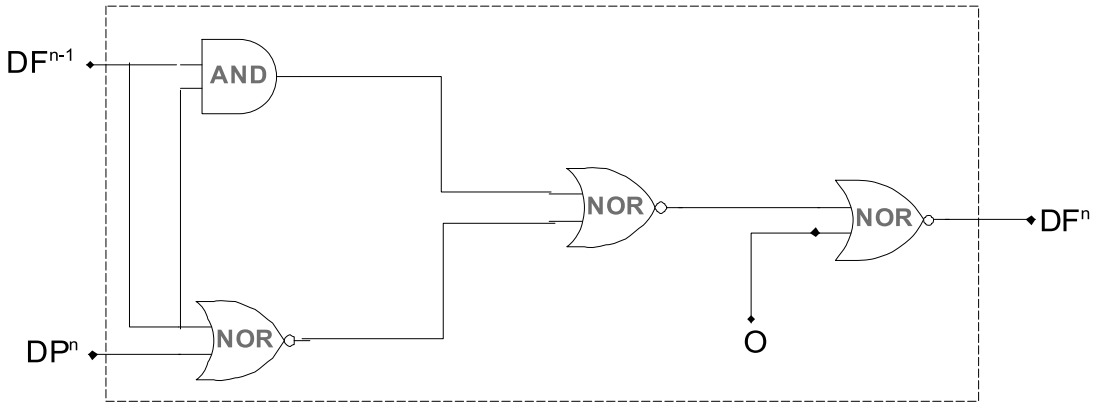

Figure 5.25:The ESC Circuit [25].

The logic is simulated and tested as shown in the figure below and the output where found to be exactly the same as that of the logic table.

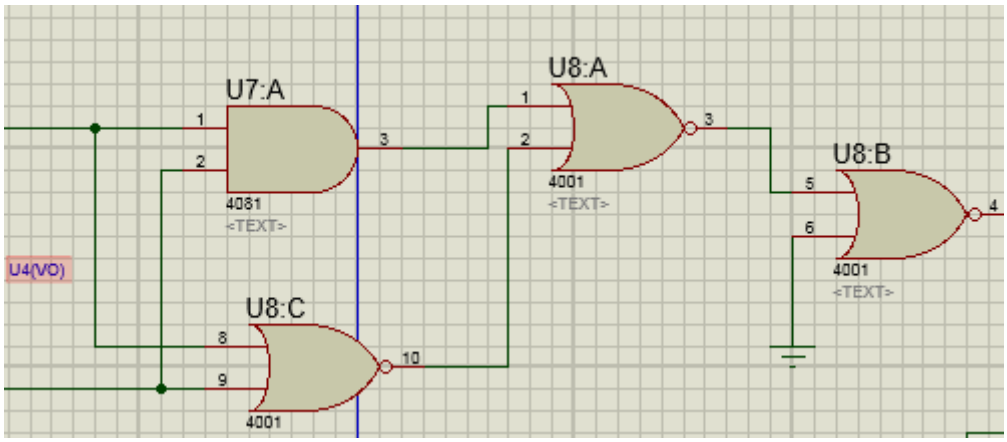

Figure 5.26: The ESC Circuit

The Boolean variable ΔF^{n-1} is supplied to the logic section via a suitable time delay flip – flip from ΔF^{n}. ΔP^{n} is derived from the output of a comparator which compares the present value of V_{PN} with the value of V_{PN} at the last sample time which is stored on a sample and hold capacitor. Thus the circuit that gives the Boolean ΔF^{n} is as shown in figure 5.27.

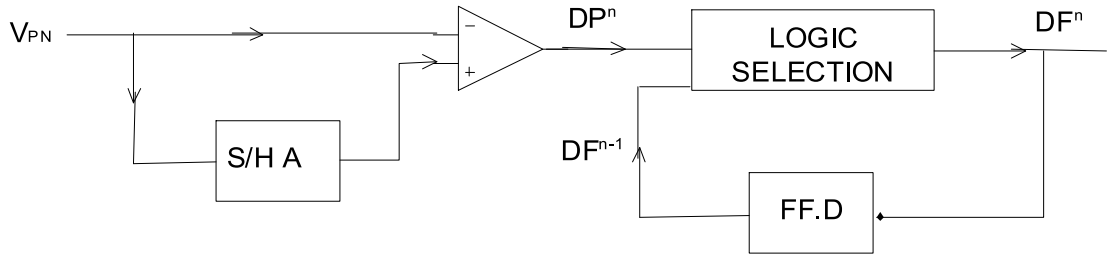

Figure 5.27: Schematic of the Boolean ΔF^n Circuit.

NOTES:

1. 1.In the ESC a flip flop is essentially a one-bit delay line with delay T seconds, and a sample and hold is a delay of T seconds for an analog quantity.
2. A sample and hold is represented by "S/H" or SH and a flip flop by FF.
3. The labels A and D used above will be referred to later.
4. Logic 1 will be volts and logic 0 will be 0 volts.

5.5.3.2. Implementing The Logic Decision

The remainder of the ESC circuit must do the following:

1. Provide the output voltage V_F (stored on a S/H capacitor).
2. Increment or decrement this value every T seconds as soon as a new decision ΔF^n is made.

These requirements are met by the circuit in Fig. 5.28.

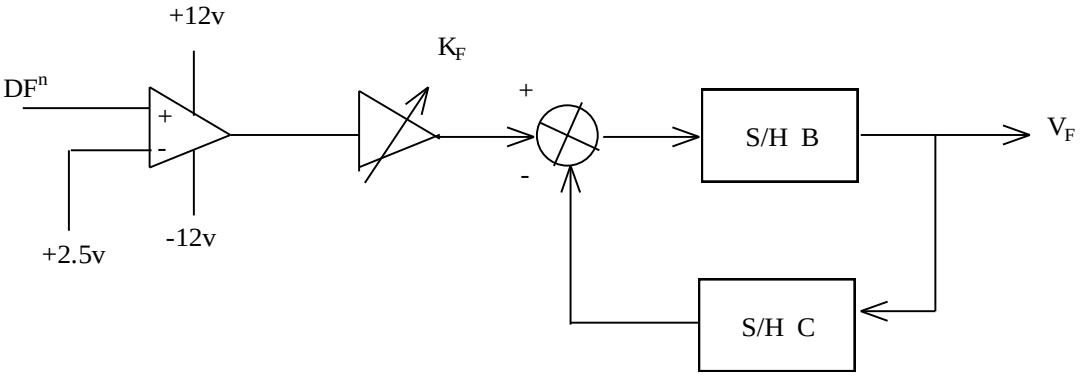

Figure 5.28: Schematic of the Logic Decision İmplementation Circuit

The comparator gives +12V for $\Delta F^n = 5V$ and $-12V$ for $\Delta F^n = 0V$. This is necessary because the S/H required and +12 and $-12V$ supply rails.

An amplifier with variable gain $K_F < 1$, provides some fraction of + or – 12 volts at one input of the adder, typically 0.2 volt. SH. B holds the output voltage V_F as does SH.C.

Every T seconds SH.B samples its input, which is in fact $V_F \pm 12K_F$ volts and this is held as the new output, V_F .

In this way V_F will respond to ΔF^n every T seconds as required, increasing if ΔF^n is 5V and decreasing if ΔF^n is 0V.

5.5.3.3. Timing

The synchronous components of the ESC must be clocked in a suitable sequence in order to ensure correct ESC operation. The full circuit of figure 5.29 Formed by connecting the ΔF^n output of figure 5.27 To the ΔF^n input of Fig. 5.29 is shown below. Clock terminals are now marked for all synchronous components.

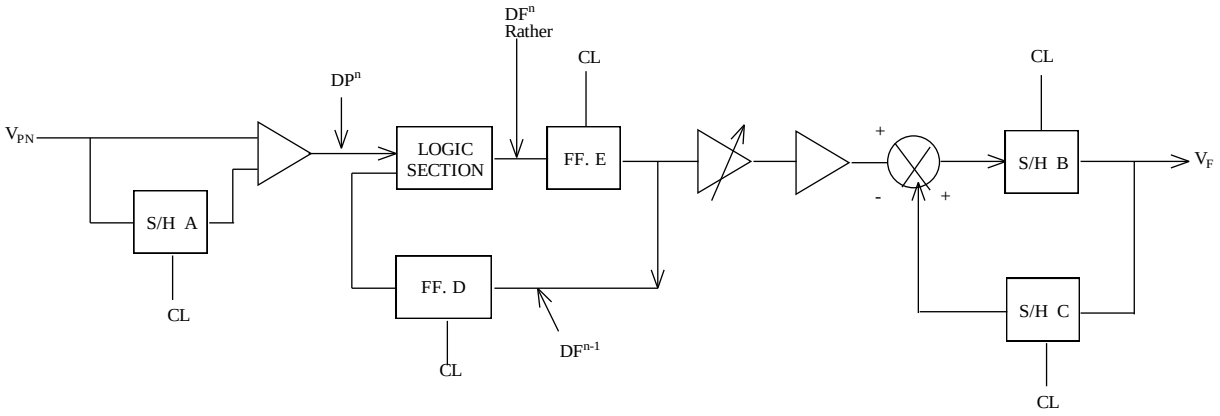

Figure 5.29: Schematic of the Timing and Logic İmplementation Circuit

5.5.3.4. Flıp Flop E

At this stage an extra delay flip flop FF.E was introduced for this reason:

A Sample and Hold circuit must sample its input for a finite length of time, say t_s .

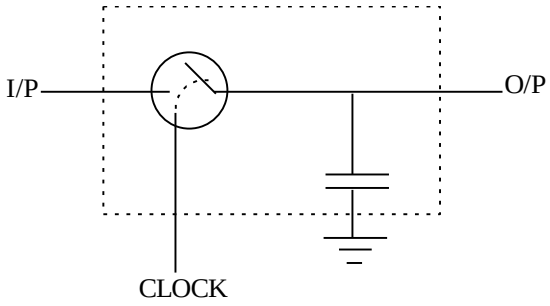

Figure 5.30: Schematic of the Sample and Hold Circuit.

The sample and hold circuit is simulated as shown in the figure below and tested with a hold time of about 20s.

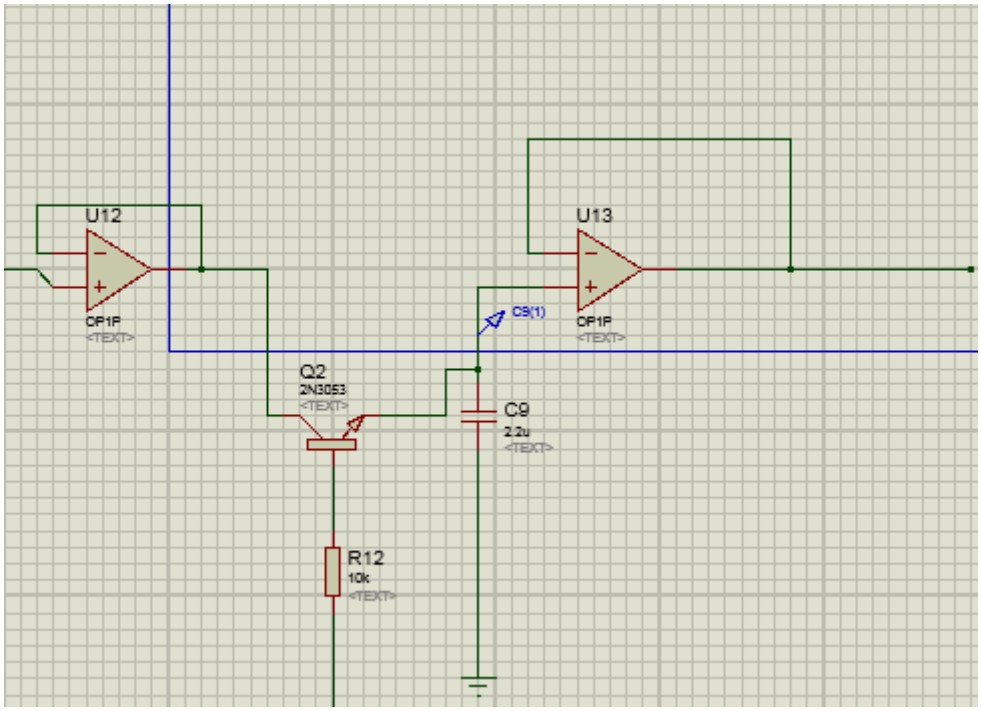

Figure 5.31: Sample and Hold Circuit [25] [26].

The out put

Figure 5.32: The Output of the Sample and Hold Circuit

For t_s seconds then, the clock controlled switch is closed and the input is connected via a buffer to the output.

Consider SH.B in the ESC, without FF.E in the circuit. For t_s seconds, while SH.B is sampling, there will be no delay element between V_{PN} and V_F in the ESC. It might therefore happen that, while is V_F changing from one voltage to the next, ıt could influence, through the external solar energy system, the input V_{PN} which is being used to determine the change in V_F that is presently occurring; i.e. the attempt to implement a particular logic decision ΔF^n could in itself change that decision. Erroneous decision would be likely to result, therefore, unless a delay is introduced between input V_{PN} and output, V_F, thus, flip flop E is introduced.

5.5.3.5. Clocking Sequence

There are three S/H's and two flip flops to be clocked. Each will be clocked every T seconds with a zero to five volts pulse of duration t_s. Three clock pulse streams are generated as shown in Fig. 5.33.

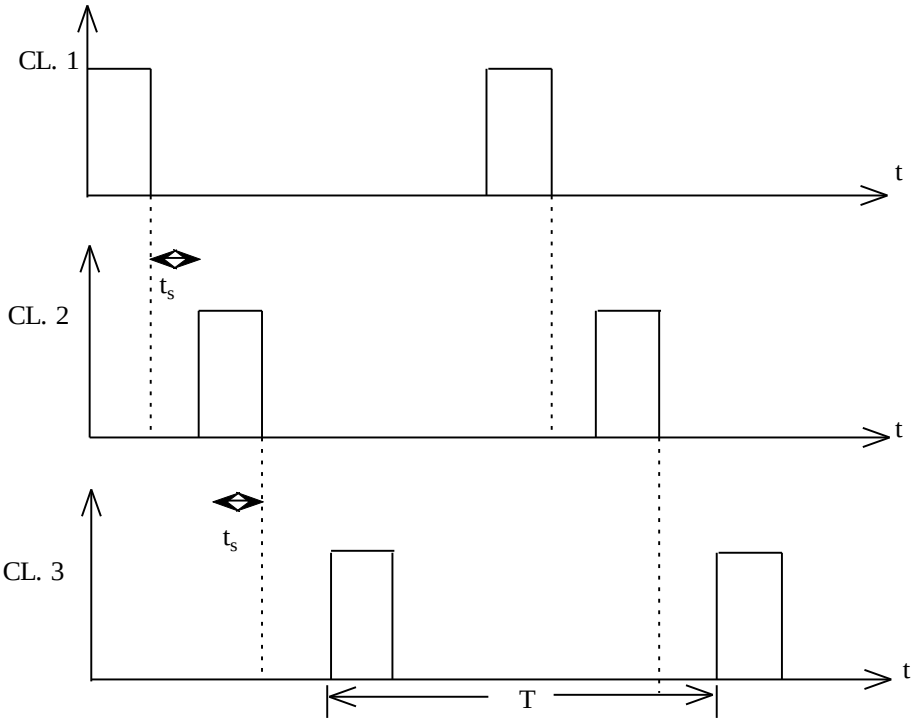

Figure 5.33: Schematic of the Clocking Sequence Output.

CL.1 is used to trigger both FF.E and SH.C

CL.2 is used to trigger both SH.A and FF.D

CL.2 is used to trigger SH.B

The reasoning behind this timing is as follows:

During the period of time required to complete a decision, it is necessary for the ESC to :

First: store the decision ΔF^n to be implemented i.e. clock FF.E

Second: store the V_{PN} value, into SH.A, that was used to make decision ΔF^n so that it can be used for decision ΔF^{n+1} .

Third: ımplement decision ΔF^n, by clocking SH.B.

This is the only acceptable clocking order (FF.E, SH.A, and SH.B) because:

1. If A is clocking before E, ΔF^n is arbitrary when sampled by E , because the comparator output, ΔP^n is arbitrary (equal inputs).

2. If B is clocked before A, then the output V_F may, through the external system, change V_{PN} before it is stored by SH.A. Thus, the actual value stored would not be the one used to make the decision.

These two points rule out all other clocking orders for FF.E, SH.A and SH.B. Now the only restriction on SH.C is that it is not clocked at the same time as SH.B. Thus SH.C can be clocked with the same pulse stream as FF.E (i.e. SH.C does not require a new pulse stream). Also, the only restriction on the clocking of FF.D is that it does not occur at the same time as that of FF.E. Thus FF.D is clocked with the same pulse stream as SH.A.

In the light of the above reasoning, the three clock streams CL.1, CL.2, CL.3 each clocking the components indicated represent the simplest acceptable clocking system.

5.5.3.6. Bridging Pulses

A further requirement on the clocking sequences is that between any two successive clock pulses, i.e. (CL.2 and CL.1) and (CL.3 and CL.2), there should be a finite time delay.

For example, without a delay between (CL.1 and CL.2), SH.A begins to open its voltage controlled switch at the instant when FF.E is storing its input ΔF^n . In reality, this instant is some finite length of time Δt_s as shown in Fig. 5.34.

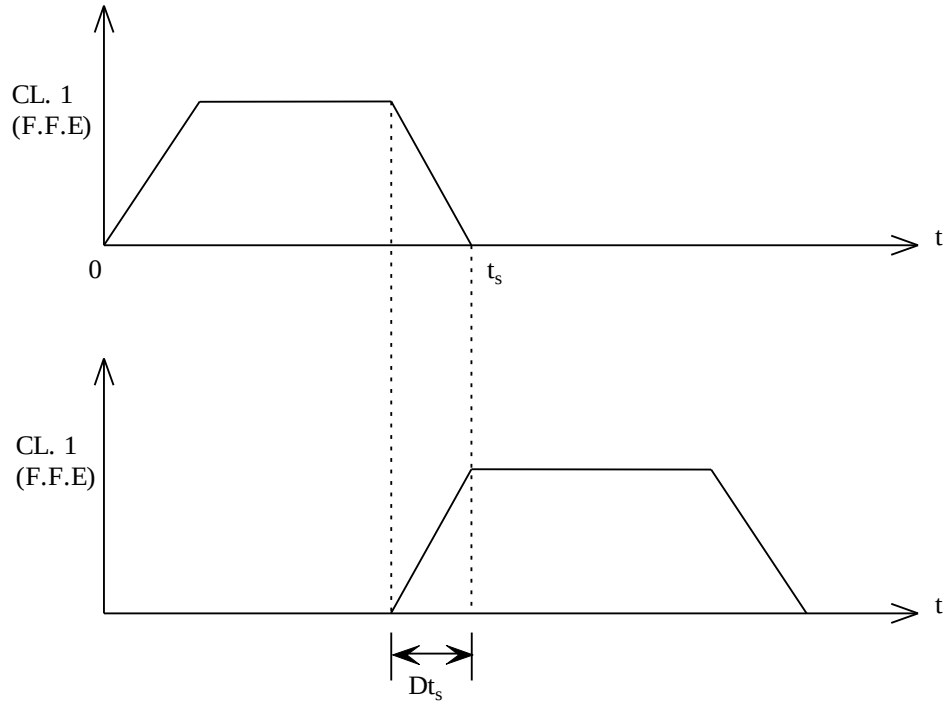

Figure 5.34: Schematic of Bridging Pulses.

During Δt_s, it is possible that the transistor which is the switch in SH.A is partially ON or CLOSED at the time as the transistor whose base is the clock of FF.E is not yet fully off. Thus to ensure this cannot happen, (and hence that the two errors of the last section cannot occur) a clock pulse width,, is introduced between (CL.1 and CL.2) and between (CL.2 and CL.3). Thus, each two consecutive clock pulses are separated by seconds as shown in the original Fig. 5.33.

NOTE:

It is possible that delays introduced by asynchronous components in the ESC circuit may remove the necessity for either or both of the bridging pulses; but this cannot be relied upon. It is also possible that time delays, through the external system may be sufficiently large so as not to give rise to the error described in 2 above. However, by developing the ESC in consideration of all possible problems ensures that it can be used for any external system without regard for a possibly short associated time delay.

5.5.3.7. Hardware

The hardware required to generate the three clock pulse streams is shown in Fig. 5.35

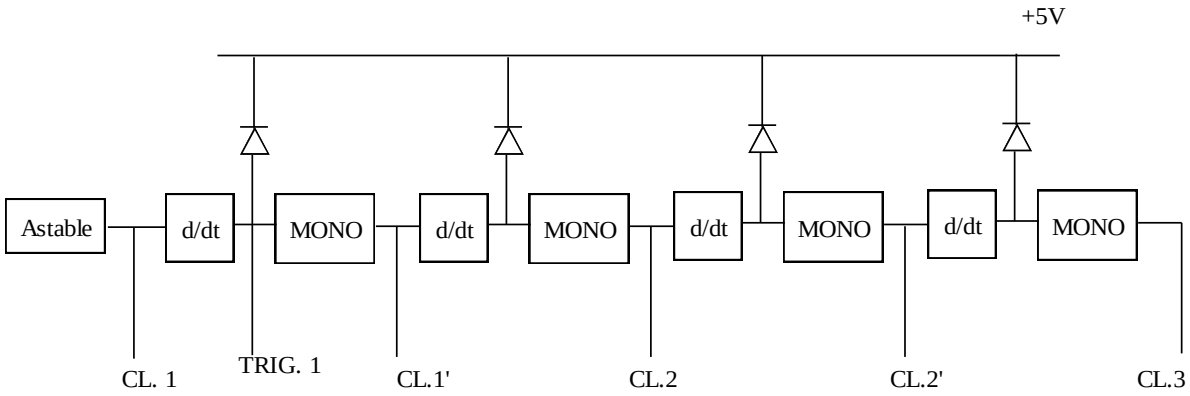

Figure 5.35: Schematic of the Clocking Sequence Circuit.

"MONO" = MONOSTABLE

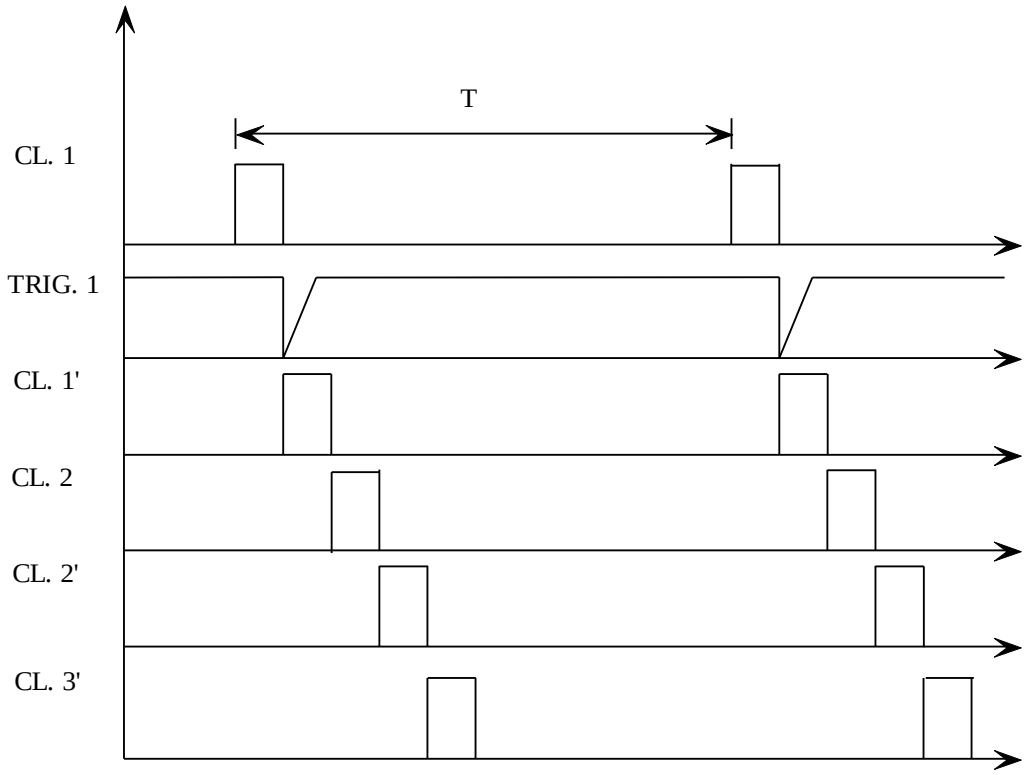

Figure 5.36: Sample Output of the Clocking Sequence Circuit.

Each monostable is triggered by the preceding output which is differentiated by a simple CR circuit. One trigger is shown in Fig.5.36 for illustration. CL.1, CL.2 and CL.3 are connected to the five synchronous components in the main part of the ESC circuit required.

t_s was adjusted to be up to about 900ms (arbitrary) by selecting appropriate monostable components. T was made variable by a pot in the astable. T can be up to 2.5 minutes (approximately).

The circuit diagram for the simulation is as shown

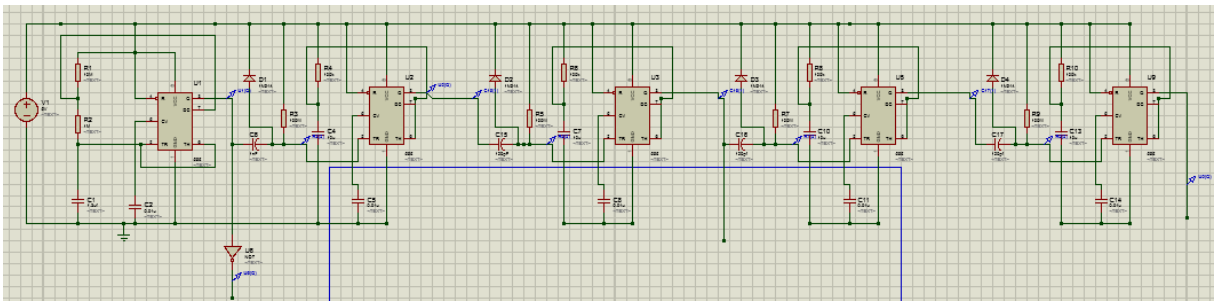

(a)

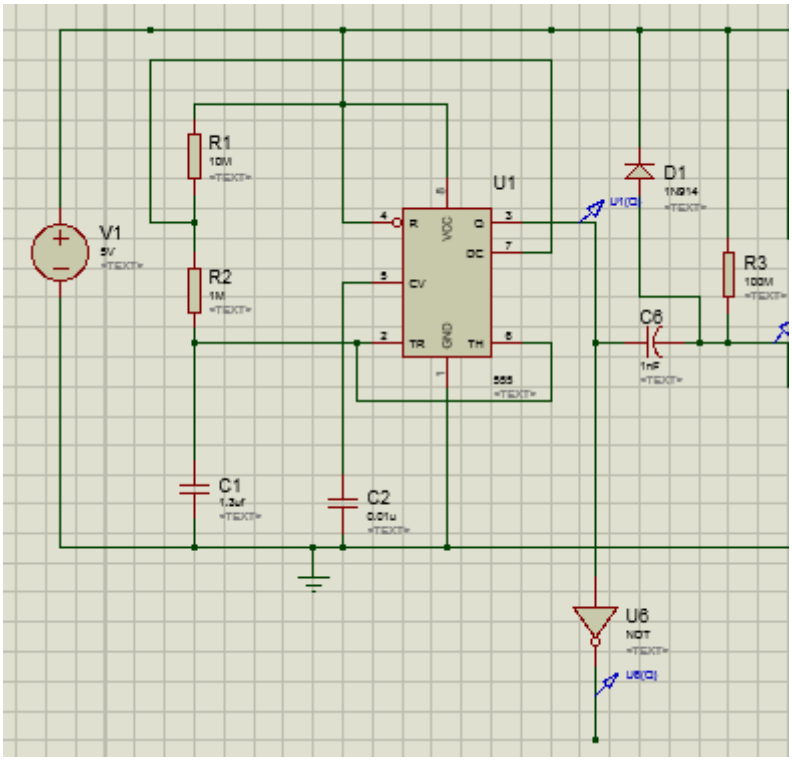

(b)

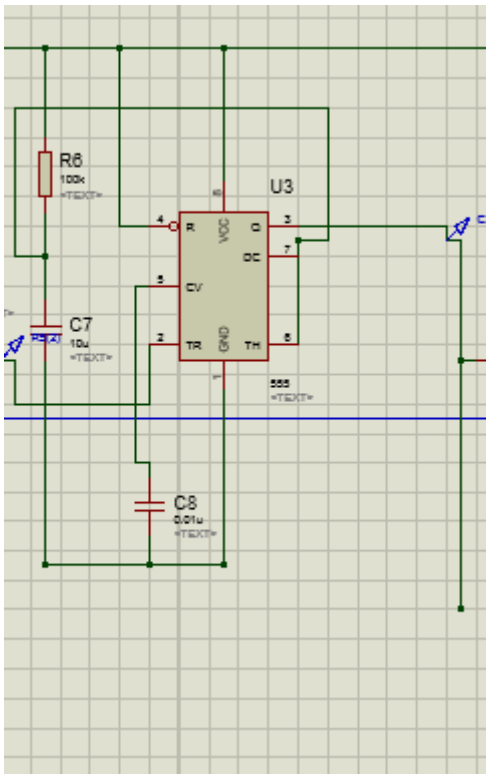

(c)

Figure 5.37: The Clocking Sequence Circuits [23] [28]

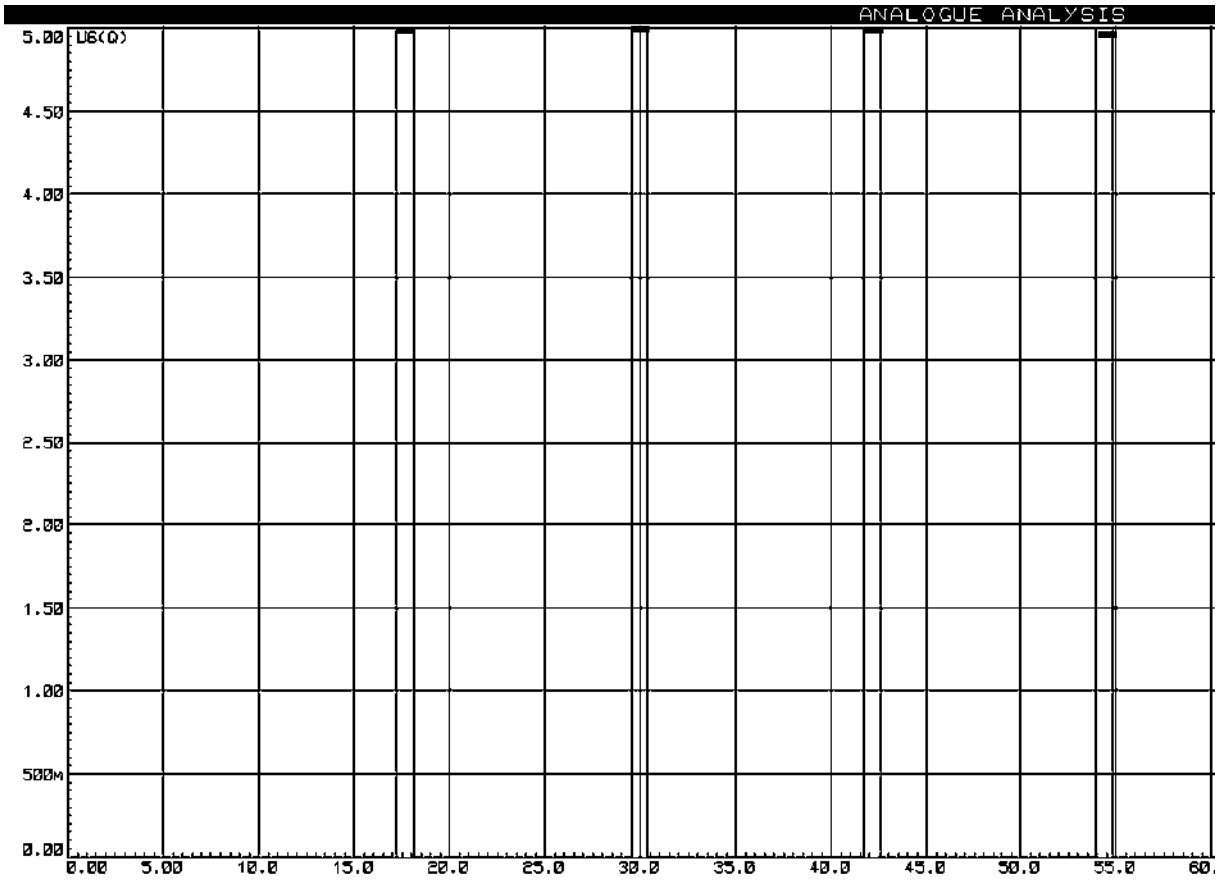

Figure 5.38: The astable output through the not gate CL1

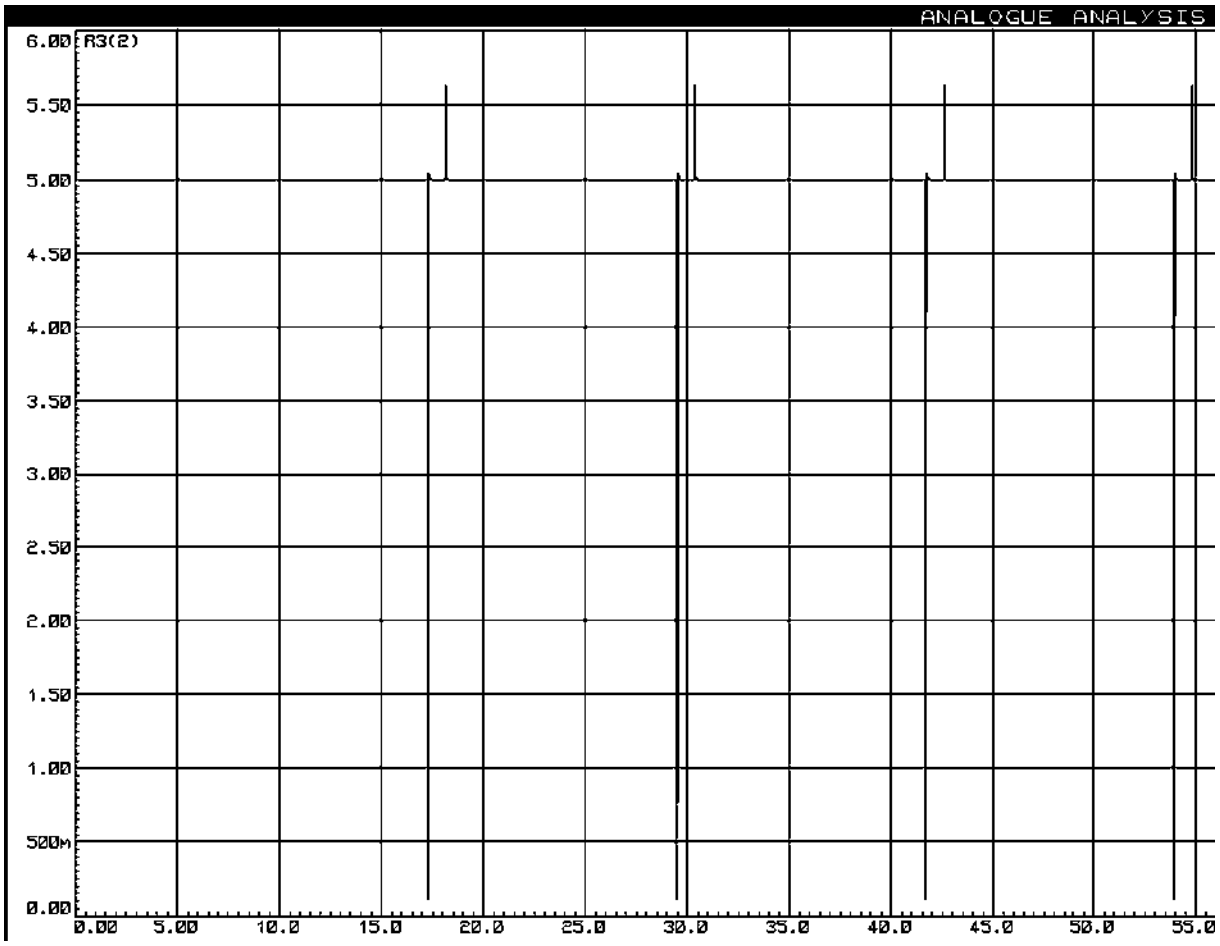

Figure 5.39: The differentiator output for triggering the firs monostable from CL1.

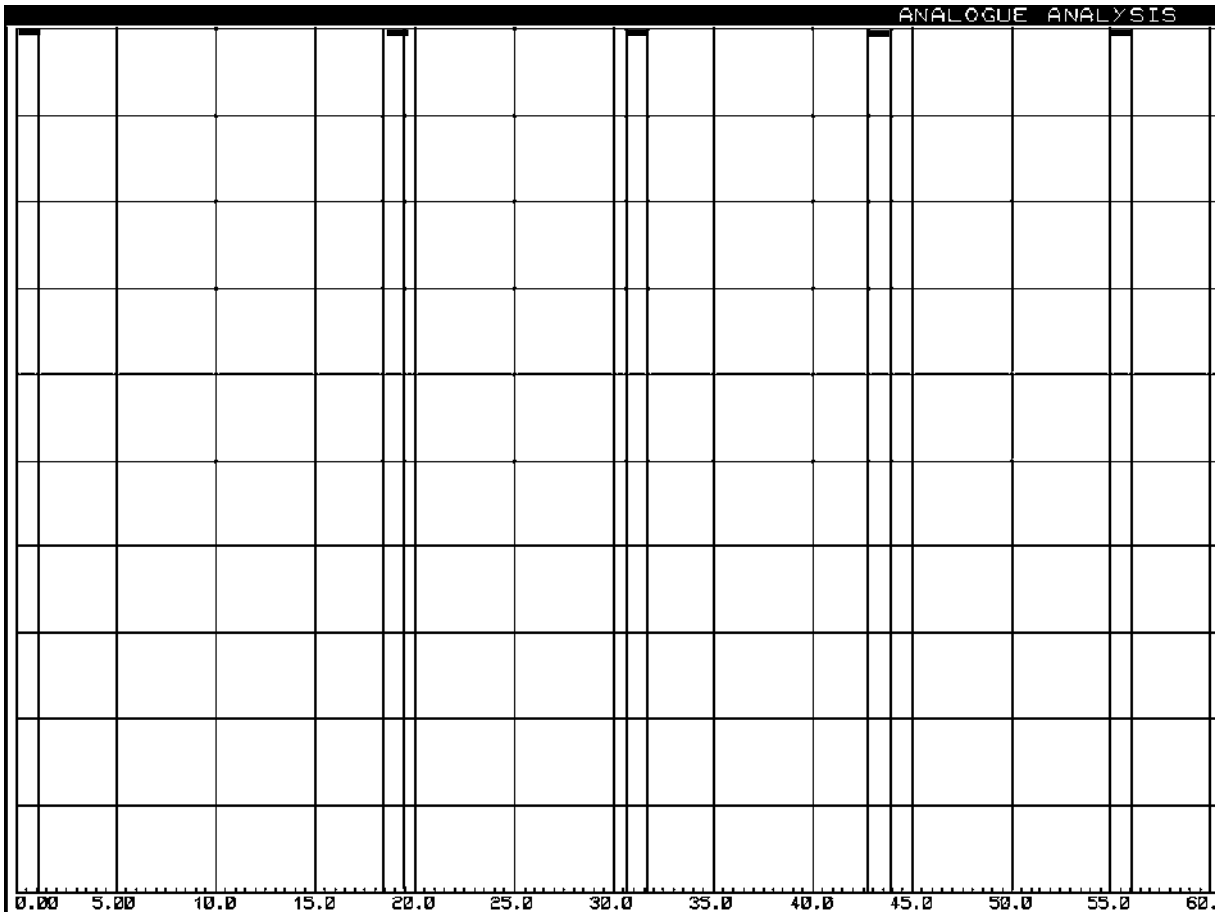

Figure 5.40: The Monostable output for CL2.

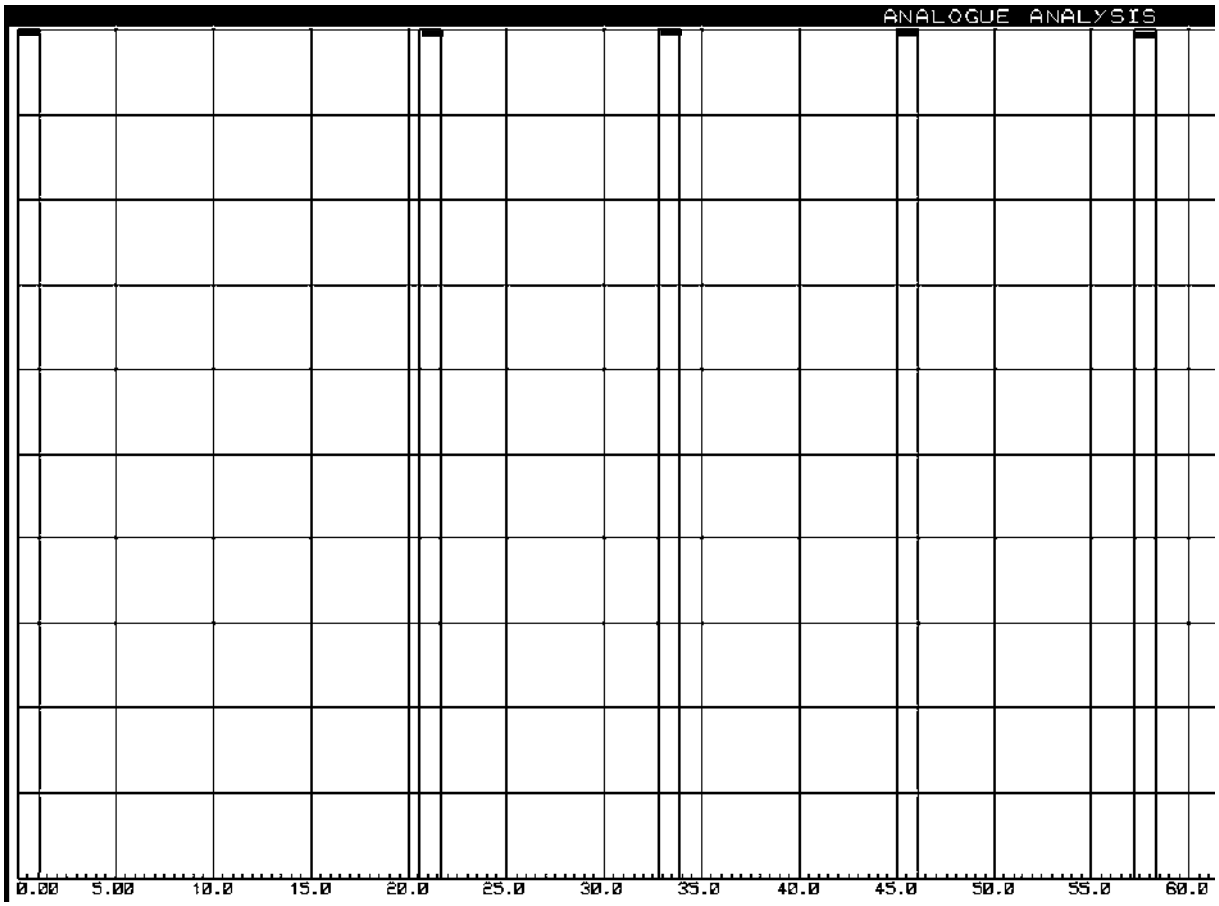

Figure 5.41: The Monostable output for CL3.

Recalling the presence of the variable – gain amplifier "K_F" we may represent the ESC, for all practical purposes by Fig.

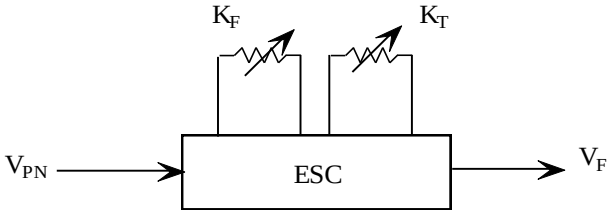

Figure 5.42: The Extremum Seeking Controller

Where the K_T pot. Adjusts the inter – sample period (up to maximum value of 150 seconds), and the K_F pot adjusts the increment/decrement to (up to a maximum of $\pm V_{cc}$)

The complete ESC circuit is shown in 5.43.

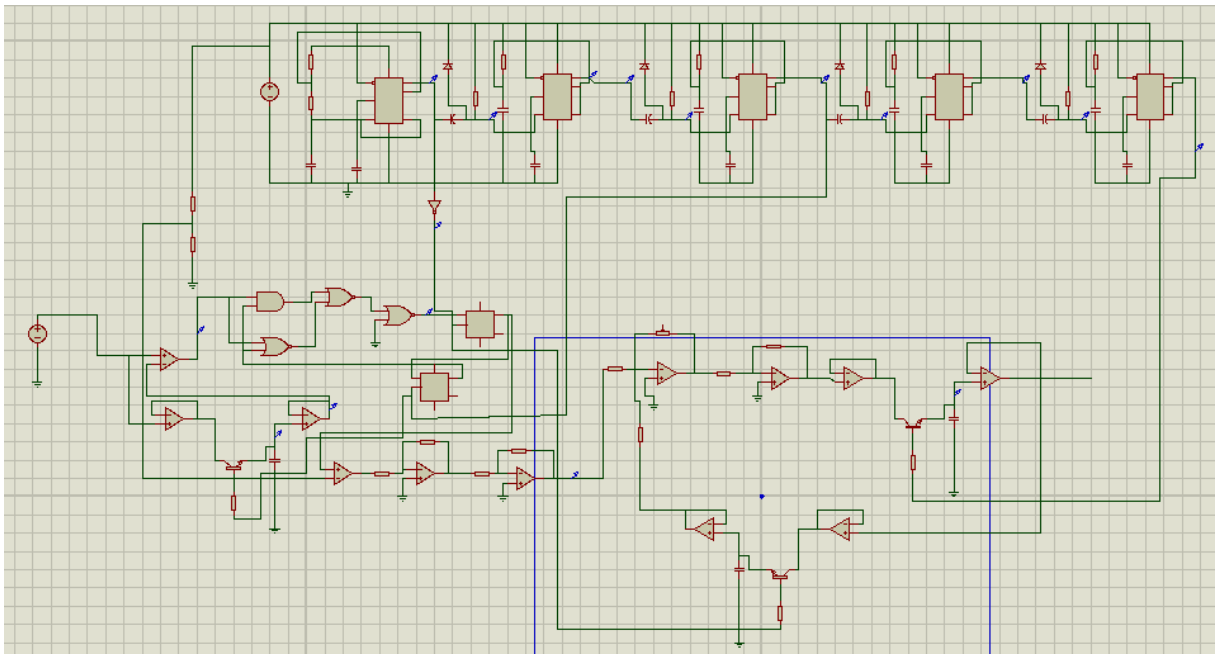

(a)

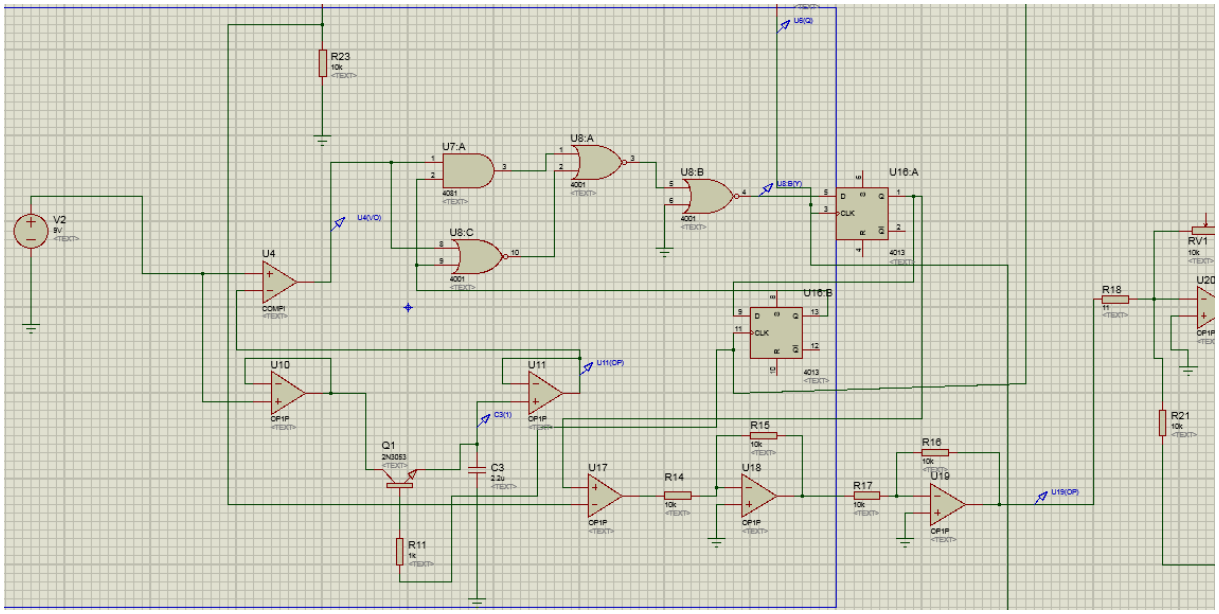
R23
10k
U7:A
U8:A
U8:B
U8:C
U16:A
U16:B
V2
8V
U4
COMP1
U10
OP1P
U11
Q1
2N3053
C3
2.2u
R11
1k
U17
R14
R15
U18
R16
U19
R17
R18
RV1
R21
U20

(b)

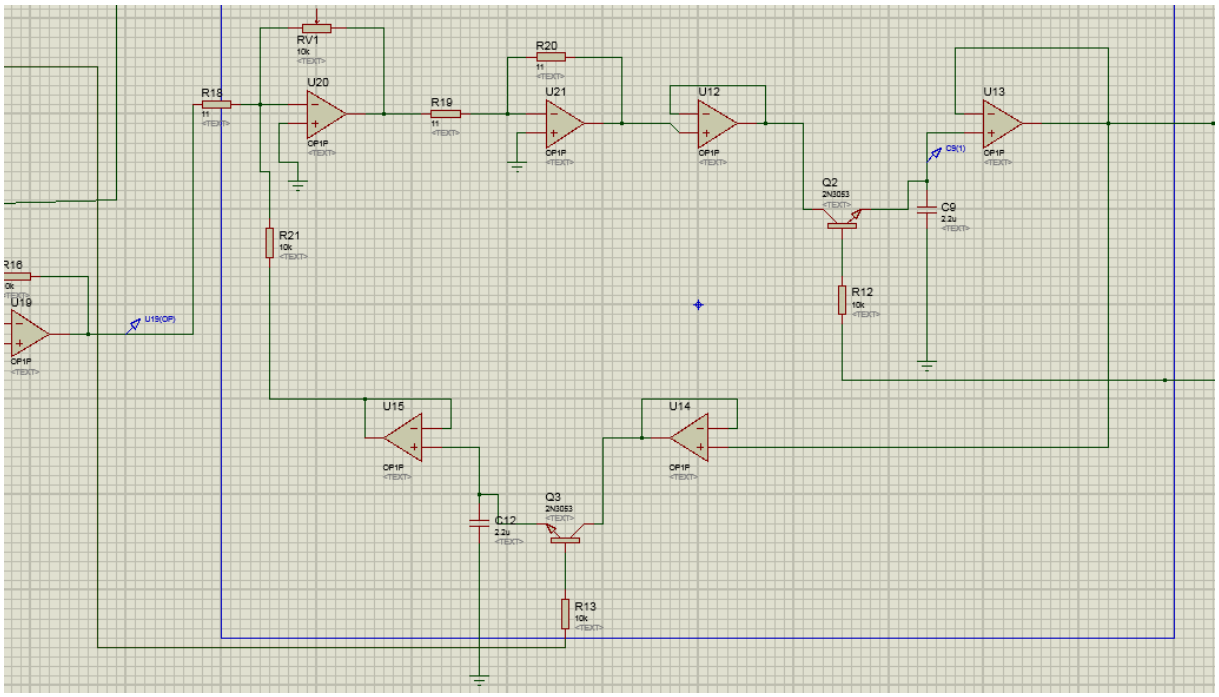

(c)

Figure 5.43: The ESC Circuit [24]

The following points are to be noted

1. The capacitor selected for use in the S/H's was a 2.2uF polystyrene capacitor. This had acceptable hysteresis and leakage levels, holding voltages with an error of less than 0.5% over 150 seconds.
2. The input V_{PN}, to the ESC is derived from the output of a multiplier filter, whose time constant was 0.8 seconds. The period T should be significantly greater than this value.

In fact, it is the solar energy system itself which will set a minimum value on T because that system takes about one minute to come to equilibrium after the pump speed is changed.

NOTES:

1. The capacitor selected for use in the S/H's was a 2.2 μF polystyrene capacitor. This had acceptable hyteresis and leakage levels, holding voltages with an error of less than 0.5% over 150 seconds.
2. The input V_{PN}, to the ESC is derived from the output of a multiplier filter, whose time constant was 0.8 seconds. The period T should be significantly greater than this value.

In fact, it is the solar energy system itself which will set a minimum value on T because that system takes about one minute to come to equilibrium after the pump speed is changed.

Finally a printed circuit Board of the ESC was built. A photocopy of the PCB mask and a photograph of the P.C.B itself are to be found at the end of this report.

5.5.4. Pump Drive Circuit

The requirement of this circuit is that it should provide a phase controlled mains-derived D.C voltage proportional to an input signal level voltage, V_F = 0 corresponds to zero motor voltage and V_F = 8V correspond to full wave rectified mains voltage.

A basic thyristor controlled motor circuit is shown in Fig. 5.44.

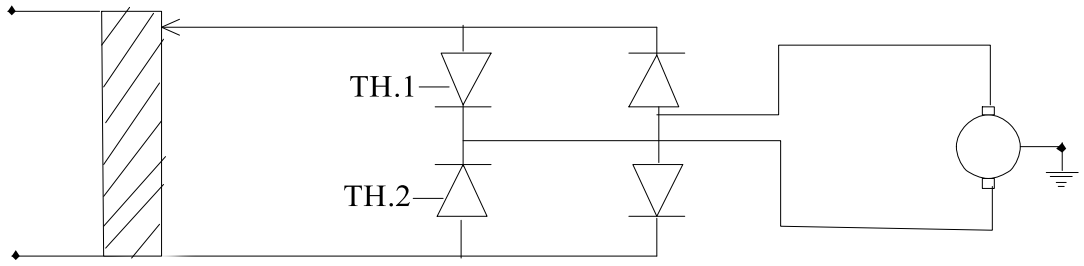

Figure 5.44: The Pump Drive Circuit

This is a modified version of full wave rectification where each mains half cycle is allowed through a thyristor to the motor only after a controlled fraction of a half period of time has passed.

To fire TH.1, it is necessary to produce a series of pulse, each two consecutive pulses being separated by 360^0 (mains cycle) and each pulse delayed by θ^0 from positive going zero crossing of the mains cycle, where θ should vary monotonically with V_F .

To fire TH.2, a similar series of pulses is required, but where each pulse is delayed by θ^0 from a negative going zero crossing of the mains cycle.

The effect of such pulses applied to the thyristor can be seen in Fig. 5.46 (j), (k), (I), the motor voltage being shown shaded in Fig. (1). To produce the pulses, the "Cosine Crossing Method" was used. This method has the property that the net area under Fig. 5.46 (I) and hence the average motor voltage can be easily made proportional to V_F .

5.5.4.1. Cosine Crossing Method

The method is illustrated with reference to the pump drive circuit shown in Fig. 5.45

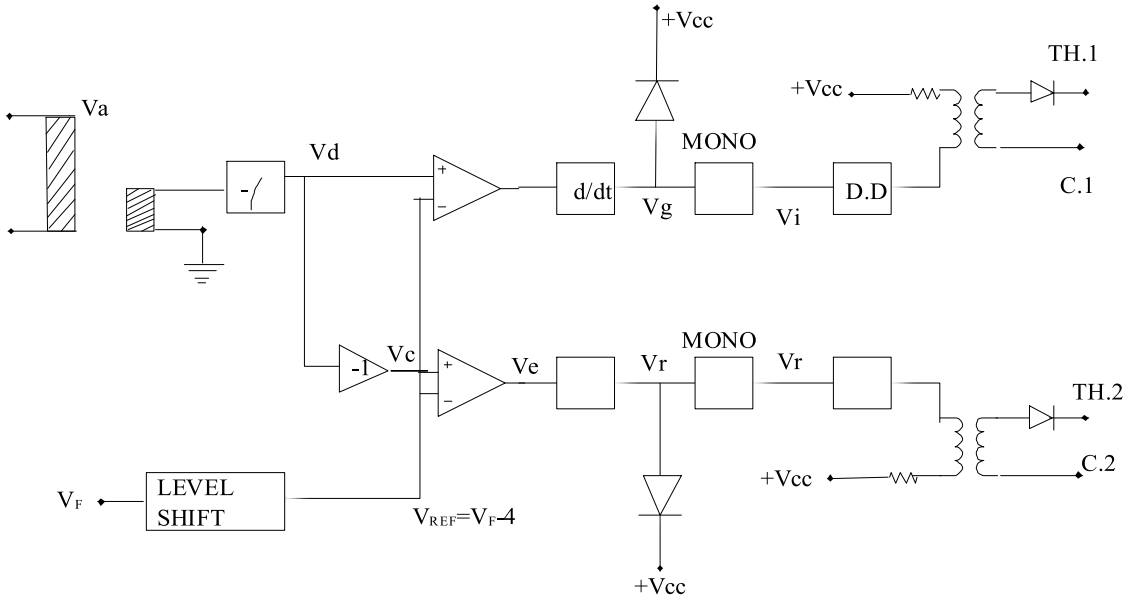

Figure 5.45: Schematic of the firing Circuit

In the circuit:

MONO: represents a monostable

D.D: represent a Darlington Driver

C.1 and C.2: represent the cathodes of thyristors 1 and 2 respectively

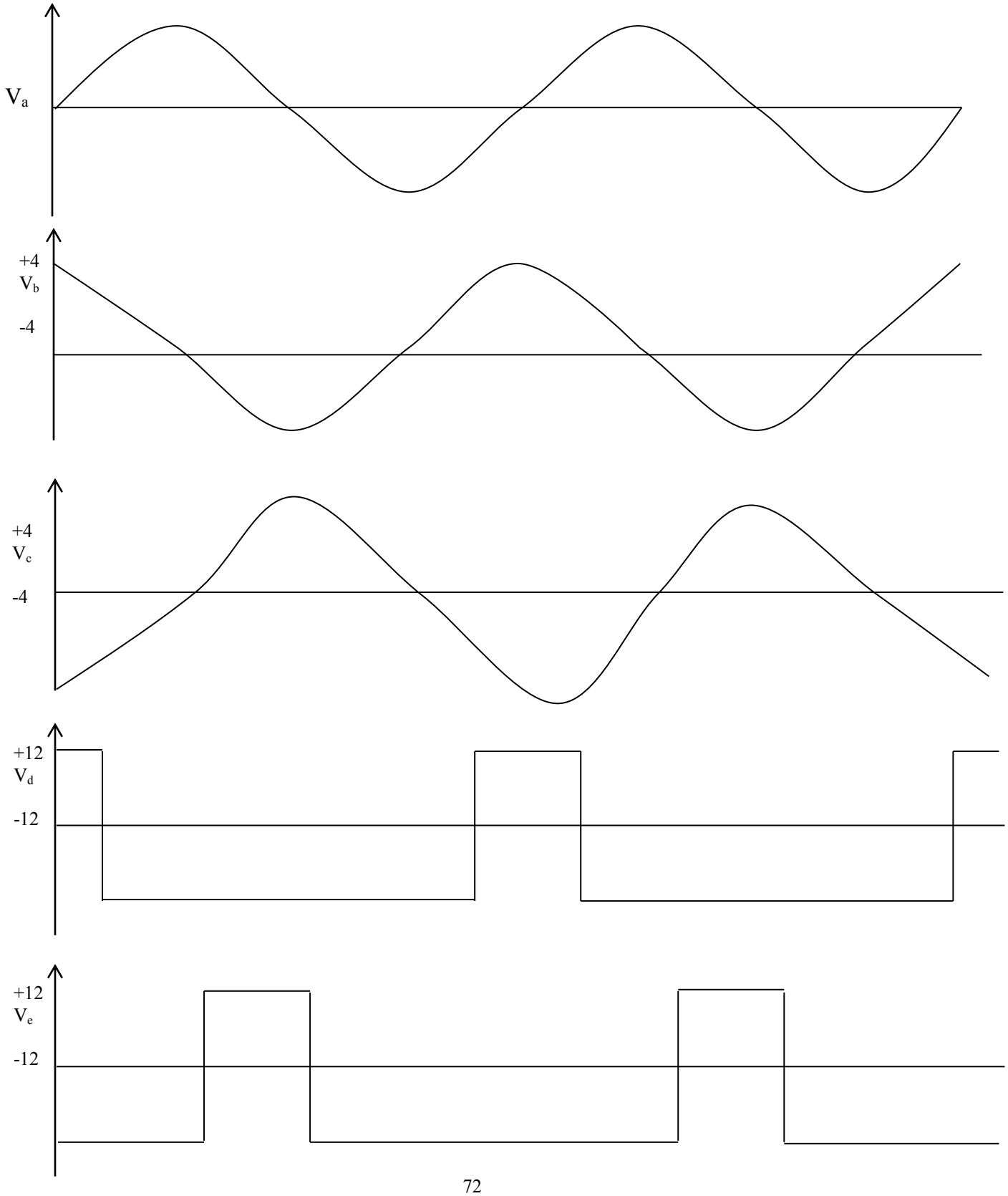
V_a
+4
V_b
-4
+4
V_c
-4
+12
V_d
-12
+12
V_e
-12

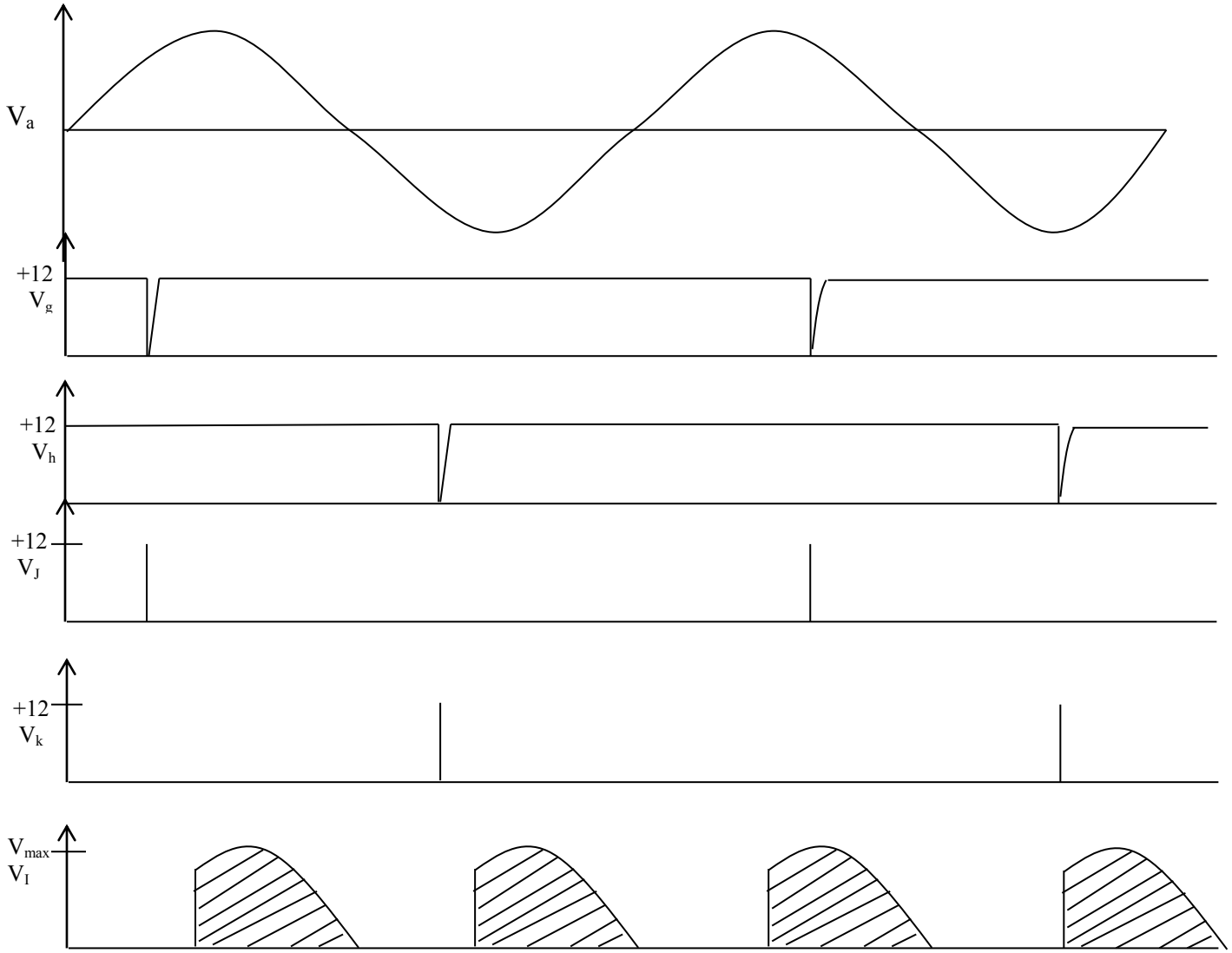

Figure 5.46: The firing circuit waves and output

An 8 volt peak to peak sinusoidal voltage is derived from the mains using a transformer. This is integrated to give a cosine wave form V_b (relative to the mains). The comparator output V_d was a pulse whose wide was that part of a mains period for which V_b is above V_{REF}. This part of the period can be seen to be,

$$2\cos^{-1}(V_{REF}/4) \qquad (5.11)$$

From Fig.5.46 (b), and so the corresponding negative pulse of V_g which is the derivative of V_d, occurs at an angle $\theta = 2\cos^{-1}(V_{REF}/4)$ radians, after the positive going zero crossing of the mains voltage.

Similarly, the pulse of V_R are derived from an inverted (180^0 phase shifted) cosine wave, and hence the pulses are 180^0 out of phase with those of V_g.

If then, pulses V_g are applied to TH.1 (after some modification, discussed later) and pulse V_R to TH.2, then the required motor voltage as shown in Fig.(1) will be produced. The average motor voltage will be:

$$V_{AV} = \frac{1}{\pi}\int_0^{\pi} V_{MAX} Sin(wt)d(wt) \tag{5.12}$$

$$V_{AV} = \frac{V_{MAX}\left[V_{REF}+4\right]}{4\pi} \tag{5.13}$$

Thus by putting

$$V_{REF} = V_F - 4 \text{ Volts} \tag{5.14}$$

The requirement that V_{AY} is proportional to V_F is satisfied; i.e. four volts is subtracted from V_F and the result voltage is input to the comparators in the above circuit.

One side of the firing circuit is shown in figure below:

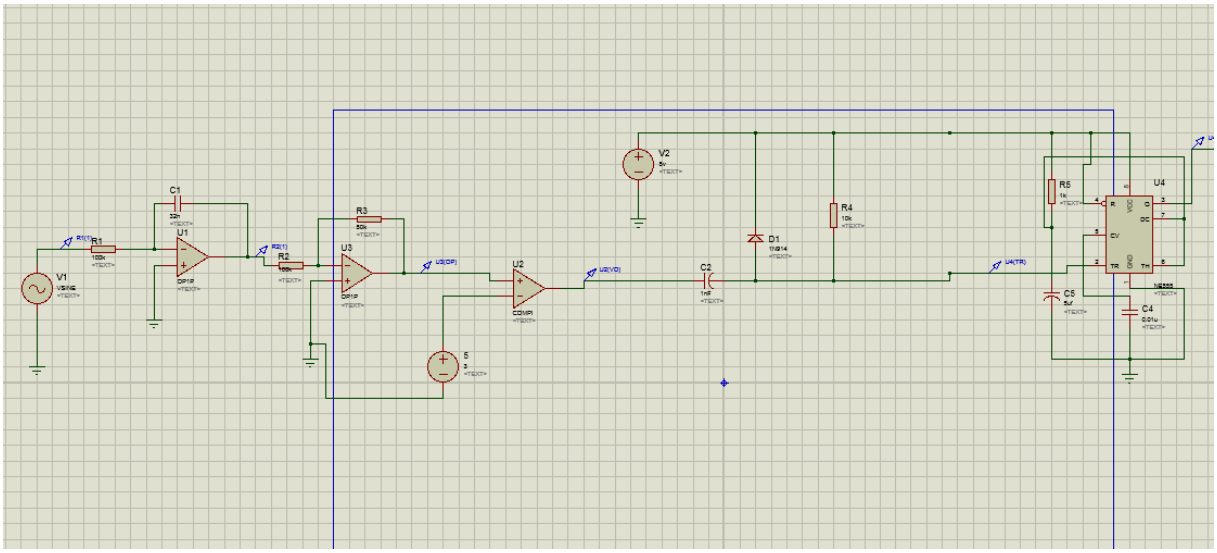

(a)

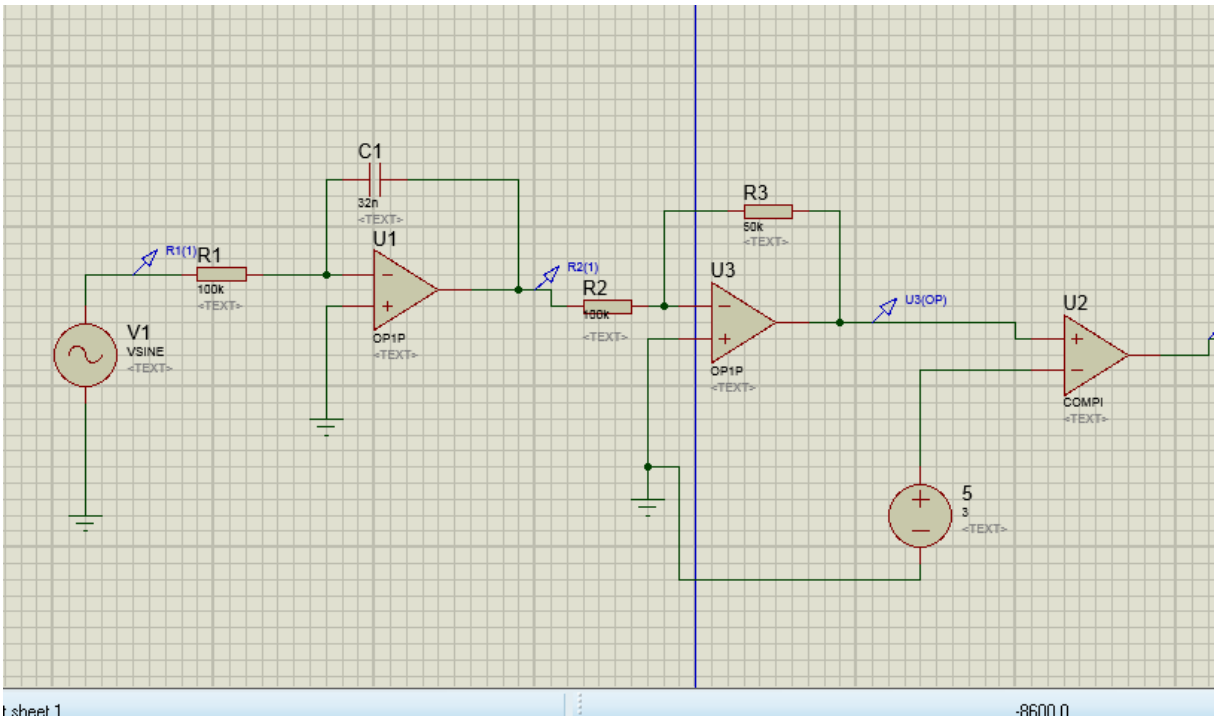

(b)

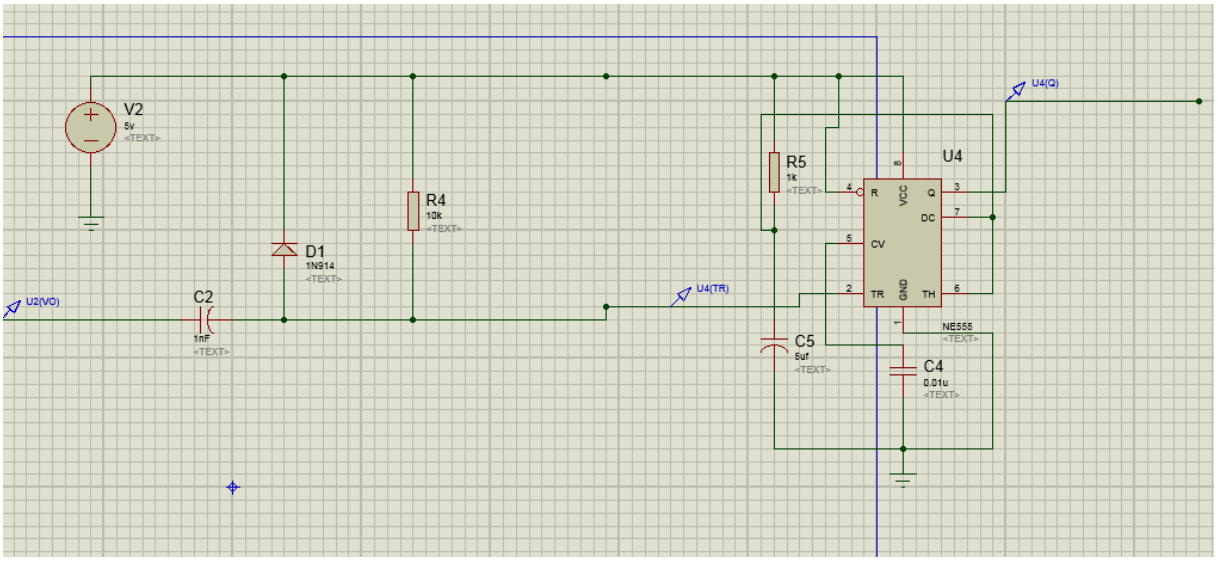

(c) V_a

Figure 5.47 The Firing circuit [23], [24], [28]

The output from the above circuit

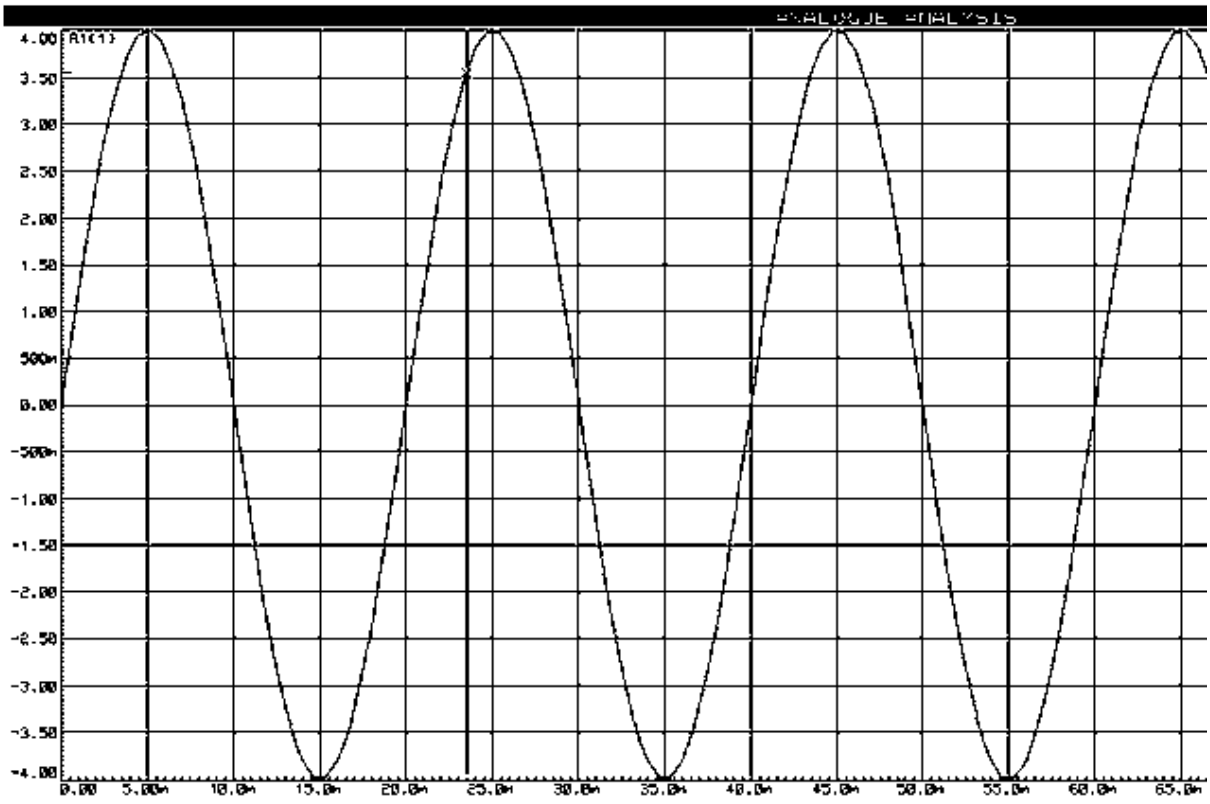

(a) V_a

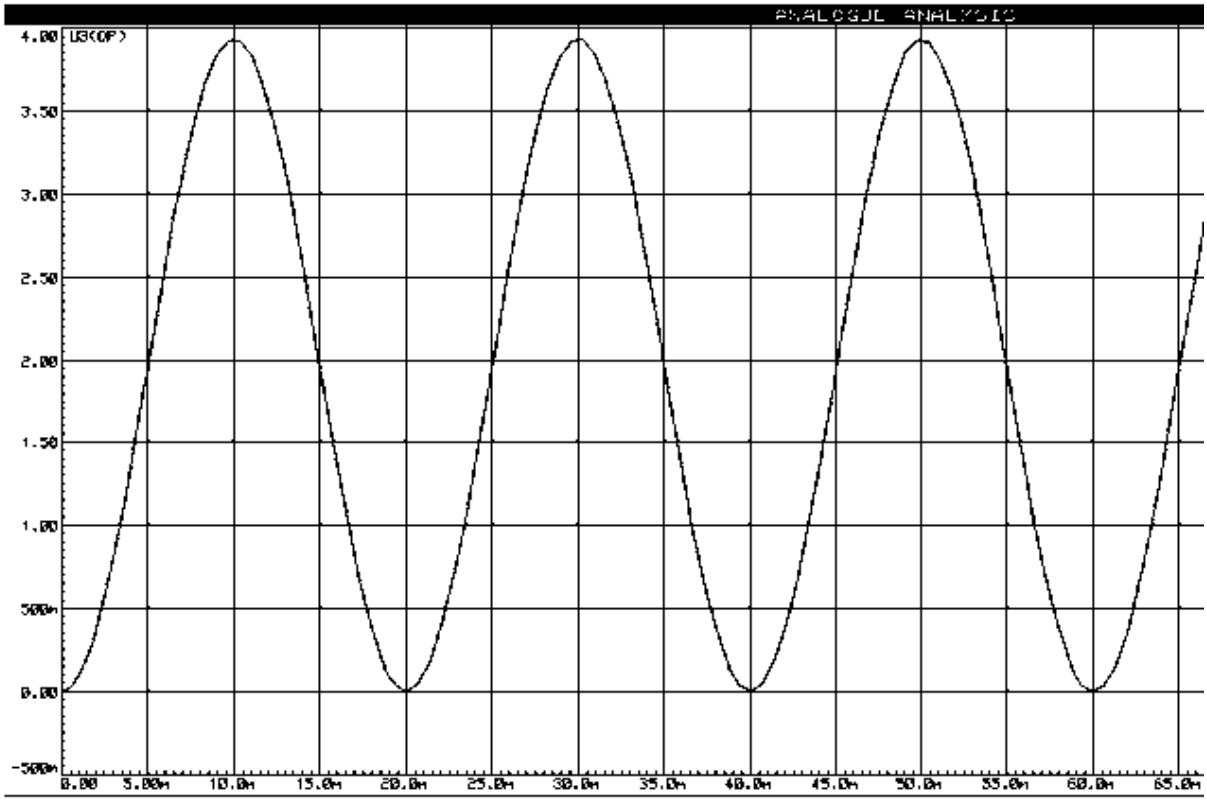
ANALOG/DL ANALYSIS
U3(OP)
4.00
3.50
3.00
2.50
2.00
1.50
1.00
500m
0.00
-500m
0.00
5.00m
10.0m
15.0m
20.0m
25.0m
30.0m
35.0m
40.0m
45.0m
50.0m
55.0m
60.0m
65.0m

(b) V_d

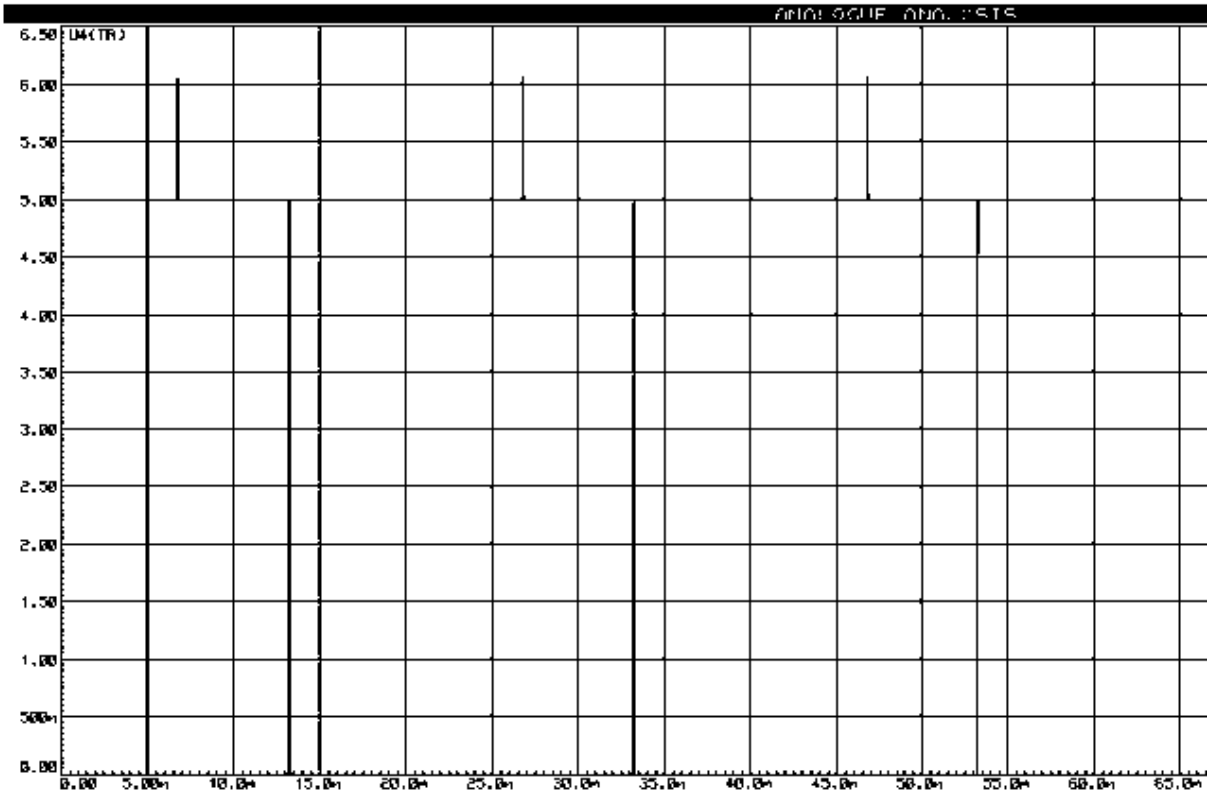
6.50
6.00
5.50
5.00
4.50
4.00
3.50
3.00
2.50
2.00
1.50
1.00
0.00
0.00
5.00n
10.0n
15.0n
20.0n
25.0n
30.0n
35.0n
40.0n
45.0n
50.0n
55.0n
60.0n
65.0n

(c) V_g

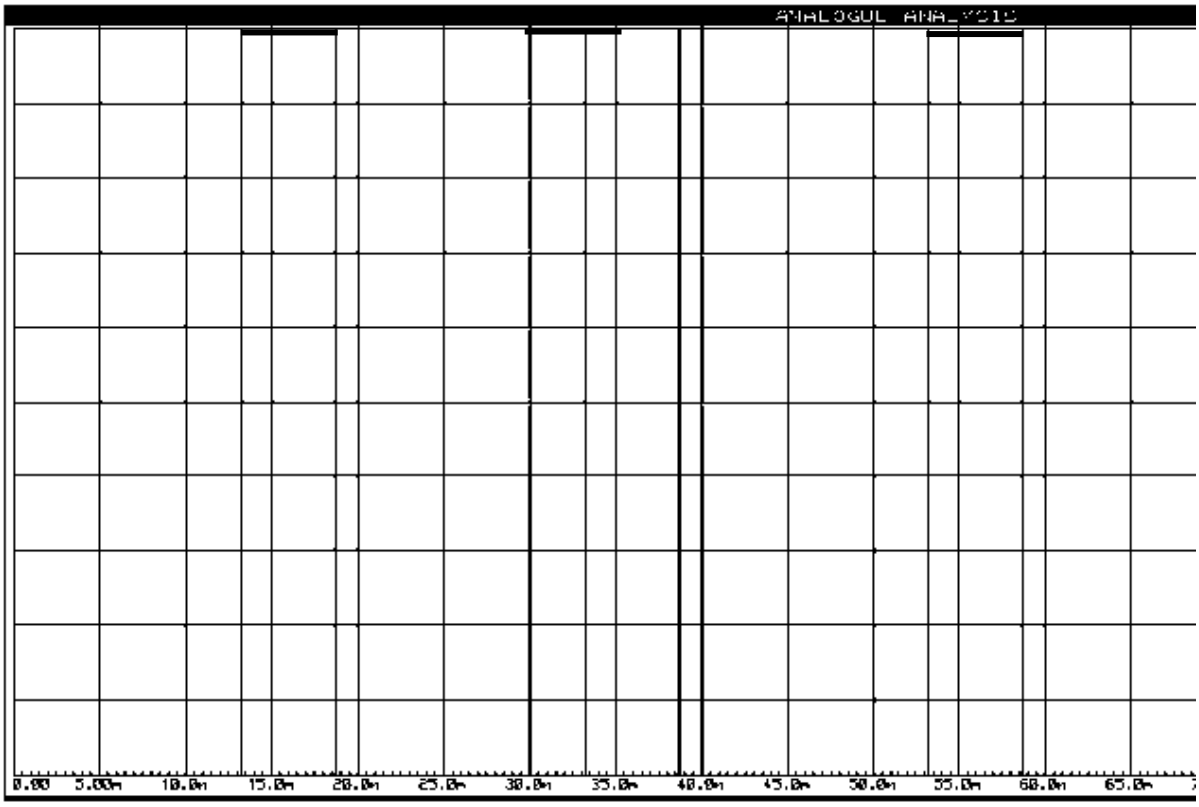

(d) V_j

Figure 5.48: The firing circuit output

5.5.4.2. Further Circuit Requırements

1. A freewheel diode across the motor is required to ensure that until a trigger current is applied to a thyristor it will not turn on. Without this diode, current may be forced through the thyristor by the inductive properties of the motor, thus turning the thyristor on too early, i.e. the diode provides an alternative path for the inductive current.

2. The monostable are required to "clean up" the pulses before they are eventually applied to the thyristor. A short monostable pulses width of less than 1 μ sec is implemented.

3. Darlington Drivers are used to give a current boost to the pulses.

4. These boosted pulses are applied to pulse transformers which provide isolation form the high voltages in the motor circuit. The output of the pulse transformer is applied across the thyristor's cathode and gate as ındıcated.

NOTE:

A simpler single-thyristor circuit was not used because it would provide only half the voltage of the dual-thyristor system used. While this would be adequate for small solar energy systems, that would not be the case for larger systems with greater pumping power requirements.

A complete pump drive circuit is shown in Appendix 2.

5.5.5. Final Stages

5.5.5.1. Tests performed, using the laboratory rig on the flow transducer revealed:

(a) The flow transducer caused a severed obstruction to flow and hence an artificially high pumping power was required.

(b) The flow transducer could not be used at flow rates above 100 1/hr.

Tests performed on the temperature differential transducer circuit revealed that, whilst at high temperature differentials the circuit's accuracy was adequate, this was not so for low values of ΔT. The problem was due mainly to the fact the change in voltage being detected was about 5m/ ^{0}c. Usıng operatıonal amplıfıers wıth D.C offset voltages of this order meant that temperature differentials could be measured with an accuracy of no more than $0.5\,^{0}c$.

This problem could have been solved by the use of very high impedance circuitry and very high gain operational amplifiers.

Furthermore, the problems of the flow-meter could have been solved by a division of flow method.

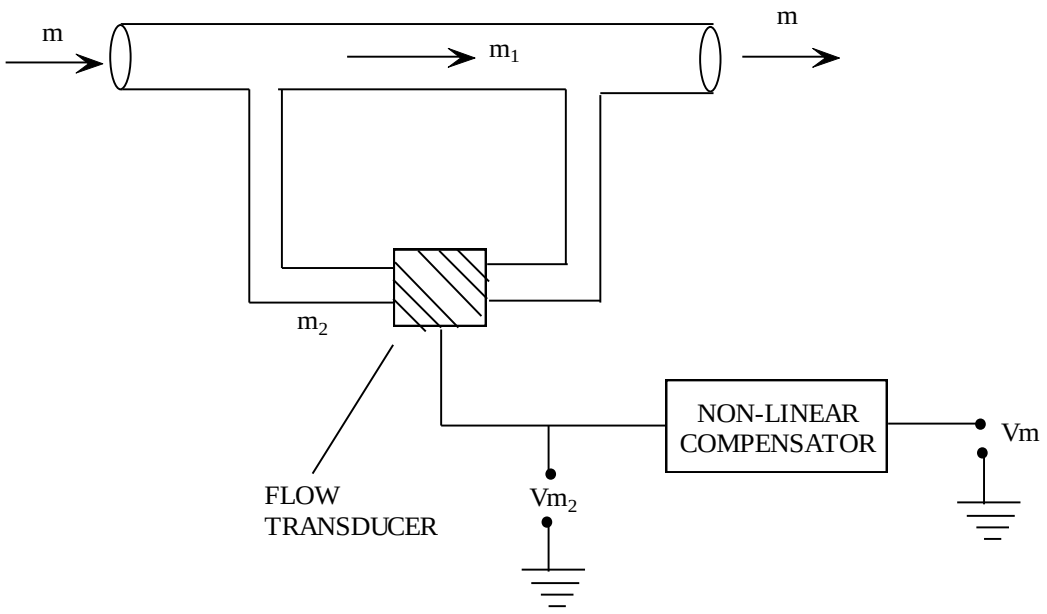

Figure 5.49: Flow meter

This is illustrated in Fig. 5.46. The m_2 would be some non-lınear function of m. This function could have been determined and a compensater built to provide V_m, proportional to m.

This would allow a larger max. Value of $\dot{m}$ than the max. Value of m_2 since m_2 can be much less than m. Also, the obstruction problem would be almost eliminated.

However, at this stage a commercial thermal power transducer –an I.S.S. CLORIUS ENERGY METER – become available. This device used a superior electromagnetic flow meter for flow detection which provided no obstruction and had a large range of flow rates (up to 2001/hr).

This device was intended by the manufacturer for use as a recorder of the thermal energy transferred from a collector over a long period of time. The available instantaneous power signal required filtering and some d.c. compensating before an acceptable V_{PTH} signal was derived. The output of the compensentor circuit was 20Mv per watt of thermal power. This circuit is shown in Appendix.

The final block diagram for the optimal Controller is shown in Fig. 5.47. Magnitudes of various signals are shown.

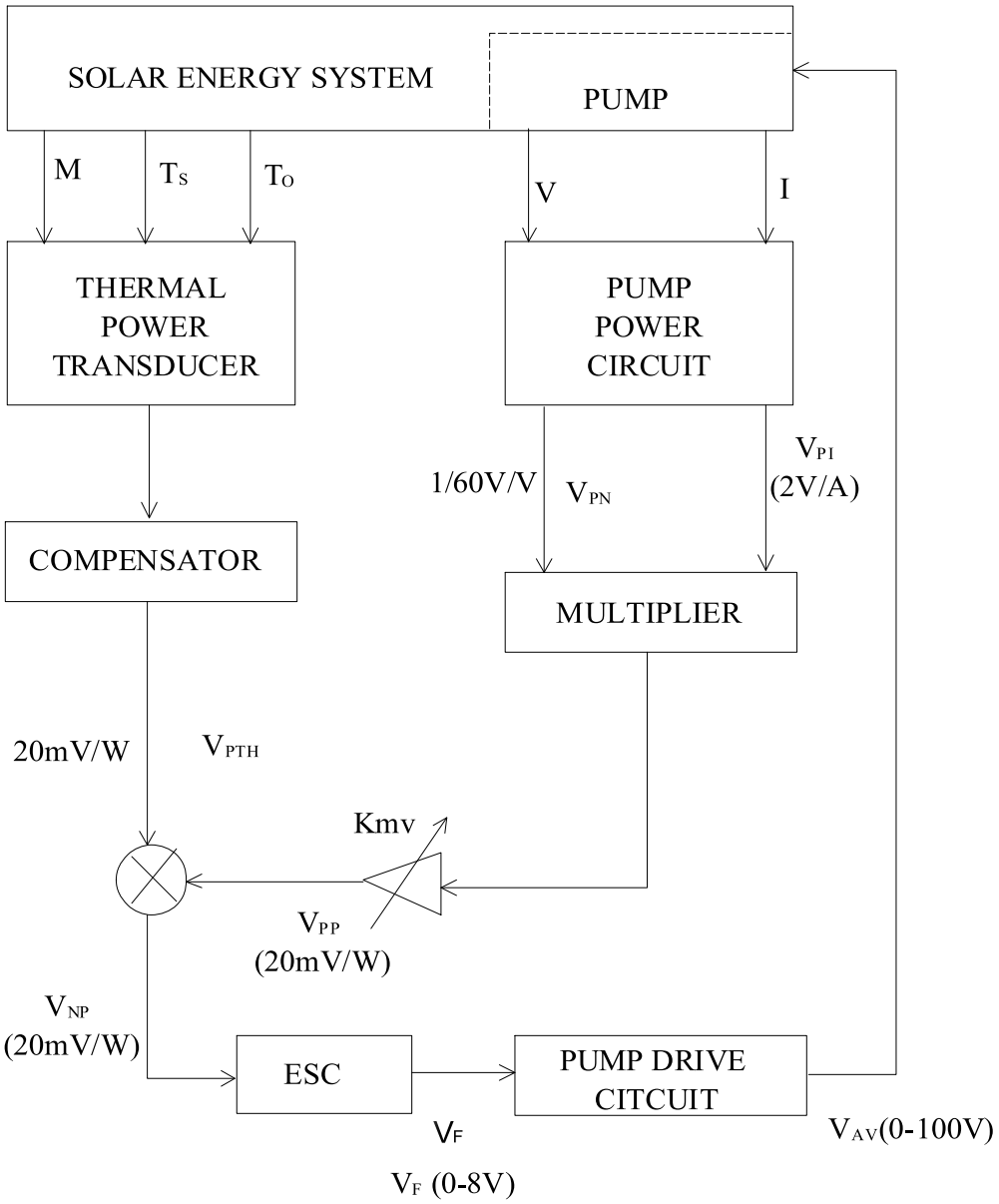

Figure 5.48: Block Diagram of the Optimal Controller

The “kmu” pot. is adjusted so that it gives an output V_{PP} such that V_{PP} is 20Mv per watt of pump power.

CHAPTER SIX

Conclusıon and Recommendations

6.1. Conclusision

The circuit components of the new temperature sensitive control system were individually designed and simulated. This makes it feasible for the real implementation of the system, but a prototype is needed to be constructed through a laboratory analysis of the individual components and setting them to a desired value based on the proposed design. The extremum seeking controller which is the heart of the control system is found to be high (i.e. 5v) when both ΔF^{n-1} and ΔP^{n} are at the same state and this result in more water flow by increasing V_F and goes to a low state when ΔF^{n-1} and ΔP^{n} are at a different state which in turn decrease the flow . Based on the simulation performed using proteus software, it can be concluded that the aim of the project has been achieved.

6.2. Recomendations

It is recommended that, for this control implementation

1. A more precision timing unit is needed in order to avoid approximatiom of some circuit components values by avoiding the tolerance effect which can temper with the desired component values. As such programmable interface controller (PIC) can be used for the timing.
2. Modern devices such as programmable logic circuit (PLC) can be used in implementing the controller in order to minimize the complexity of the circuit.

REFERANCES

1. Hasan, M. R., Arifin, K., Rahman, A., & Azad, A. (2011, September). Design, implementation and performance of a controller for uninterruptible solar hot water system. In *Industrial Engineering and Engineering Management (IE&EM), 2011 IEEE 18Th International Conference on* (pp. 584-588). IEEE.

2. Solar world, solar water heating advantages and disadvantages, http://solarword.blogspot.com.tr/2013/01/solar-water-heating-systems-advantages.html

3. Controller operation, http://www.omega.com/temperature/Z/pdf/z118.pdf

4. Madhukeshwara, N., & Prakash, E. S. (2012). An investigation on the performance characteristics of solar flat plate collector with different selective surface coatings. *International Journal of Energy & Environment*, *3*(1).

5. Report by Doctor Hussein Valizadeh,Mevlana university,konya,Turkey

6. National Renewable Energy Laboratory (NREL), (1996), Residential Solar Heating Collectors, U.S. Department of Energy (DOE)

7. Solar energy conversion text book (from Dr. Hussein valizadeh)

8. Stine, W. B., & Geyer, M. (2001). Power from the Sun (p. 12). Power from the sun. net.

9. Madhukeshwara, N., & Prakash, E. S. (2012). An investigation on the performance characteristics of solar flat plate collector with different selective surface coatings. International Journal of Energy & Environment, 3(1).

10. Evacuated Tube collector.

11 passive solar water heating,.http://ded.mo.gov/division-of-energy/renewables/missouri-s-solar-energy-resource/passive-solar-water-heating,.

12. Types Of Solar Domestic Hot Water System, http://www.lacleantech.net/solar_hot_water_systems.pdf

13. End uses of the solar energy radiantec company, .http://www.radiantsolar.com/pdf/section2.pdf.

14. System Types, http://www.fsec.ucf.edu/en/consumer/solar_hot_water/homes/system_types .htm

15. Struckmann, Fabio. "Analysis of a flat-plate solar collector." Heat and Mass Transport, Project Report, 2008MVK160 (2008).

16 solar water heaters, alternative energy, http://www.altenergy.org/renewables/solar-water-heaters.html.

17. A.M, El – Nashar, Evacuated Tube Collectors, Renewable Energy System and Desalination – vol-II, Encyclopedia of Desalination And Water Resources (DESWARE).

18. Kalogirou, S. A. (2004). Solar thermal collectors and applications. Progress in energy and combustion science, 30(3), 231-295.

19. module 1.5 – control action http://www.see.ed.ac.uk/~jwp/control06/controlcourse/restricted/course/second/course/lecture5.html, .

21. Basic Control Theory http://www.spiraxsarco.com/resources/steamengineeringtutorials/basic -control-theory/basic-control-theory.asp.

21. Indutrial Training Program, Variable Speed Drives, A Way To Lower Life Cycle Costs, U.S Department of Energy.

22. Frequency To Voltage Converter, http://www.next.gr/converters/frequency-to-voltage/frequency-to-voltage-converter-l12074.html

23. Understanding 555 Timer, http://www.electronicshub.org/understanding-555-timer/

24. Jung, W. G. (Ed.). (2005). *Op amp applications handbook*. Newnes.

25. Basic Gates And Function, http://www.ee.surrey.ac.uk/Projects/CAL/digital-logic/gatesfunc/index.html

26. Mosfet As A Switch, http://www.electronics-tutorials.ws/transistor/tran_7.html

27. Opamp Voltage Follower, Sample And Hold Circuit, http://ecetutorials.com/analog-electronics/opamp-voltage-follower-sample-and-hold-circuit/

28. RC Integrator And Differentiator, http://ecetutorials.com/analog-electronics/opamp-voltage-follower-sample-and-hold-circuit/